molecules

MDPI

Article

Half-Sandwich Type Platinum-Group Metal Complexes of *C*-~~glucosaminyl~~ Glucosaminyl Azines: Syntheses, Antineoplastic and Antimicrobial Activities

István Kacsir[1,2,†], Adrienn Sipos[3,4,5,†], Evelin Major[6], Nikolett Bajusz[6], Attila Bényei[7], Péter Buglyó[8], László Somsák[1], Gábor Kardos[6], Péter Bai[3,4,5,9,10,*] and Éva Bokor[1,*]

[1] Department of Organic Chemistry, University of Debrecen, P.O. Box 400, H-4002 Debrecen, Hungary; kacsir.istvan@science.unideb.hu (I.K.); somsak.laszlo@science.unideb.hu (L.S.)
[2] Doctoral School of Chemistry, University of Debrecen, P.O. Box 400, H-4002 Debrecen, Hungary
[3] Department of Medical Chemistry, Faculty of Medicine, University of Debrecen, Egyetem Tér 1., H-4032 Debrecen, Hungary; siposadri@med.unideb.hu (A.S.)
[4] The Hungarian Academy of Sciences, Center of Excellence, Hungary
[5] MTA-DE Cell Biology and Signaling Research Group ELKH, Debrecen, Hungary
[6] Department of Metagenomics, University of Debrecen, H-4032 Debrecen, Hungary; evelin-major@med.unideb.hu (E.M.), bajusz.nikolett@med.unideb.hu (N.B.), kg@med.unideb.hu (K.G.)
[7] Department of Physical Chemistry, Faculty of Sciences and Technology, University of Debrecen, Egyetem Tér 1., H-4032 Debrecen, Hungary; benyei.attila@science.unideb.hu (A.B.)
[8] Department of Inorganic & Analytical Chemistry, Faculty of Sciences and Technology, University of Debrecen, Egyetem Tér 1., H-4032 Debrecen, Hungary; buglyó@science.unideb.hu (P.Buglyó)
[9] NKFIH-DE Lendület Laboratory of Cellular Metabolism, H-4032 Debrecen, Hungary
[10] Research Center for Molecular Medicine, Faculty of Medicine, University of Debrecen, H-4032 Debrecen, Hungary
† These authors have contributed equally to this work and share first authorship.
* Correspondence: bokor.eva@science.unideb.hu (É.B.); baip@med.unideb.hu (P.Bai), Tel.: +36-525-129-00 (ext. 22474) (É.B.); +36-524-123-45 (P.Bai)

Abstract: While platinum-based compounds, as cisplatin, build the backbone of the chemotherapy, the use of these compounds is limited by resistance and toxicity driving the development of novel complexes with cytostatic properties. In this study we synthesized a set of half-sandwich complexes of platinum-group metal ions (Ru(II), Os(II), Ir(III), Rh(III)) with an N,N-bidentate ligand comprised of a *C*-glucosaminyl group and a heterocycle, such as pyridine, pyridazine, pyrimidine, pyrazine and quinoline. The sugar-containing ligands themselves are unknown compounds, and have been obtained by nucleophilic additions of the lithiated heterocycles to *O*-perbenzylated 2-nitro-glucal. Reduction of the adducts and, where necessary, subsequent protecting group manipulations furnished the above *C*-glucosaminyl heterocycles in their *O*-perbenzylated, *O*-perbenzoylated and *O*-unprotected forms. The derived complexes were tested on A2780 ovarian cancer cells. Pyridine, pyrazine and pyridazine-containing complexes proved to be cytostatic and cytotoxic on A2780 cells, while pyrimidine and quinoline derivatives were inactive. The best complexes contained pyridine as the heterocycle. Furthermore, the metal ion with polyhapto arene/arenyl moiety also impacted on the biological activity of the complexes. Ruthenium complexes with *p*-cymene and iridium complexes with Cp* had the best performance on ovarian cancer cells followed by osmium complexes with *p*-cymene and then by rhodium complexes with Cp*. Finally, the chemical nature of the protective groups on the hydroxyl groups of the carbohydrate moiety were also key determinants of the bioactivity, namely, *O*-benzyl groups were superior to *O*-benzoyl groups. The IC_{50} values of the complexes were in the low micromolar range and, importantly, the complexes were less active against primary, untransformed human dermal fibroblasts, however the anticipated therapeutic window is narrow. The bioactive complexes exerted cytostasis on a set of carcinomas, as cell models of glioblastoma, breast and pancreatic cancer. Furthermore, the same complexes had bacteriostatic

Citation: Kacsir, I.; Sipos, A.; Major, E.; Bajusz, N.; Bényei, A.; Buglyó, P.; Somsák, L.; Kardos, G.; Bai, P.; Bokor, É. **Half-Sandwich Type Platinum-Group Metal Complexes of *C*-glucosaminyl Azines: Syntheses, Antineoplastic and Antimicrobial Activities.** *Molecules* **2023**, *26*, x. https://doi.org/10.3390/xxxxx

Academic Editor(s):

Received: date
Revised: date
Accepted: date
Published: date

properties against multiresistant Gram-positive *Staphylococcus aureus* and *Enterococcus* clinical isolates in the low micromolar range.

Keywords: ruthenium; osmium; iridium; rhodium; half-sandwich complex; *C*-glucosaminyl heterocycles; azines; *Staphylococcus aureus*; *Enterococcus*; MRSA; VRE; cytostasis; ovarian cancer

1. Introduction

Registered platinum complexes (cisplatin, oxaliplatin, carboplatin) constitute the backbone of modern oncological chemotherapy in multiple solid tumors with poor prognosis, including a large set of carcinomas, as ovarian cancer, sarcomas and hematological malignancies [1,2]. The applicability of platinum compounds is limited by platinum resistance and toxicity [3-8].

Novel organometallic compounds of other platinum-group metals such as complexes of ruthenium [2,9-15], osmium [9,11,12,14,16-19], iridium [11,14,17,20,21] or rhodium [11,14,20,22] are being developed for the replacement of platinum drugs and were reported to have better toxicity profiles as compared to platinum-based drugs [23-26]. The anticancer potential of such platinum-group metal complexes is also supported by three ruthenium derivatives, NAMI-A [27], KP1019/1339 (IT-139, BOLD100) [28] and TLD-1433 [29], which have already been in different phases of clinical trials against neoplastic diseases as bladder or lung cancer.

In the quest for potential substitutes of the platins, the half-sandwich type complexes of platinum-group metal ions (e.g. Ru(II), Os(II), Ir(III), Rh(III)) with a large number of representatives displaying anticancer potencies [14,15,19,21,22] have emerged as a promising compound class. In addition to the antineoplastic effects, several members of these piano stool complexes have different antimicrobial (e.g. antibacterial [30-39], antiparasitic [40-42], antiviral [30,43] and antifungal [44]) properties.

We have recently reported a series of half-sandwich complexes having five-membered chelate rings, constructed by the use of *N*- and *C*-glycopyranosyl heterocyclic N,N-bidentate ligands (Figure 1, **I**) [32,45,46]. Several representatives of **I** displayed low micromolar or in certain cases submicromolar (e.g. **Ia**) cytostatic activities against and also proved to be selective for cancer cells. The antiproliferative potency of these complexes is thought to be related to reactive oxygen species production [32,45,46]. It is to be mentioned that the complexes having antineoplastic activities (e.g. **Ia**) were also shown to be effective against Gram positive multiresistant bacteria [31,32]. A short summary about the structure-activity relationships (SAR) of these complexes is presented in Figure 1, while for a more detailed explanation of the SAR the reader is kindly referred to our previous publications [31,32,45,46]. One of the most important structural motifs related to biological efficacy is the presence of the sugar moiety *O*-protected with large hydrophobic acyl, preferably with benzoyl groups. This feature contributes in a large extent to the favorably increased lipophilic character of the biologically active complexes [32,45,46].

Apart from the above complexes, there are only two more literature examples for half-sandwich complexes with sugar-based N,N-chelators. 1,4-Bis(β-D-glycopyranosyl)tetrazenes [47] (e. g. **II**) as well as methyl 2,3-diamino-2,3-dideoxy-hexopyranosides [48] (e. g. **III**) were incorporated into the coordination sphere of the reported complexes. The antineoplastic effects of these organometallics were also studied and some of them were found to be cytotoxic at low micromolar concentrations against various cancer cells (**II** and **III** represent the most efficient compounds of the respective series) [47,48].

Based on the structures of the sugar-derived ligands of complexes **I** and **III**, we have considered that *C*-glucosaminyl N-heterocycles, having an N-donor atom in the glycon, and another one in the heterocylic aglycon part, are capable of forming half-sandwich type complexes with six-membered chelate ring. In the present study, the preparation of a series of *C*-glucosaminyl azines and their incorporation as N,N-bidentate ligands into complexes of type **IV** have been envisaged. Biological studies to reveal the anticancer and antibacterial potencies of the new organometallic compounds have also been foreseen.

formázott: Betűtípus: 9 pt

With the exception of the glycosyl heterocyclic ligand, the main structural elements of the new complexes as depicted in formula **IV** have been designed to be identical to those of complexes **I** with biological activities. In addition, the replacement of the *O*-benzoyl groups of the monosaccharide unit by *O*-benzyl groups has also been envisaged in order to examine the effect of an ether-type protection on the biological efficiency of the complexes.

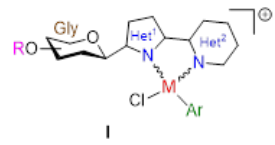

I

Structure-activity relationships showing increasing biological activities:

R = H/$COCH_3$ inactive; R = COC_nH_{2n+1} (n = 3-7) < COPh

Gly = D-xylo < D-gluco ~ D-galacto

Het^1 = 1,2,4-oxadiazole < 1,3,4-oxadiazole < 1,2,3-triazole

Het^2 = 2-pyridyl < 2-quinolinyl

M = Ir(III)/Rh(III) with Ar = Cp* < Ru(II)/Os(II) with Ar = *p*-cymene

Biologically most effective complex of the series:

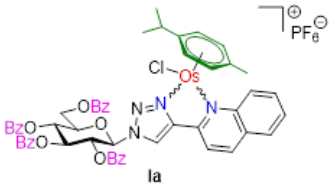

Ia

Antineoplastic activity:

Cancer cell line	IC_{50} [μM]
A2780 (ovarian, cisplatin resistant)	0.43
ID8 (ovarian)	0.36
Capan2 (pancreatic adenocarcinoma)	1.35
Saos (sarcoma)	1.29

Antimicrobial activity:

MIC = 5-20 μM on Gram-positive multiresistant bacteria

-*Staphylococcus aureus*

-*Enterococcus species*

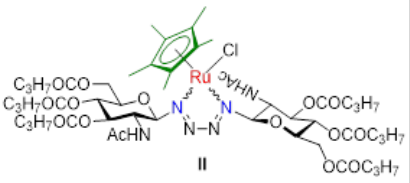

II

Antineoplastic activity:

Cancer cell line	IC_{50} [μM]
A2780 (ovarian)	0.36
SK-OV-3 (ovarian, cisplatin resistant)	2.01
MDA-MB-231 (breast)	1.02

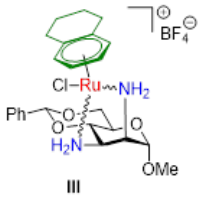

III

Antineoplastic activity:

Cancer cell line	IC_{50} [μM]
DAN-G (pancreas)	28.5
LCLC-103H (lung)	4.39
SISO (cervical)	2.79

Target compounds of this study:

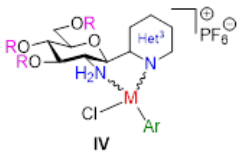

IV

R = H, COPh, CH_2Ph

M = Ru(II)/Os(II) with Ar = *p*-cymene, Ir(III)/Rh(III) with Ar = Cp*

Het^3 =

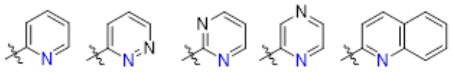

107

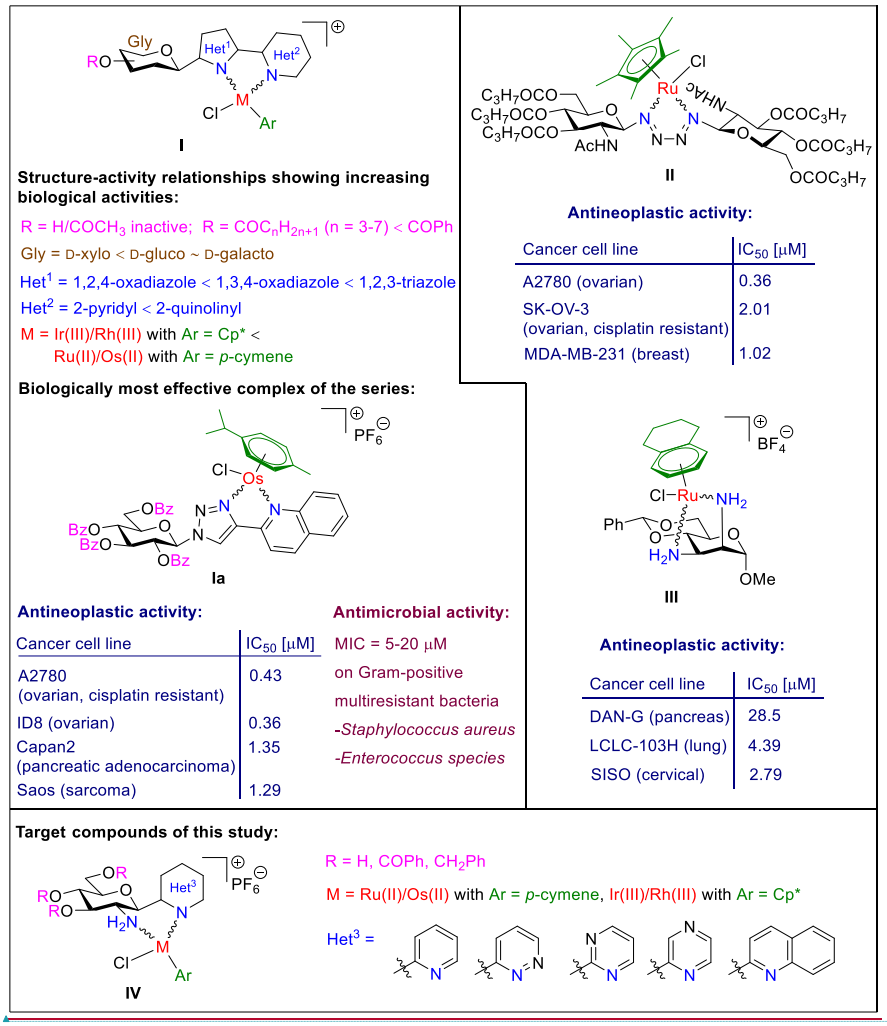

Figure 1. Preliminaries and target compounds of the present work.

2. Results

2.1. Chemistry

For the preparation of the planned *C*-glucosaminyl azine type N,N-chelators 3,4,6-tri-*O*-benzyl-2-nitro-D-glucal [49] (**1**) was used as the starting material with the expectation that a common general procedure can be elaborated by using additions to the double bond of organometallic nucleophiles derived from the respective heterocycles [50]. In line with these plans, nitro-Michael addition [51-53] of **1** with lithiated six-membered heterocycles, pre-formed from the corresponding halogenated heterocycles with *n*-buthyl lithium or generated *in situ* (Table 1, *i*), resulted in a set of *C*-(2′-deoxy-2′-nitro-3′,4′,6′-tri-*O*-benzyl-β-D-glucopyranosyl)azines **2a-e** in good to acceptable yields.

Megváltozott a mezőkód

formázott: Betűtípus: 10 pt
formázott: Betűtípus: 8 pt
formázott: Betűtípus: 10 pt
formázott: Betűtípus: 10 pt
formázott: Betűtípus: 10 pt
formázott: Betűtípus: 10 pt
formázott: Betűtípus: 10 pt
formázott: Betűtípus: 8 pt

In the next step, the reduction of the nitro group of compounds **2** showed a much less uniform behavior. To get *O*-perbenzylated *C*-glucosaminyl azines reduction of the nitro group of **2a-e** by Zn-HCl (*ii*) was investigated first. This transformation of **2a** to the expected 2-glucosaminyl pyridine **3a** was smoothly accomplished in good yield. Similar reactions of nitro derivatives **3b-e** led, however, to multicomponent reaction mixtures, from which only the 2-glucosaminyl pyrazine **3d** could be isolated in low yield. Unfortunately, our further attempts to obtain the glucosamine derivatives **3d,e** from **2d,e** under different reductive conditions also failed, either no reaction took place (Fe, *cc*HCl, THF-H_2O 1 : 1, 0 °C; $SnCl_2$, dry EtOH, reflux; $SiCl_3H$, DIPEA, dry CH_3CN, 0 °C; $B_2(OH)_4$, THF-H_2O 1 : 1, 80 °C) or formation of inseparable product mixtures (Sn, *cc*HCl, THF-H_2O 1 : 1, 0 °C) was observed.

Table 1. Synthesis of *C*-(2′-deoxy-2′-nitro-3′,4′,6′-tri-*O*-benzyl-β-D-glucopyranosyl)azines and their transformation into *C*-(2′-amino-2′-deoxy-3′,4′,6′-tri-*O*-benzyl-β-D-glucopyranosyl)azines.

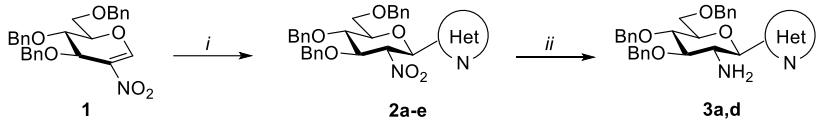

1 **2a-e** **3a,d**

Conditions: *i*) 1.2-2.0 equiv. of Het-Hlg (Hlg = Br, I), 2.5 M solution of *n*-Bu-Li in hexane (1.2-2.0 equiv.), dry THF, -78 °C; *ii*) Zn powder, *cc*HCl or 2M aq. HCl, THF-H_2O (2 : 1), r.t.

Het		Conditions and yields (%)			
			2		**3**
a		*i*	52	*ii*	64
b		*i*	13	*ii*	NI*
c		*i*	71	*ii*	NI*
d		*i*	63	*ii*	7
e	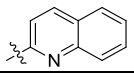	*i*	60	*ii*	NI*

*Could not be isolated.

Next, the synthesis of *O*-unprotected *C*-glucosaminyl azines was examined starting from compounds **2a-e** and **3a** (Table 2). A BCl_3-mediated *O*-debenzylation of the pyridine derivative **3a** gave the *O*-unprotected analog **5a** in moderate yield (*i*). This reaction was repeated in the presence of the cation scavenger pentamethylbenzene [54] (*ii*) to give compound **5a** in excellent yield.

Attempted transformation of compounds **2a-e** into **5a-e** in one step involving simultaneous *O*-debenzylation and reduction of the nitro group by catalytic hydrogenation (Pd(C) or $Pd(OH)_2$, cat. *cc*HCl, EtOH, reflux,) was unsuccessful, in each case decomposition of the starting materials **2a-e** was observed. Therefore, the synthesis of the glucosamine derivatives **5a-e** from **2a-e** was performed in a two-step procedure. First, the *O*-benzyl protecting groups of **2a-e** were removed by BCl_3 (*i*) to give *C*-(2′-deoxy-2′-nitro-β-D-

formázott: Betűtípus: 10 pt
formázott: Betűtípus: 7 pt
formázott: Behúzás: Bal: 0 cm
formázott: Betűtípus: Nem Félkövér
formázott: Betűtípus: 7 pt
formázott: Betűtípus: Nem Félkövér
formázott: Betűtípus: Nem Félkövér
formázott: Balra zárt, Behúzás: Bal: 1,25 cm
táblázatot formázott
formázott: Sorkizárt, Behúzás: Bal: 4,6 cm, Sorköz: Többszörös 0,95 s.
formázott: Térköz Előtte: 12 pt
formázott: Betűtípus: 8 pt

glucopyranosyl)azines **4a-e** in high yields. Reduction of the nitro group of **4a-e** was then examined under two conditions. Catalytic hydrogenation of **4c** and **4d** (*iii*) gave the desired pyrimidine- and pyrazine-containing *C*-glucosaminyl derivatives **5c** and **5d**, respectively, in acceptable yields. The same conditions (*iii*) applied to compounds **4a,b,e** resulted in complex product mixtures, in which the desired *C*-glucosaminyl pyridine **5a**, pyridazine **5b** and quinoline **5e** were detected by TLC analysis, however, could not be separated in pure state. Treatment of **4e** with Sn powder in the presence of *cc*HCl (*iv*) was also carried out to give the target **5e** in acceptable yield.

Table 2. Synthesis of *C*-(2′-amino-2′-deoxy-β-D-glucopyranosyl)azines.

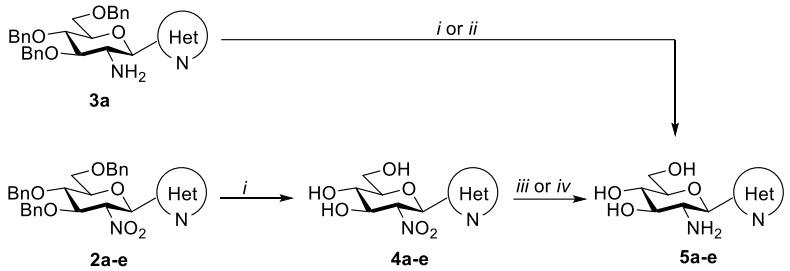

Conditions: *i*) 1M solution of BCl_3 in CH_2Cl_2 (5 equiv.), dry CH_2Cl_2, -78 °C; *ii*) 1M solution of BCl_3 in CH_2Cl_2 (4 equiv.), pentamethylbenzene (9 equiv.), dry CH_2Cl_2, -78 °C; *iii*) H_2, Pd(C), dry EtOH, reflux; *iv*) Sn powder, *cc*HCl, THF-H_2O (2 : 1), r.t.

Het		Conditions and yields (%)			
			4		5
a		*i*	85	*i* *ii* *iii*	42 (from **3a**) 95 (from **3a**) NI* (from **4a**)
b		*i*	89	*iii* *iv*	NI* (from **4b**) NI* (from **4b**)
c		*i*	98	*iii*	38 (from **4c**)
d		*i*	78	*iii*	66 (from **4d**)
e	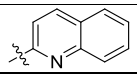	*i*	76	*iii* *iv*	NI* (from **4e**) 29 (from **4e**)

*The formation of the expected product was detected, but the compound could not be isolated in pure state.

Towards *O*-perbenzoylated *C*-glucosaminyl azines, a direct exchange of the *O*-benzyl protecting groups to benzoyl groups by a $Zn(OTf)_2$ mediated reaction [55] of compounds **2a-d** with benzoyl chloride (Table 3, *i*) was performed to obtain *C*-(2′-deoxy-2′-nitro-3′,4′,6′-tri-*O*-benzoyl-β-D-glucopyranosyl)azines **6a-d** in good to excellent yields. Subsequent reduction of the nitro group of the pyridine derivative **6a** by Zn-HCl (*ii*) afforded the *O*-perbenzoylated glucosamine derivative **7a** in moderate yield. Analogous reactions (*ii*) carried out with compounds **6b-d** led to complex reaction mixtures, from which the desired *C*-glucosaminyl heterocycles **7b-d** could not be isolated. For the transformation of **6b-d** into **7b-d** further experiments under various reductive conditions (e.g. H_2, Pd(C) or

formázott: Behúzás: Bal: 0 cm
formázott: Betűtípus: Nem Félkövér
formázott: Betűtípus: 7 pt
formázott: Betűtípus: Nem Félkövér
formázott: Betűtípus: Nem Félkövér
formázott: Balra zárt, Behúzás: Bal: 0,25 cm
táblázatot formázott
formázott: Térköz Előtte: 12 pt
formázott: Betűtípus: 8 pt

Pd(OH)$_2$, dry EtOH, reflux; $SnCl_2$, dry EtOH, reflux; Sn, *cc*HCl, THF-H_2O 1 : 1, 0 °C; $B_2(OH)_4$, THF-H_2O 1 : 1, 80 °C) were also tried, however, none of them were successful.

Due to the above difficulties, another three-step procedure starting from **5c-e** was applied to get the planned **7c-e** (Table 3). Thus, the NH_2 group of **5c-e** was protected first as a carbamate by using Boc_2O (*iv*) and the resulting **8c-e** were then *O*-perbenzoylated upon treatment with benzoyl chloride (*v*) to give the *O*- and *N*-protected glucosaminyl derivatives **9c-e**. Finally, an acid-mediated liberation of the NH_2 group in **9c-e** (*vi*) was carried out providing the final products **7c-e** in high yields.

As mentioned earlier, the 3-(2′amino-2′-deoxy-β-D-glucopyranosyl)pyridazine **5b** could not be obtained in pure state from **4b** (Table 2). In order to get the *O*-perbenzoylated **9b**, a consecutive three-step procedure starting from **4b** was accomplished to avoid the need of using pure intermediate **5b** (Table 3). Thus, the $NO_2 \rightarrow NH_2$ transformation carried out by catalytic hydrogenation of **4b** (*iii*), followed by the Boc-protection of the amino group of intermediate **5b** (*iv*) and subsequent *O*-perbenzoylation of the resulting **8b** (*v*) furnished the desired glucosaminyl pyridazine **9b** in acceptable overall yields (27% for three steps). Then, standard *N*-Boc-deprotection (*vi*) gave the desired **7b** in high yield.

formázott: Betűtípus: 8 pt

178

Table 3. Synthesis of *C*-(2′-amino-2′-deoxy-3′,4′,6′-tri-*O*-benzoyl-β-D-glucopyranosyl)azines

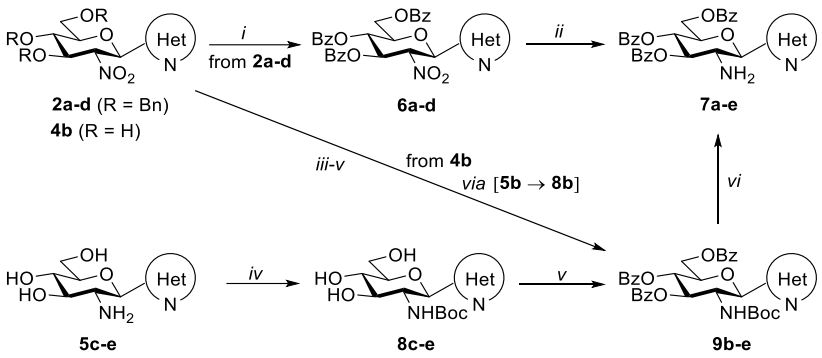

Conditions: *i*) 6 equiv. of benzoyl chloride, 2 equiv. of $Zn(OTf)_2$, dry $ClCH_2CH_2Cl$, r.t.; *ii*) Zn powder, *cc*HCl or 2M aq. HCl, THF-H_2O (2 : 1), r.t.; *iii*) H_2, Pd(C), dry EtOH, reflux; *iv*) 2 equiv. of Boc_2O, 1,4-dioxane-H_2O (1 : 1), r.t.; *v*) 7.2 equiv. of benzoyl chloride, dry pyridine, 60 °C; *vi*) 2 equiv. of CF_3COOH, dry CH_2Cl_2, r.t.

Het		Conditions and yields (%)							
		6	**7**		**8**		**9**		
a		*i*	88	*ii*	38 (from **6a**)	-	-	-	-
b		*i*	97	*ii* *vi*	NI* (from **6b**) 88 (from **9b**)	*iv*	NI*	*iii-v*	27** (from **4b**)
c		*i*	45	*ii* *vi*	NI* (from **6c**) 96 (from **9c**)	*iv*	67	*v*	80 (from **8c**)
d		*i*	82	*ii* *vi*	NI* (from **6d**) 96 (from **9d**)	*iv*	67	*v*	71 (from **8d**)
e	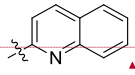	*i*	-	*vi*	84 (from **9e**)	*iv*	80	*v*	81 (from **8e**)

*Could not be isolated. **Overall yield for three steps.

179

180

formázott: MDPI_3.1_text, Az ázsiai és latin betűs szöveg közötti térköz beállítása, Az ázsiai szöveg és a számok közötti térköz beállítása

formázott: Betűtípus: 9 pt

formázott: Betűtípus: 7 pt

formázott: Balra zárt, Térköz Előtte: 12 pt, Utána: 6 pt, Sorköz: Többszörös 0,95 s.

formázott: Betűtípus: 9 pt

táblázatot formázott

formázott: Betűtípus: 10 pt

formázott: Sorköz: szimpla

formázott: Betűtípus: 10 pt, Félkövér

formázott: Betűtípus: 10 pt

formázott: Betűtípus: 10 pt

formázott: Betűtípus: 10 pt

formázott: Betűtípus: 10 pt

formázott: Betűtípus: 10 pt

formázott: Betűtípus: 10 pt

formázott: Betűtípus: 10 pt

formázott: Betűtípus: 10 pt

formázott: Betűtípus: 10 pt

formázott: Betűtípus: 10 pt

formázott: Betűtípus: 10 pt

formázott: Betűtípus: 10 pt

formázott: Betűtípus: 10 pt

formázott: Betűtípus: 10 pt

Next, the newly prepared heterocyclic glucosamine derivatives were used as N,N-bidentate ligands in the formation of platinum-group metal half-sandwich complexes.

Treatment of the *O*-perbenzylated 2-glucosaminyl pyridine with dichloro(η⁶-*p*-cymene)ruthenium(II) and -osmium(II) and dichloro(pentamethylcyclopentadienyl)iridium(III) and -rhodium(III) dimers (**Ru-/Os-/Ir-/Rh-dimer**) in the presence of the halide abstractor $TlPF_6$ afforded the expected cationic complexes **Ru-3a**, **Os-3a**, **Ir-3a** and **Rh-3a**, respectively, with six-membered chelate rings (Table 4, entries 1-4). Analogous Ru(II) and Os(II) complexes **Ru-3d**, **Os-3d** with the pyrazine derivative **3d** were also obtained under similar conditions (entries 5 and 6, respectively).

Our previous studies [45,46] on other series of half-sandwich complexes constructed with glycopyranosyl azole ligands revealed that the *O*-protection of the hydroxyl groups of the sugar moiety by large apolar protecting groups played a pivotal role in achieving significant biological effects. Complexes containing *O*-unprotected monosaccharide-based ligands proved to be biologically inactive. Nevertheless, for a comparative study of the new set of platinum-group metal complexes presented here, compound **Ru-5a** incorporating *O*-deprotected 2-glucosaminyl pyridine **5a** was also synthesized (Table 4, entry 7).

Table 4. Synthesis of half-sandwich platinum-group metal complexes with the *O*-perbenzylated and *O*-unprotected *C*-glucosaminyl azines

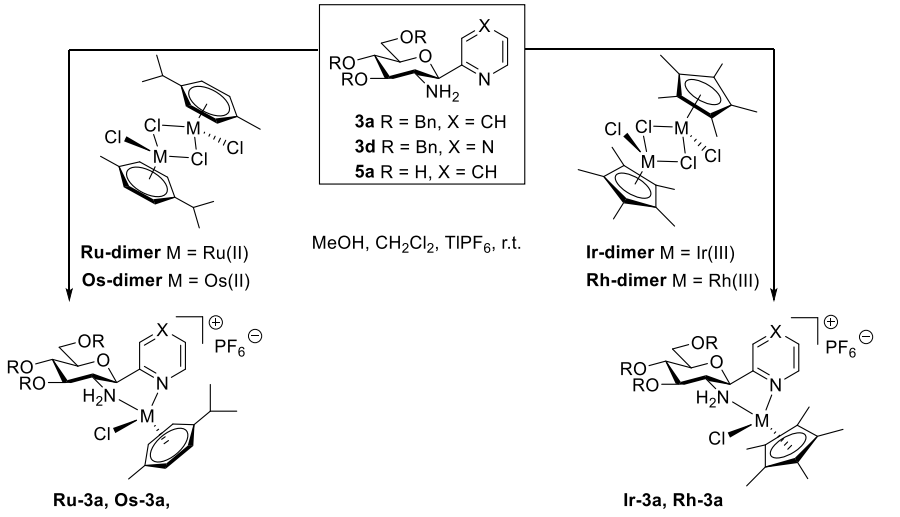

Entry	Ligand	R	X	M	Product	Yield (%)*
1	**3a**	Bn	CH	Ru(II)	**Ru-3a**	74
2				Os(II)	**Os-3a**	64
3				Ir(III)	**Ir-3a**	93
4				Rh(III)	**Rh-3a**	83

formázott: Betűtípus: 10 pt

formázott: Térköz Előtte: 12 pt, Utána: 6 pt, Sorköz: Többszörös 0,95 s.

formázott: Betűtípus: 10 pt, Félkövér

formázott: Betűtípus: 10 pt

formázott: Betűtípus: 10 pt

formázott: Betűtípus: 10 pt

formázott: Betűtípus: 10 pt

5	**3d**	Bn	N	Ru(II)	**Ru-3d**	33
6		Bn	N	Os(II)	**Os-3d**	47
7	**5a**	H	CH	Ru(II)	**Ru-5a**	43

*Each complex was isolated as single diastereoisomer.

The complexations of the *O*-perbenzoylated *C*-glucosaminyl azines **7a-e** with the dimeric chloro-bridged platinum-group metal complexes **Ru-dimer**, **Os-dimer**, **Ir-dimer** and **Rh-dimer** were also performed under the same conditions as described above to give the planned half-sandwich type complexes **Ru-7a–Ru-7e**, **Os-7a–Os-7e**, **Ir-7a–Ir-7e** and **Rh-7a–Rh-7e**, respectively, in good to excellent yields (Table 5).

Table 5. Synthesis of half-sandwich platinum-group metal complexes with the *O*-perbenzoylated *C*-glucosaminyl azines

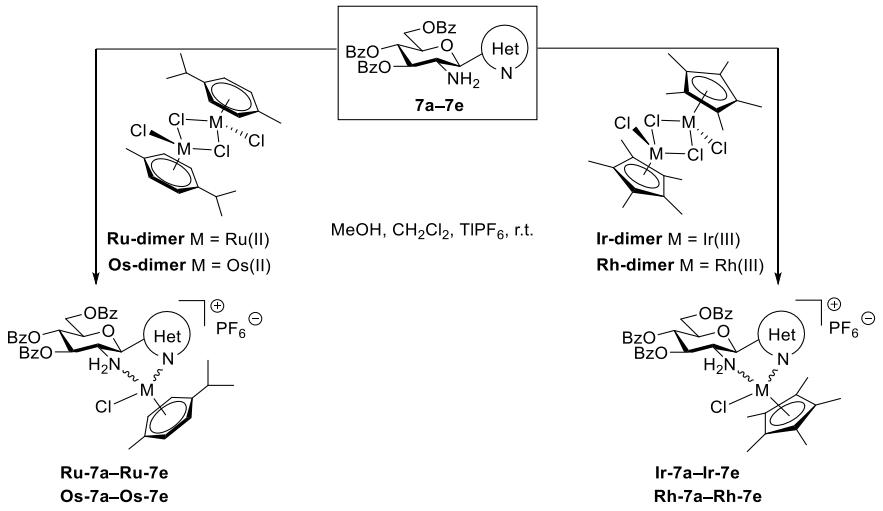

Entry	Ligand	Het	M	Product	Yield (%)	Number of isomers
1	**7a**		Ru(II)	**Ru-7a**	81	1
2			Os(II)	**Os-7a**	43	1
3			Ir(III)	**Ir-7a**	76	1
4			Rh(III)	**Rh-7a**	86	1
5	**7b**		Ru(II)	**Ru-7b**	88	2 (d.r. = 2 : 1)*
6			Os(II)	**Os-7b**	73	2 (d.r. = 5 : 4)*
7			Ir(III)	**Ir-7b**	69	2 (d.r. = 9 : 1)*
8			Rh(III)	**Rh-7b**	86	2 (d.r. = 5 : 1)*

formázott: Betűtípus: 10 pt
formázott: Betűtípus: 10 pt
formázott: Betűtípus: 10 pt
formázott: Betűtípus: 10 pt
formázott: Térköz Előtte: 12 pt
formázott: Betűtípus: 9 pt
formázott: Térköz Előtte: 12 pt, Utána: 6 pt, Sorköz: Többszörös 0,95 s.
formázott: Betűtípus: 10 pt, Félkövér
formázott: Betűtípus: 10 pt
formázott: Betűtípus: 10 pt
formázott: Betűtípus: 10 pt
formázott: Betűtípus: 10 pt
formázott: Betűtípus: 10 pt
formázott: Betűtípus: 10 pt
formázott: Betűtípus: 10 pt
formázott: Betűtípus: 10 pt
formázott: Betűtípus: 10 pt

9		Ru(II)	**Ru-7c**	99	1
10	**7c** 	Os(II)	**Os-7c**	98	1
11		Ir(III)	**Ir-7c**	99	1
12		Rh(III)	**Rh-7c**	99	1
13		Ru(II)	**Ru-7d**	91	1
14	**7d** 	Os(II)	**Os-7d**	91	1
15		Ir(III)	**Ir-7d**	99	1
16		Rh(III)	**Rh-7d**	96	1
17		Ru(II)	**Ru-7e**	82	1
18	**7e** 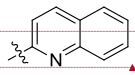	Os(II)	**Os-7e**	96	1
19		Ir(III)	**Ir-7e**	88	1
20		Rh(III)	**Rh-7e**	90	1

* Diastereomeric ratio (d.r.)

In most of the complexations presented in Tables 4 and 5 a single diastereoisomer of the complexes was formed. As an exception, the reactions of **7b** yielded complexes **Ru-7b**, **Os-7b**, **Ir-7b** and **Rh-7b** as mixtures of two diastereoisomers (Table 5, entries 5-8).

A single crystal of complex **Ru-3a** could be obtained by slow evaporation of a $CHCl_3$-MeOH solvent mixture. Search of the Cambridge Structural Database (Ver 5.43, Update November 2021) [56] resulted in 98 hits for similar Ru·Cl·η^6··NH_2··N coordination. However, our structure is rather unique as the Ru-Cl distance is the minimum one in this family of compounds by 2.374(5) Å, average 2.416(15) Å, while the angle of the arene ring and the N-N-Ru plane is rather high by 60.7°, average 57(2)°. Moreover, none of the hits contains pyranose ring attached to one coordinated amino nitrogen atom in any position. In a more detailed search of Ru·Cl·η^6··NH_2 coordination revealed more than 200 hits and the Ru-Cl distance is also in the very short region there and the average is also 2.42 Å. The ring puckering analysis [57] indicates that C1-O5 ring has a chair conformation (Θ = 19.6(18)°, Φ = 275(5)°), which is in good agreement with the NMR data related to the coupling constants of the proton resonances of the sugar skeleton.

The X-ray crystallography analysis of **Ru-3a** provided unequivocal evidence for the existence of the six-membered chelate ring and revealed the spatial arrangement of structural elements in the coordination sphere of the Ru(II) ion (Figure 2). Thus, following the general convention [58], the absolute configuration of the stereogenic Ru(II) was assigned to be *R*. The absolute configuration is confirmed by the analysis of the anomalous dispersion data as the Flack parameter [59] is 0.055 (Table S3).

formázott: Betűtípus: 10 pt
formázott: Betűtípus: 10 pt
formázott: Betűtípus: 10 pt
formázott: Betűtípus: 10 pt
formázott: Betűtípus: 10 pt
formázott: Betűtípus: 10 pt
formázott: Betűtípus: 10 pt
formázott: Betűtípus: 10 pt
formázott: Betűtípus: 10 pt
formázott: Betűtípus: 10 pt
formázott: Betűtípus: 10 pt
formázott: Betűtípus: 10 pt
formázott: Betűtípus: 10 pt
formázott: Betűtípus: 10 pt
formázott: Térköz Előtte: 12 pt
formázott: Betűtípus: 10 pt

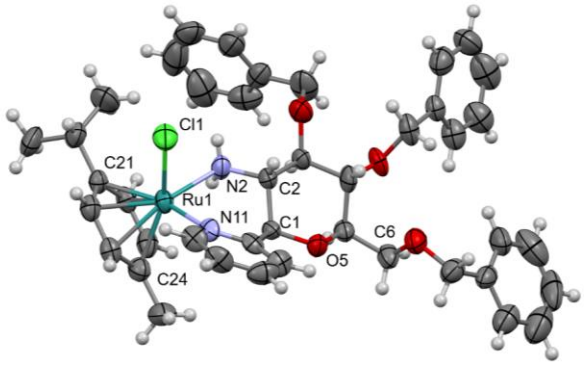

Figure 2. ORTEP view of **Ru-3a** at a 50% probability level, with a partial numbering scheme. The PF_6^- counter ion is omitted for clarity. Selected bond distance (Å) and bond length (°) data: Ru(1)-N(2) 2.153(13), Ru(1)-N(11) 2.091(14), Ru(1)-Cl(1) 2.374(5), Ru(1)-C_{Ar}(avg) 2.180(16), C(1)-C(2) 1.536(19), N(11)-Ru(1)-N(2) 87.3(5), N(11)-Ru(1)-Cl(1) 85.0(4), N(2)-Ru(1)-Cl(1) 82.4(4). For further details see the supporting information.

For structure elucidation of the prepared compounds ^{1}H and ^{13}C NMR measurements were also performed. Comparing the ^{1}H NMR spectroscopic data of the complexes to those of the starting **Ru/Os/Ir/Rh-dimers** and the *C*-glucosaminyl heterocyclic ligands, several significant changes in the chemical shifts could be noticed. Some of them are representatively highlighted in the superposition of the ^{1}H NMR spectra of **Ru-dimer**, **3a** and **Ru-3a** (Figure 3).

As a consequence of the complexation, the H-2' signal of the sugar skeleton of **3a** shifted upfield by 1.2 ppm (**B**), while the H-5′ resonance showed a 0.3 ppm downfield shift (**C**). Such changes in the chemical shifts of H-2′ and H-5′ are characteristic not only for **Ru-3a**, but also for all complexes isolated as a single isomer (**Os/Ir/Rh-3a**, **Ru/Os-3d**, **Ru-5a**, **Ru/Os/Ir/Rh-7a**, **Ru/Os/Ir/Rh-7c-d**) and the major component of the diastereomeric mixtures of **Ru/Os/Ir/Rh-7b** ($\Delta = \delta_{complex}-\delta_{ligand}$ = (-1.3) – (-0.5) ppm for H-2′ and (+0.3) – (+0.6) ppm for H-5′; Table S1). It is to be noted that the formation of the minor stereoisomers of **Ru/Os/Ir/Rh-7b** from ligand **7b** resulted in practically no (for **7b** → **Ir/Rh-7b**) or less significant changes (+0.15 ppm for **7b** → **Ru/Os-7b**) in the chemical shift of the H-5′ signal (Table S1).

The transformation of **Ru-dimer** into **Ru-3a** significantly affected the proton resonances of the *p*-cymene moiety. For example, the signal of C*H*$_3$ attached to the benzene ring displayed remarkable upfield shifts (0.46 ppm) as a result of the complexation (**E**). A similar trend in the appearance of this C*H*$_3$ signal was observed for all single isomeric Ru(II) and Os(II) complexes (**Os/Ir/Rh-3a**, **Ru/Os-3d**, **Ru-5a**, **Ru/Os/Ir/Rh-7a**, **Ru/Os/Ir/Rh-7c-d**) and for the main components of complexes **Ru-7b** and **Os-7b** ($\Delta = \delta_{complex}-\delta_{dimer}$ = (-0.3) – (-0.6) ppm for C_6H_4-C*H*$_3$, Table S1). In case of the minor isomers of **Ru-7b** and **Os-7b** the same signal indicated a slight downfield shift ($\Delta = \delta_{complex}-\delta_{dimer}$ = ~+0.1 ppm, Table S1) relative to that of the corresponding **Ru-dimer** and **Os-dimer**, respectively.

These data strongly suggest that in each complex obtained as a single isomer (**Os/Ir/Rh-3a**, **Ru/Os-3d**, **Ru-5a**, **Ru/Os/Ir/Rh-7a**, **Ru/Os/Ir/Rh-7c-d**) and in the major component of **Ru/Os/Ir/Rh-7a** the absolute configuration of the metal centre is identical to that of the reference complex **Ru-3a**.

For a more detailed collection of the comparative spectroscopic data pls. see Table S1 in the Supplementary Materials.

formázott: Kiemelt

formázott: Betűtípus: 10 pt

formázott: Betűtípus: 10 pt

formázott: Betűtípus: 10 pt

formázott: Betűtípus: 10 pt

formázott: Betűtípus: 10 pt

formázott: Betűtípus: 10 pt

formázott: Betűtípus: 10 pt

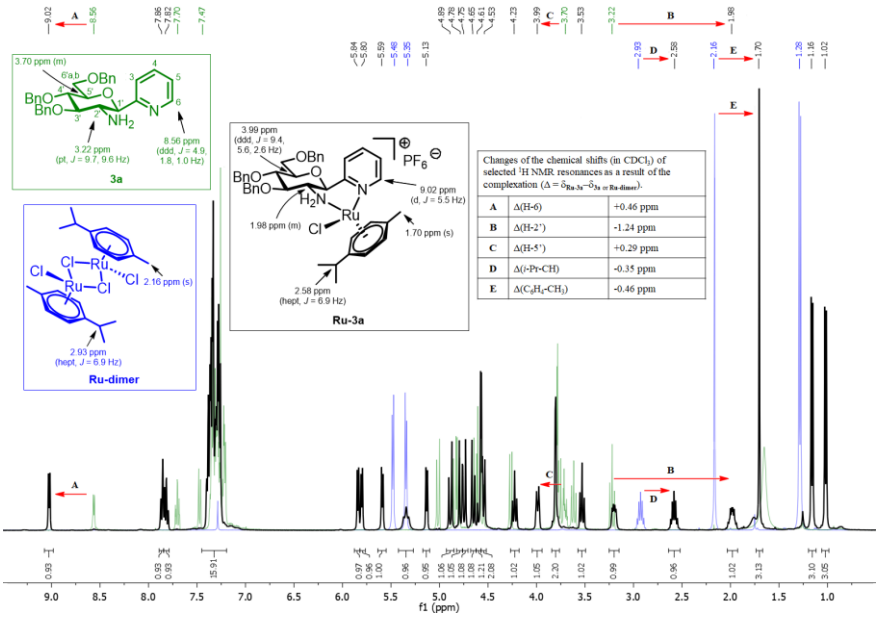

Figure 3. Superposition of the ^{1}H-NMR spectra of ligand **3a** (green) and complexes **Ru-dimer** (blue) and **Ru-3a** (black) in $CDCl_3$, and highlights of the changes of some characteristic resonances as a result of the complexation.

2.2. Cell biology

2.2.1. C-Glucosaminyl azines exert cytostatic activity

The complexes described above are intended for replacing registered platinum complexes. Platinum complexes constitute the core of the chemotherapy regimen used in ovarian cancer [8], therefore, we used a cellular model of ovarian cancer, A2780, and primary human dermal fibroblasts as models of non-transformed cells (controls). For the characterization of the complexes we used the MTT assay after 4 hours of treatment for the detection of early toxicity and the SRB assay 48 hours after treatment for the detection of cytostasis [60-62].

First, we assessed the complexes of ligands **7a-e**. The complexes of the pyridine- and pyridazine-containing ligands **7a** and **7b** had superior bioactivity over the complexes of ligands **7c**, **7d** and **7e**, having pyrimidine, pyrazine and quinoline aglycon part, respectively (Figures 4 and 5, Table 6). Complexes of **7a-e** induced early toxicity, as evidenced from the MTT assays. The complexes of the ligand **7a** were the most effective in inducing early toxicity with IC_{50} values ranging between 9-14 μM and the complexes reached over 90% inhibition (Figure 4, Table 6). Other complexes did not reach over 90% inhibition, although induced early toxicity (Figures 4 and 5, Table 6). In terms of long-term cytostatic activity, the complexes of **7a** and **7b** exerted complete inhibition of cell growth in SRB assays with IC_{50} values between 4-9 μM (Figure 4, Table 6). Complexes of ligands **7c-e** did not inhibit cell proliferation fully up to 100 μM (Figure 5, Table 6). The best IC_{50} values fell into the low micromolar range, **Ru-3a** and **Ir-3a** had IC_{50} values of 1.86 and 1.69 μM, respectively.

In general, the IC_{50} values of the Ru(II)-containing complexes were lower than those of the Os(II), Ir(III) and Rh(III) analogs constructed with the same ligand (e.g. **Ru-7a** vs.

formázott: Betűtípus: Dőlt

Ir-7a, **Os-7a** and **Rh-7a**; Table 6). In terms of effectiveness, the Ru-containing complexes were followed by the corresponding iridium complexes, then by the osmium and, finally, by the rhodium complexes (Figures 4 and 5, Table 6). Of note, the difference between Ru, Os, Ir and Rh complexes was not as pronounced as we observed in our prior studies with glycosyl azole type ligands [32,45,46]. Furthermore, the free ligands **7a**, **7c**, **7d** and **7e** effectively induced cytostasis (Figures 4 and 5, Table 6).

We further investigated the complexes of **7a** and **7b** on human primary dermal fibroblasts, as these complexes were efficient in inducing cytostasis. Testing the complexes on primary, non-transformed cells informs us on the selectivity of the complexes between transformed cancer cells, modelled by A2780 cells and primary, non-transformed cells, modelled by primary fibroblasts. The complexes of **7a** and **7b** induced early toxicity (10-70% maximal inhibition) and long-term cytostasis on primary dermal fibroblasts (25-60% maximal inhibition), however, with lower efficacy as compared to A2780 cells (Figure 4, Table 6).

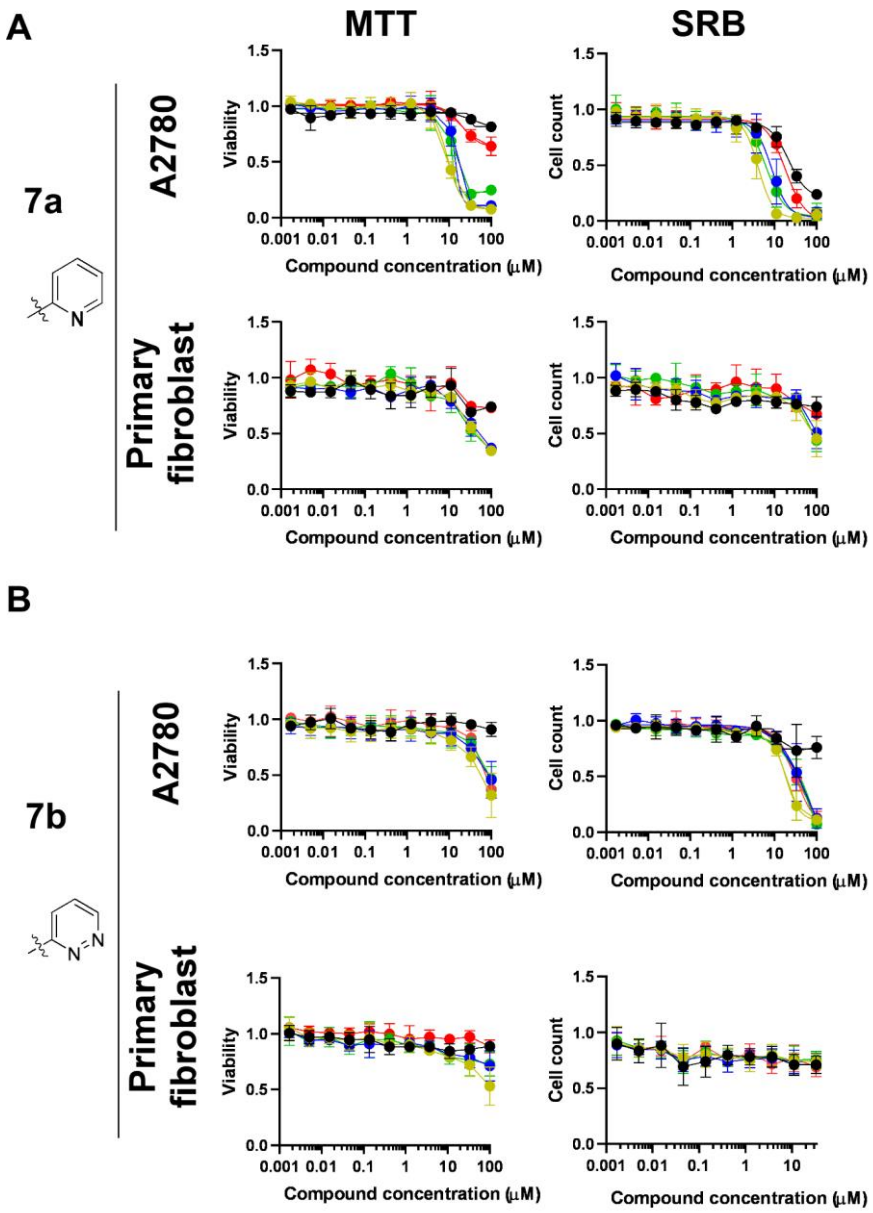

Figure 4. Assessment of the free ligands **7a,b** and their complexes (**Ru/Os/Ir/Rh-7a**, **Ru/Os/Ir/Rh-7b**) for cytotoxic and cytostatic activity. For MTT assays $3x10^3$ A2780 cells or $4x10^3$ primary fibroblasts were plated to 96 well plates. For SRB assays $1.5x10^3$ A2780 cells or $2x10^3$ primary fibroblasts were plated to 96 well plates. Cells were treated with the compounds in the concentrations indicated for either 4 hours for an MTT assay or for 48 hours for an SRB assay. Data is represented as average

formázott: Térköz Utána: 0 pt

± SD, from three biological replicates; individual assays were performed in duplicates. Values were normalized for vehicle treated cells, absorbance for vehicle treated cells equals to 1. Statistical significance was assessed using one-way ANOVA test comparing all values to the lowest concentration of a compound. Before the test normality was assessed using the Shapiro-Wilk test and the post-hoc test was chosen accordingly. For better visibility the p values and distributions are presented in an excel sheet at https://figshare.com/s/9ec2a005e6b9e5874c07. Nonlinear regression was performed on the datasets indicated in Table 6.

Color code: black – free ligand (**7a** or **7b**), khaki – ruthenium complex (**Ru-7a** or **Ru-7b**), blue – osmium complex (**Os-7a** or **Os-7b**), green - iridium complex (**Ir-7a** or **Ir-7b**), red – rhodium complex (**Rh-7a** or **Rh-7b**).

formázott: Betűszín: Fekete

formázott: MDPI_5.1_figure_caption, Sorkizárt, Behúzás: Első sor: 0 cm

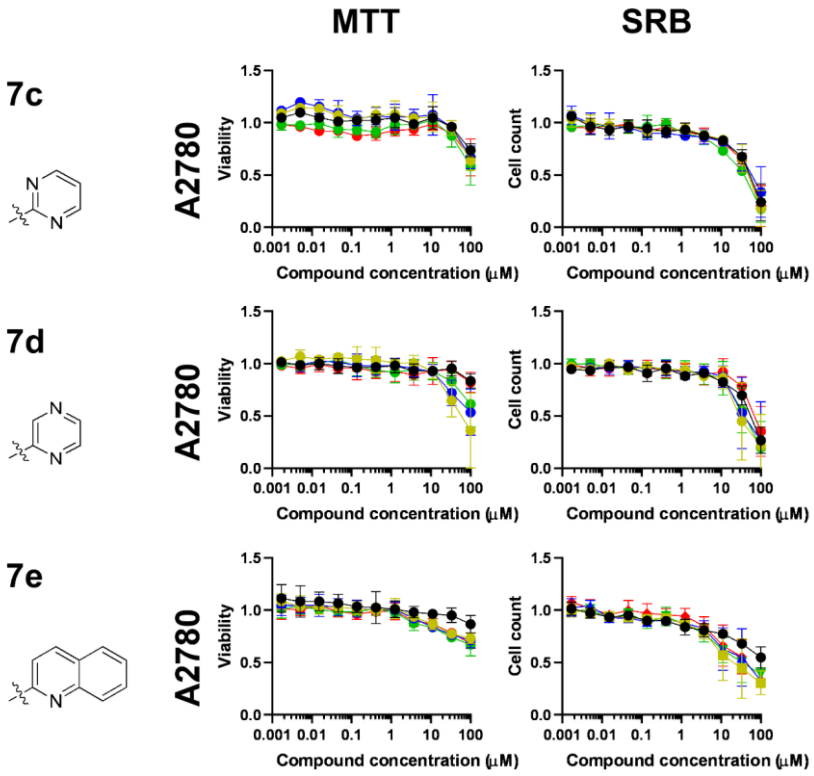

Figure 5. Assessment of the free ligands **7c-e** and their complexes (**Ru/Os/Ir/Rh-7c**, **Ru/Os/Ir/Rh-7d**, **Ru/Os/Ir/Rh-7e**) for cytotoxic and cytostatic activity. For MTT assays $3x10^3$ A2780 cells, for SRB assays $1.5x10^3$ A2780 cells were plated to 96 well plates. Cells were treated with the compounds in the concentrations indicated for either 4 hours for an MTT assay or for 48 hours for an SRB assay. Data is represented as average ± SD, from three biological replicates; individual assays were performed in duplicates. Values were normalized for vehicle treated cells, absorbance for vehicle treated cells equals to 1. Statistical significance was assessed using one-way ANOVA test comparing all values to the lowest concentration of a compound. Before the test normality was assessed using the Shapiro-Wilk test and the post-hoc test was chosen accordingly. For better visibility the p values and distributions are presented in an excel sheet at https://figshare.com/s/9ec2a005e6b9e5874c07. Nonlinear regression was performed on the datasets indicated in Table 6.

formázott: Térköz Utána: 0 pt

Color code: black – free ligand (**7c** or **7d** or **7e**), khaki – ruthenium complex (**Ru-7c** or **Ru-7d** or **Ru-7e**), blue – osmium complex (**Os-7c** or **Os-7d** or **Os-7e**), green - iridium complex (**Ir-7c** or **Ir-7d** or **Ir-7e**, red – rhodium complex (**Rh-7c** or **Rh-7d** or **Rh-7e**).

Table 6. Kinetic and LogD values of the complexes assessed in the present manuscript.

	A2780						Fibroblast						LogD
	MTT			SRB			MTT			SRB			
	Max inhibition	IC_{50}	Hill	Max inhibition	IC_{50}	Hill	Max inhibition	IC_{50}	Hill	Max inhibition	IC_{50}	Hill	
3a	70.22	ND	ND	>90	36.23	1.33	32.22	ND	ND	75	ND	ND	
Ru-3a	>90	8.02	1.68	>90	1.86	2.98	80.22	ND	ND	75	9.62	2.87	2.72
Os-3a	85.65	ND	ND	>90	2.13	2.12	69.36	ND	ND	75	15.08	3.09	1.78
Ir-3a	82.71	ND	ND	>90	1.69	1.41	80.22	ND	ND	75	14.14	2.12	3.18
Rh-3a	25.36	ND	ND	>90	9.81	1.11	37.82	ND	ND	75	ND	ND	1.64
3d	ND	ND	ND	13.07	ND	ND	18.39	ND	ND	13.15	ND	ND	
Ru-3d	>90	19.34	2.33	>90	3.77	2.31	80.31	ND	ND	64.44	ND	ND	2.06
Os-3d	86.83	32.34	1.98	>90	6.83	2.52	73.24	ND	ND	30.17	ND	ND	2.64
5a	ND	ND	ND	ND	ND	ND							
Ru-5a	ND	ND	ND	ND	ND	ND							-1.91
7a	18.61	ND	ND	76.24	ND	ND	27.02	ND	ND	26.00	ND	ND	
Ru-7a	>90	9.15	2.54	>90	4.11	2.46	65.18	ND	ND	56.31	ND	ND	1.15
Os-7a	>90	13.77	ND	>90	8.58	2.26	65.18	ND	ND	49.00	ND	ND	2.15
Ir-7a	>90	11.64	ND	>90	6.20	1.96	65.18	ND	ND	56.31	ND	ND	1.08
Rh-7a	35.97	ND	ND	>90	18.25	1.88	27.02	ND	ND	32.56	ND	ND	1.20
7b	9.12	ND	ND	18.38	ND	ND	11.39	ND	ND	ND	ND	ND	
Ru-7b	68.22	ND	ND	>90	17.78	2.57	47.04	ND	ND	ND	ND	ND	1.39
Os-7b	53.39	ND	ND	>90	56.37	1.26	27.22	ND	ND	ND	ND	ND	1.32
Ir-7b	53.39	ND	ND	77.58	ND	ND	27.22	ND	ND	ND	ND	ND	1.17
Rh-7b	62.85	ND	ND	>90	31.98	1.97	11.39	ND	ND	ND	ND	ND	1.41
7c	26.30	ND	ND	79.53	ND	ND							
Ru-7c	33.13	ND	ND	66.28	ND	ND							1.31
Os-7c	33.13	ND	ND	66.28	ND	ND							1.59
Ir-7c	41.53	ND	ND	82.52	ND	ND							1.40
Rh-7c	33.13	ND	ND	79.53	ND	ND							1.13
7d	18.08	ND	ND	73.37	ND	ND							
Ru-7d	64.04	ND	ND	80.44	ND	ND							1.26
Os-7d	46.72	ND	ND	80.44	ND	ND							1.42
Ir-7d	38.71	ND	ND	80.44	ND	ND							1.30
Rh-7d	18.08	ND	ND	64.76	ND	ND							1.04
7e	13.56	ND	ND	45.20	ND	ND							
Ru-7e	27.04	ND	ND	67.50	ND	ND							2.22
Os-7e	27.04	ND	ND	67.50	ND	ND							2.21

formázott: Betűszín: Fekete
formázott: MDPI_5.1_figure_caption, Sorkizárt
formázott: Betűtípus: Félkövér
táblázatot formázott
formázott: Betűtípus: Félkövér
formázott: Betűtípus: Félkövér

Ir-7e	27.04	ND	ND	61.28	ND	ND		1.39
Rh-7e	31.89	ND	ND	67.32	ND	ND		1.66

ND – not detectable.

2.2.2. *O*-Benzyl protective groups improve, while the *O*-deprotection abrogates the cytostatic activity of the complexes

Next we assessed the complexes constructed by the *O*-perbenzylated *C*-glucosaminyl heterocycles **3**. Due to the synthetic difficulties of this series of the ligands, only the complexes of the pyridine and pyrazine derivatives **3a** and **3d**, respectively, were available for further analysis.

The complexes of **3a**, such as **Ru-3a**, **Os-3a** and **Ir-3a** exerted considerable early toxicity as judged from the MTT assays, wherein **Ru-3a** induced early toxicity with an IC_{50} value of 8.02 μM on A2780 cells (Figure 6, Table 6). Interestingly, **Rh-3a**-induced early toxicity was negligible on A2780 cells (Figure 6, Table 6). With regard to cytostasis, complexes **Ru-3a**, **Os-3a**, **Ir-3a** and **Rh-3a** were cytostatic on A2780 cells with micromolar IC_{50} values, whereas ligand **3a** had an IC_{50} value above 30 μM (Figure 6A, Table 6). The complexes were active on primary human dermal fibroblasts. **Ru-3a**, **Os-3a** and **Ir-3a** exerted ≥70% inhibition in MTT assays, while **3a** and **Rh-3a** exerted ~30-40% inhibition (Figure 6A, Table 6). In SRB assays **3a** and all corresponding complexes (**Ru-3a**, **Os-3a**, **Ir-3a**, **Rh-3a**) exerted full inhibition and for **Ru-3a**, **Os-3a** and **Ir-3a** it was possible to determine the IC_{50} values that fell into the range of ~10-15 μM (Figure 6A, Table 6).

Next, we assessed **3d** and its ruthenium and osmium complexes **Ru-3d** and **Os-3d**. **Ru-3d** and **Os-3d** exerted early toxicity on A2780 and human primary dermal fibroblast cells in low micromolar concentrations (Figure 6B, Table 6). The ligand **3d** had no activity in MTT assays on A2780 and human primary dermal fibroblast cells in low micromolar concentrations (Figure 6, Table 6). Similar to their activity in the MTT assay, **Ru-3d** and **Os-3d** exerted early toxicity in SRB assays on A2780 cells in low micromolar concentrations, while **3d** did not exert considerable activity in SRB assays on A2780 cells (Figure 6B, Table 6). In contrast to their activity in MTT assays, **3d** and **Os-3d** did not inhibit cell proliferation in SRB assays and **Ru-3d** had only minor effect on primary human dermal fibroblasts (Figure 6B, Table 6).

formázott: Betűtípus: Dőlt

formázott: Betűtípus: Dőlt

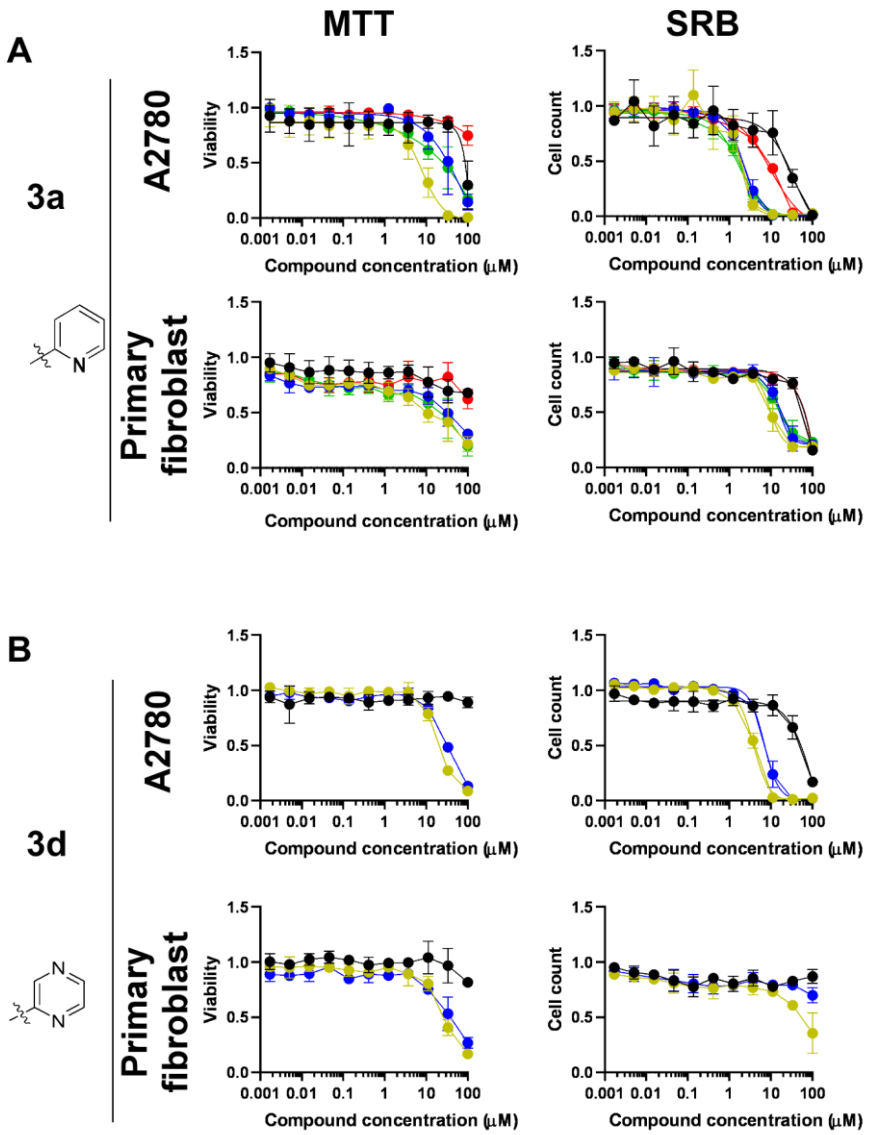

Figure 6. Assessment of the free ligands **3a** and **3d** and their complexes (**Ru/Os/Ir/Rh-3a** and **Ru/Os-3d**) for cytotoxic and cytostatic activity. For MTT assays $3x10^3$ A2780 cells or $4x10^3$ primary fibroblasts were plated to 96 well plates. For SRB assays $1.5x10^3$ A2780 cells or $2x10^3$ primary fibroblasts were plated to 96 well plates. Cells were treated with the compounds in the concentrations indicated for either 4 hours for an MTT assay or for 48 hours for an SRB assay. Data is represented as average ± SD, from three biological replicates; individual assays were performed in duplicates. Values were normalized for vehicle treated cells, absorbance for vehicle treated cells equals to 1. Statistical significance was assessed using one-way ANOVA test comparing all values to the lowest concentration

formázott: Térköz Utána: 0 pt

of a compound. Before the test normality was assessed using the Shapiro-Wilk test and the post-hoc test was chosen accordingly. For better visibility the p values and the distributions are presented in an excel sheet at https://figshare.com/s/9ec2a005e6b9e5874c07_Nonlinear regression was performed on the datasets indicated in Table 6.

Color code: black – free ligand (**3a** or **3d**), khaki – ruthenium complex (**Ru-3a** or **Ru-3d**), blue – osmium complex (**Os-3a** or **Os-3d**), green - iridium complex (**Ir-3a**), red – rhodium complex (**Rh-3a**).

We assessed the effect of the *O*-deprotection of the carbohydrate moiety that was shown to abrogate the bioactivity similar to our previous observations [45-47]. We used the free ligand, **5a**, that is the deprotected equivalent of **3a** and **7a**, and its ruthenium complex **Ru-5a**. Ligand **5a** and its ruthenium complex **Ru-5a** did not exhibit any biological activity on A2780 cells either in MTT or SRB assays (Figure 7, Table 6).

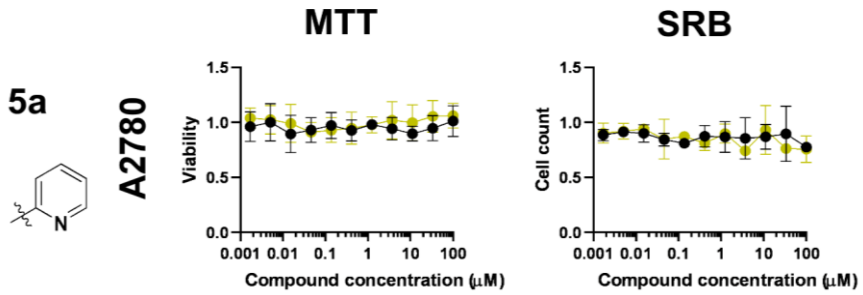

Figure 7. Assessment of the free ligand **5a** and its ruthenium complex **Ru-5a** for cytotoxic and cytostatic activity. For MTT assays $3x10^3$ A2780 cells, for SRB assays $1.5x10^3$ A2780 cells were plated to 96 well plates. Cells were treated with the compounds in the concentrations indicated for either 4 hours for an MTT assay or for 48 hours for an SRB assay. Data is represented as average ± SD, from three biological replicates; individual assays were performed in duplicates. Values were normalized for vehicle treated cells, absorbance for vehicle treated cells equals to 1. Statistical significance was assessed using one-way ANOVA test comparing all values to the lowest concentration of a compound. Before the test normality was assessed using the Shapiro-Wilk test and the post-hoc test was chosen accordingly. For better visibility the p values and the distributions are presented in an excel sheet at https://figshare.com/s/9ec2a005e6b9e5874c07_Nonlinear regression was performed on the datasets indicated in Table 6. Color code: black – free ligand (**5a**), khaki – ruthenium complex (**Ru-5a**).

2.2.3. Compound **Ru-3a** is cytostatic on multiple carcinoma cell lines

Carbohydrate-containing ruthenium, osmium and iridium complexes with similar structure were shown to be effective on a large set of carcinoma, sarcoma and lymphoma cell lines [32,45-47,63-67], therefore, we assessed the bioactivity of these complexes on other carcinoma cell lines. For this assay we chose **Ru-3a** and the corresponding ligand **3a**, as this complex had one of the best IC_{50} value on A2780 cells (IC_{50}= 1.86 μM) and had the best-performing protective group attached.

In agreement with the prior art, **Ru-3a** inhibited the proliferation of another ovarian cancer cell line (ID8), a glioblastoma cell line (U251), a breast carcinoma cell line (MCF7), and a pancreatic adenocarcinoma cell line (Capan2) with IC_{50} values in the low micromolar range falling between 2-4 μM (Figure 8, Table 7). Importantly, **3a** was also active on these cell lines with IC_{50} values falling between 10-30 μM (Figure 8, Table 7).

formázott: Betűszín: Fekete

formázott: MDPI_5.1_figure_caption, Sorkizárt

formázott: Térköz Előtte: 12 pt, Utána: 6 pt

formázott: Betűtípus: Félkövér

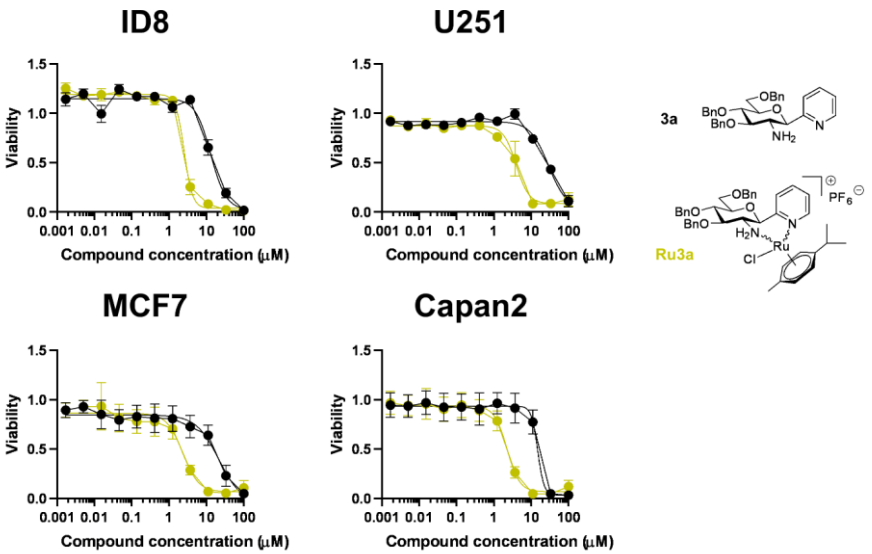

Figure 8. Assessment of the free ligand **3a** and complex **Ru-3a** for cytostatic activity in multiple carcinomas. 2x10³ ID8 or 3x10³ U251 or 3x10³ MCF7 or 3x10³ Capan2 cells were plated to 96 well plates. Cells were treated with the compounds in the concentrations indicated for 48 hours then an SRB assay was performed. Data is represented as average ± SD, from three biological replicates; individual assays were performed in duplicates. Values were normalized for vehicle treated cells, absorbance for vehicle treated cells equals to 1. Statistical significance was assessed using one-way ANOVA test comparing all values to the lowest concentration of a compound. Before the test normality was assessed using the Shapiro-Wilk test and the post-hoc test was chosen accordingly. For better visibility the p values and the distributions are presented in an excel sheet at https://figshare.com/s/9ec2a005e6b9e5874c07. Nonlinear regression was performed on the datasets indicated in Table 7.

Table 7. The kinetic values of compounds **3a** and **Ru-3a** on cancer cell lines other than A2780.

	ID8			U251			MCF7			Capan2		
	SRB			SRB			SRB			SRB		
	Max inhibition	IC_{50}	Hill	Max inhibition	IC_{50}	Hill	Max inhibition	IC_{50}	Hill	Max inhibition	IC_{50}	Hill
3a	>90	13.05	2.10	>90	29.36	1.77	>90	21.33	1.43	>90	14.99	ND
Ru-3a	>90	2.54	3.87	>90	3.97	2.55	>90	2.30	2.02	>90	2.25	2.55

ND- Not detectable.

2.2.4. The complexes with cytostatic properties are bacteriostatic on Gram positive multi-resistant Staphylococcus aureus and Enterococcus isolates

Prior investigations by us [31,32] and others [30-39,68-75] showed that complexes of the platinum-group metals (platinum, palladium, ruthenium, osmium, iridium and rhodium) can exert bacteriostatic activity. Furthermore, we showed that those compounds were bacteriostatic that were also cytostatic in neoplasia models [31,32,45,46]. Therefore, we assessed **Ru/Os/Ir/Rh-3a**, **Ru/Os-3d**, **Ru/Os/Ir/Rh-7a** and **Ru/Os/Ir/Rh-7b** complexes and the corresponding free ligands. Free ligands and rhodium complexes did not exert bacteriostatic activity on any of the strains and isolates investigated. In contrast to that, the remaining ruthenium, osmium and iridium complexes (**Ru/Os/Ir-3a**, **Ru/Os-3d**,

formázott: Nincs aláhúzás

formázott: Betűtípus: Félkövér

formázott: Betűtípus: Félkövér

táblázatot formázott

formázott: Betűtípus: Félkövér

Ru/Os/Ir-7a and **Ru/Os/Ir-7b**) had bacteriostatic activity on the reference strain of *Enterococcus faecalis* and *Staphylococcus aureus*, VRE, and MRSA with the exception of **Os-3d** on the reference strain of *Enterococcus faecalis* and **Ir-7b** on the reference strain of *Staphylococcus aureus* (Figure 9, Table 8). Ruthenium and osmium complexes were characterized by the lowest MIC values, followed by iridium complexes. The ruthenium complexes of **3a** and **7a** had the lowest MIC values on the reference strain and clinical isolates of *Staphylococcus aureus* and *Enterococcus faecalis* highlighting the superior performance of pyridine-containing complexes in terms of their bacteriostatic activity similar to their higher performance as cytostatic agents.

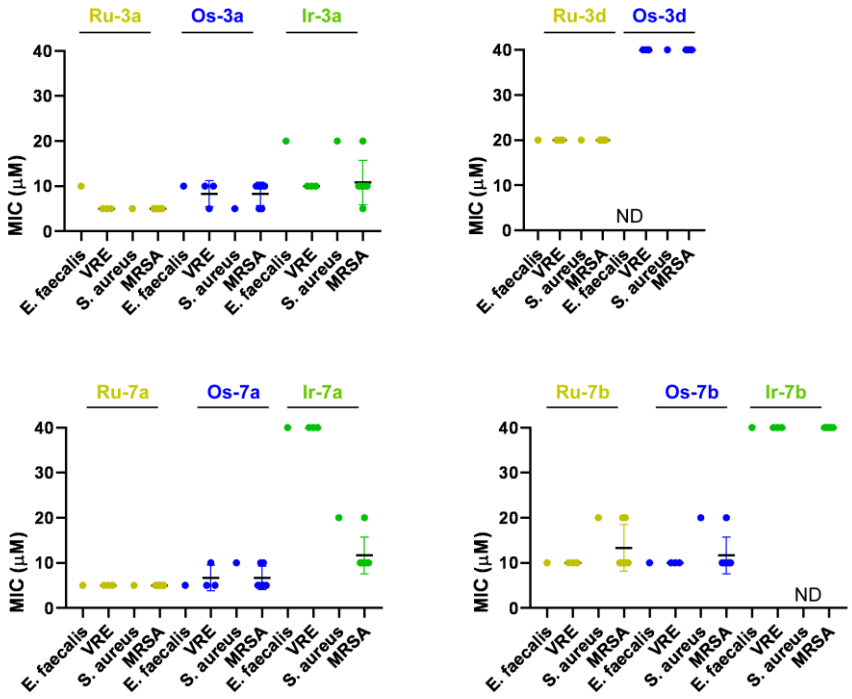

Figure 9. Complexes of the *C*-glucosaminyl heterocycles **3a**, **3d**, **7a** and **7b** exert bacteriostatic activity against reference strains and clinical VRE and MRSA isolates. The MIC values of the complexes were determined against the reference strains of *S. aureus* (ATCC29213) and *E. faecalis* (ATCC29212) and against clinical VRE and MRSA isolates by microdilution assays (repeated at least twice in duplicates) as described in Materials and Methods. Abbreviations: MRSA – methicillin-resistant *Staphylococcus aureus*, VRE – vancomycin-resistant *Enterococcus*, ND – not detected, MIC>40 μM, Veh - vehicle. Color code: khaki – ruthenium complex, blue – osmium complex, green - iridium complex.

Table 8. The MIC values [μM] of a subset of ligands and complexes.

	3a	**Ru-3a**	**Os-3a**	**Ir-3a**	**Rh-3a**	**3d**	**Ru-3d**	**Os-3d**
E. faecalis ATCC 29212	>40	10	10	20	>40	>40	20	>40
27085 VRE	>40	5	10	10	>40	>40	20	40

25 051 VRE	>40	5	5	10	>40	>40	20	40		
25 498 VRE	>40	5	10	10	>40	>40	20	40		
S. aureus ATCC 29213	>40	5	5	20	>40	>40	20	40		
24 408 MRSA	>40	5	10	10	>40	>40	20	40		
24 328 MRSA	>40	5	5	10	>40	>40	20	40		
20 426 MRSA	>40	5	5	10	>40	>40	20	40		
24 268 MRSA	>40	5	10	5	>40	>40	20	40		
24 035 MRSA	>40	5	10	20	>40	>40	20	40		
24 272 MRSA	>40	5	10	10	>40	>40	20	40		

	7a	**Ru-7a**	**Os-7a**	**Ir-7a**	**Rh-7a**	**7b**	**Ru-7b**	**Os-7b**	**Ir-7b**	**Rh-7b**
E. faecalis ATCC 29212	>40	5	5	40	>40	>40	10	10	40	>40
27085 VRE	>40	5	10	40	>40	>40	10	10	40	>40
25 051 VRE	>40	5	5	40	>40	>40	10	10	40	>40
25 498 VRE	>40	5	5	40	>40	>40	10	10	40	>40
S. aureus ATCC 29213	>40	5	10	20	>40	>40	20	20	>40	>40
24 408 MRSA	>40	5	5	10	>40	>40	10	10	40	>40
24 328 MRSA	>40	5	5	20	>40	>40	20	20	40	>40
20 426 MRSA	>40	5	10	10	>40	>40	10	10	40	>40
24 268 MRSA	>40	5	5	10	>40	>40	10	10	40	>40
24 035 MRSA	>40	5	10	10	>40	>40	10	10	40	>40
24 272 MRSA	>40	5	5	10	>40	>40	20	10	40	>40

	7e	**Ru-7e**	**Os-7e**	**Ir-7e**	**Rh-7e**	**Vehicle control**
E. faecalis ATCC 29212	>40	>40	>40	>40	>40	>40
27085 VRE	>40	>40	>40	>40	>40	>40
25 051 VRE	>40	>40	>40	>40	>40	>40
25 498 VRE	>40	>40	>40	>40	>40	>40
S. aureus ATCC 29213	>40	>40	>40	>40	>40	>40
24 408 MRSA	>40	>40	>40	>40	>40	>40
24 328 MRSA	>40	>40	>40	>40	>40	>40
20 426 MRSA	>40	>40	>40	>40	>40	>40
24 268 MRSA	>40	>40	>40	>40	>40	>40
24 035 MRSA	>40	>40	>40	>40	>40	>40
24 272 MRSA	>40	>40	>40	>40	>40	>40

3. Discussion

In this study we described a set of half-sandwich type platinum-group metal complexes with *O*-protected *C*-glucosaminyl heterocyclic N,N-bidentate ligands. Among these, the pyridine-containing complexes had the lowest IC_{50} and MIC values followed by the pyrazine- and pyridazine-containing ones, while their pyrimidine and quinoline counterparts proved to be inactive (Figure 10A).

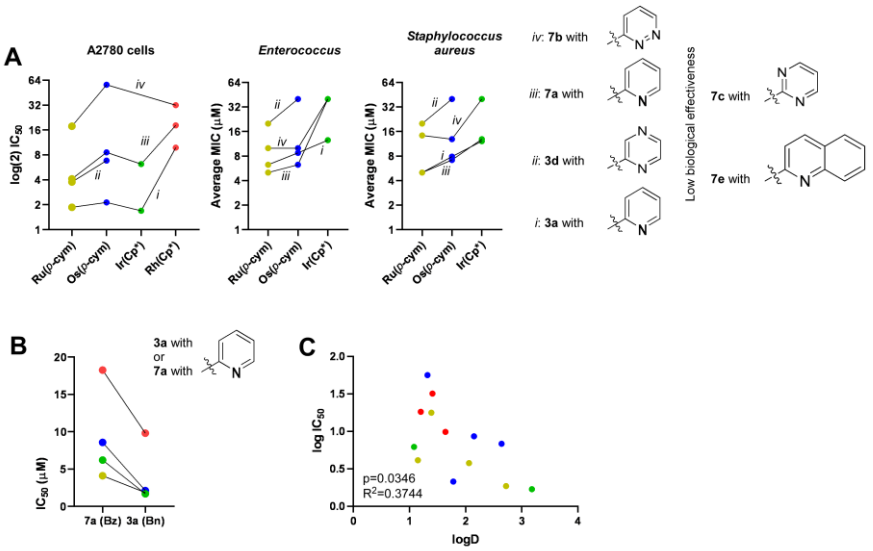

Figure 10. Correlations between the structural features and the bioactivity of the complexes with *O*-protected *C*-glucosaminyl azines in neoplastic cell models. **(A)** The effect of the heterocyclic aglycon and the arene/arenyl-metal ion parts on the IC_{50} and average MIC values. The MIC values of the reference strain and the multiresistant clinical isolates were averaged. **(B)** The effect of the *O*-protective groups (benzoyl (Bz) vs. benzyl (Bn) groups) on the IC_{50} values of the **7a** and **3a** complexes. **(C)** Correlation between the apolar character (LogD values) and the bioactivity (IC_{50} values) of the complexes. The logD values and the corresponding logIC_{50} values were plotted and Pearson's correlation was calculated. Color code: khaki – ruthenium complex, blue – osmium complex, green - iridium complex, red – rhodium complex.

Another important structural feature of the complexes is the metal ion with the polyhapto arene/arenyl moiety. In this study, ruthenium complexes with *p*-cymene and iridium complexes with Cp* had the best performance on ovarian cancer cells followed by osmium complexes with *p*-cymene and then by rhodium complexes with Cp* (Figure 10A). This is at odds with our previous observations, where we identified osmium complexes with the most potent cytostatic properties, followed by ruthenium complexes and with a large gap, iridium complexes [32,45,46]. Furthermore, rhodium complexes were inactive on cellular models of carcinomas [32,45,46] in contrast to our current results. However, the effect of the metal ions with polyhapto arene/arenyl moiety proved to be similar in terms of the bacteriostatic effects as in our previous experience [31,32], where the ruthenium complexes had the lowest MIC values followed by osmium and then by iridium complexes (Figure 10A). Rhodium complexes did not exert bacteriostatic properties.

Prior studies have shown that the chemical composition of the protective groups of the sugar part plays a key role in the bioactivity of monosaccharide-containing half-sandwich complexes to show the *O*-benzoyl protected ones to be the most effective [32,47]. In this study, besides the *O*-benzoyl protected *C*-glucosaminyl pyridine **7a** and pyrazine **7d** complexes also their *O*-benzylated counterparts (complexes **3a** and **3d**, respectively) were tested. Importantly, the benzyl-protected compounds had better IC_{50} values in cancer cell models than the benzoyl-protected ones (Figure 10B). Interestingly, the bacteriostatic properties of the benzyl/benzoyl-protected compounds did not differ drastically (Figures 9 and 10A).

Based on the positive LogD values (Table 6), all complexes with *O*-benzyl and *O*-benzoyl protective groups are lipophilic. The lipophilic character of the complexes is a prerequisite of their biological activity [31,32,45-47,63]. In fact, among the currently identified complexes the readout of apolarity (logD) and the IC_{50} value correlate (Figure 10C). Apparently, increasing the apolar character of the complexes improves the biological effectiveness that is further strengthened by the fact that when the protective groups are absent, as in **Ru-5a** or in comparable members of the previously reported series [45,46], the bioactivity of the complexes is lost.

An unexpected observation was that the *C*-glucosaminyl heterocycles used as ligands, namely pyridines **3a** and **7a**, pyridazine **7b**, pyrimidine **7c**, pyrazines **3d** and **7d** and quinoline **7e** showed cytostatic effects which proved comparable to that of the respective complexes on A2780 cells. In addition, **3a** induced cytostasis in primary human fibroblasts, as well. To the best of our knowledge, such effects have not yet been described with *C*-glycosyl heterocycles, therefore, this finding deserves further investigations.

The cytostatic compounds identified in this study were active on other carcinoma cell lines (glioblastoma, breast cancer and pancreatic adenocarcinoma) as well as on another cellular model of ovarian cancer, ID8. Prior art assessing complexes of similar structure underscores the widespread activity of such complexes evidencing bioactivity in carcinoma cell lines as MDA-MD-231 and MCF7 breast cancer cells [45,47], colon cancer [63-66], lung cancer [63], cervical carcinoma (HeLa) cells [67], U251 glioblastoma cells [45], or Capan2 pancreatic adenocarcinoma cells [45,46], L428 Hodgkin lymphoma [32,46] and Saos osteosarcoma [32,46] apart from ovarian cancer. Of note, these cell models include a diverse set of carcinomas, hematological malignancies and a sarcoma.

Importantly, the complexes with cytostatic property were less active on primary, non-transformed human dermal fibroblasts. While this property of the complexes suggests a selectivity for transformed neoplastic cells over non-transformed cells, the anticipated therapeutic window is relatively narrow as compared to previous observations on complexes with ligands of similar [32,45,46] or different structure [76,77].

4. Conclusion

Hereby, a set of half-sandwich complexes of platinum-group metal ions (Ru(II), Os(II), Ir(III), Rh(III)) with six-membered *C*-glucosaminyl heterocycles were synthesized. These complexes exerted cytostatic properties against a set of carcinomas with low micromolar IC_{50} values, while they were less active against primary, untransformed human dermal fibroblasts anticipating a narrow therapeutic window for the compounds. Furthermore, the same complexes had bacteriostatic properties against multiresistant Gram-positive *Staphylococcus aureus* and *Enterococcus* clinical isolates in the low micromolar range. The molecular mechanism of the cytostatic and bacteriostatic properties of the compounds is currently under investigation in our laboratory and the results will be published in due course.

formázott: Kiemelt

5. Materials and methods

5.1. Synthesis

5.1.1. General methods

Optical rotations were determined by a P-2000 polarimeter (Jasco, Easton, MD, USA) at room temperature. The ^{1}H and ^{13}C NMR spectra were recorded with DRX360 (360/90 MHz for $^{1}H/^{13}C$), DRX400 (400/100 MHz for $^{1}H/^{13}C$) or Bruker Asvance II 500 (500 for ^{1}H) spectrometers (Bruker, Karlsruhe, Germany). Chemical shifts are referenced to Me_4Si (^{1}H-NMR) or to the residual solvent signals (^{13}C-NMR). The more detailed proton-signal assignments for compounds **3a**, **5a**, **7a**, **Ru-3a**, **Ru-5a**, **Ru-7a**, **Ir-7a**, **Ru-7b** and **Os-7b** are based on COSY correlations. The HRMS data were determined in positive ionisation mode using a Bruker maXis II (ESI-HRMS) spectrometer. DC Kieselgel 60 F_{254} plates (Sigma-Aldrich, Saint Louis, MO, USA) were used for TLC analysis, and the spots on the plates were visualised under UV light and developed by gentle heating. For column chromatographic purification Kieselgel 60 silica gel (Molar Chemicals, Halásztelek, Hungary, particle size 0.063–0.2 mm) was applied. Among anhydrous solvents, EtOH (VWR Chemicals), pyridine (VWR Chemicals) and 1,2-dichloroethane (Sigma-Aldrich) were purchased from the indicated suppliers, while the others were obtained by applying standard distillation methods. Anhydrous CH_2Cl_2 was prepared by distillation from P_4O_{10} and stored over 4 Å molecular sieves, while THF was distilled first from sodium benzophenone ketyl, and also re-distillied from $LiAlH_4$ directly before using. 2-Bromopyridine (TCI), 3-bromopyridazine (Fluorochem), 2-iodopyrimidine (Fluorochem), 2-iodopyrazine (Fluorochem), 2-bromoquinoline (TCI), dichloro(η^6-*p*-cymene)ruthenium(II) dimer (**Ru-dimer**, Strem Chemicals, Newburyport, MA, USA), dichloro(pentamethylcyclopentadienyl)iridium(III) dimer (**Ir-dimer**, Acros Organics), dichloro(pentamethylcyclopentadienyl)rhodium(III) dimer (**Rh-dimer**, Alfa Aesar) and $TlPF_6$ (Strem Chemicals) are commercially available chemicals. Dichloro(η^6-*p*-cymene)osmium(II) dimer [78] (**Os-dimer**) and 3,4,6-tri-*O*-benzyl-2-nitro-D-glucal [49,79] (**1**) were synthesized by the adaptation of literature procedures.

5.1.2. General procedure I for the preparation of *C*-(2′-deoxy-2′-nitro-3′,4′,6′-tri-*O*-benzyl-β-D-glucopyranosyl)heterocycles **2a-e**

Method A: In a dry round bottom flask the corresponding halogenated heterocycle (4.33 mmol, 2 eq.) was dissolved in freshly distilled dry THF (10 mL). The stirred solution was cooled down to –78 °C and a 2.5 M solution of *n*-butyllithium in *n*-hexane (1.74 mL, 4.33 mmol, 2 eq.) was added dropwise over 10 minutes and the stirring was continued for 5 minutes to form the corresponding lithiated heretocycle. In another dry round bottom flask, containing activated 4 Å molecular sieves (powder, 0.2 g), 2-nitroglucal **1** (1.0 g, 2.17 mmol) was dissolved in freshly distilled dry THF (10 mL). After cooling this solution to –78 °C the solution of the freshly prepared lithiated heretocyle was added. The reaction mixture was then stirred at –78 °C and the transformation was monitored by TLC (1 : 4 EtOAc-hexane). When the TLC indicated complete disappearance of **1** the reaction was quenched by the addition of sat. aq. NH_4Cl solution (100 mL) and allowed to warm to rt. The molecular sieves were then filtered off. The filtrate was diluted with EtOAc (200 mL) and extracted with water (100 mL) and brine (100 mL). The separated organic phase was dried over $MgSO_4$, filtered, and the solvents were removed under reduced pressure. The residue was purified by column chromatography.

Method B: In a dry round bottom flask 2-nitroglucal **1** (1.0 g, 2.17 mmol) and the corresponding halogenated heterocycle (2.60 mmol, 1.2 eq.) were dissolved in freshly distilled dry THF (20 mL). The stirred solution was cooled down to –78 °C and a 2.5 M solution of *n*-butyllithium in *n*-hexane (1.04 mL, 2.60 mmol, 1.2 eq.) was added over 15 minutes by means of a syringe pump. The stirring was continued for an additional 15 minutes at the same temperature. After completion of the reaction (~ 0.5 hour) judged by TLC (1 : 2 EtOAc-hexane) the reaction was quenched by the addition of sat. aq. NH_4Cl solution (100

formázott: Betűtípus: 8 pt

formázott: Betűtípus: Dőlt

formázott: Betűtípus: Dőlt

formázott: Betűtípus: 8 pt

formázott: Betűtípus: Félkövér

mL) and allowed to warm to rt. The mixture was diluted with EtOAc (200 mL) and extracted with water (100 mL) and brine (100 mL). The separated organic phase was dried over $MgSO_4$, filtered, and the solvents were removed under reduced pressure. The residue was purified by column chromatography.

5.1.3. General procedure II for cleavage of the *O*-benzyl protecting groups of the *O*-perbenzylated *C*-glycopyranosyl heterocycle **2a-e**, **3a** to get compounds **4a-e** and **5a**

A solution of the corresponding *O*-perbenzylated *C*-glycopyranosyl heterocycle **2a-e** or **3a** in dry CH_2Cl_2 (10 mL / 100 mg substrate) was cooled down to –78 °C and a 1 M solution of BCl_3 in CH_2Cl_2 (5 eq.) was added dropwise over 5 minutes. The reaction mixture was stirred at this temperature until the TLC (9 : 1 $CHCl_3$-MeOH) showed the completion of the reaction. After that, the reaction was quenched by the addition of MeOH (10 mL) and allowed to warm to rt. The solvents were then removed under reduced pressure and the residue was purified by column chromatography.

5.1.4. General procedure III for the preparation of C-(2′-deoxy-2′-nitro-3′,4′,6′-tri-*O*-benzoyl-β-D-glucopyranosyl)heterocycles **6a-d**

To a solution of the corresponding *C*-(2′-deoxy-2′-nitro-3′,4′,6′-tri-*O*-benzyl-β-D-glucopyranosyl)heterocycle **2a-d** in dry dichloroethane (10 mL / 100 mg substrate) $Zn(OTf)_2$ (2 eq.) and benzoyl chloride (6 eq.) were added and the reaction mixture was stirred at rt. After completion of the reaction judged by TLC (1 : 2 EtOAc-hexane) the reaction mixture was diluted with CH_2Cl_2 (40 mL) and extracted with sat. aq. $NaHCO_3$ solution (50 mL) then with water (50 mL). The separated organic phase was dried over $MgSO_4$, filtered and the solvents were removed under diminished pressure. The crude product was purified by column chromatography.

5.1.5. General procedure IV for the preparation of *C*-(2′-(tert-butoxycarbonyl)amino-2′-deoxy-β-D-glucopyranosyl)heterocycles **8c-e**

To a solution of the corresponding *C*-(2′-amino-2′-deoxy-β-D-glucopyranosyl)azine **5c-e** in a 1 : 1 mixture of water and 1,4-dioxane (5 mL / 50 mg substrate) Boc_2O (2 eq.) was added, and the reaction mixture was stirred at rt. When the TLC (9 : 1 $CHCl_3$-MeOH) showed complete transformation of the staring material (~ 1 day) the solvents were removed under reduced pressure. The residue was purified by column chromatography.

5.1.6. General procedure V for the preparation of *C*-(2′-(tert-butoxycarbonyl)amino-2′-deoxy-3′,4′,6′-tri-*O*-benzoyl-β-D-glucopyranosyl)heterocycles **9c-e**

To a solution of the corresponding *C*-(2′-(*tert*-butoxycarbonyl)amino-2′-deoxy-β-D-glucopyranosyl)azine **8c-e** in dry pyridine (5 mL / 100 mg substrate) benzoyl chloride (1.2 eq. / OH group) was added at rt. The reaction mixture was stirred at 60 °C for 1 hour. Since the TLC (1 : 1 EtOAc-hexane) showed incompleteness of the reaction, an additional portion of benzoyl chloride (1.2 eq. / OH group) was added to the reaction mixture and the heating was continued for 1 hour. The reaction mixture was allowed to cool to rt and further stirred overnight. The reaction mixture was then diluted with CH_2Cl_2 (50 mL) and extracted with sat. aq. solution of $NaHCO_3$ (25 mL), then with water (25 mL). The separated organic phase was dried over $MgSO_4$, filtered and the solvents were removed under diminished pressure. The residue was purified by column chromatography.

5.1.7. General procedure VI for the preparation of C-(2′-amino-2′-deoxy-3′,4′,6′-tri-*O*-benzoyl-β-D-glucopyranosyl)heterocycles **7b-e** from compounds **9b-e**

The corresponding *C*-(2′-(*tert*-butoxycarbonyl)amino-2′-deoxy-3′,4′,6′-tri-*O*-benzoyl-β-D-glucopyranosyl)azine **9b-e** was dissolved in dry CH_2Cl_2 (5 mL / 100 mg substrate) and trifluoroacetic acid (2 eq.) was added. The reaction mixture was stirred at rt until the TLC

formázott: Betűtípus: Dőlt
formázott: Betűtípus: Dőlt
formázott: Betűtípus: Dőlt
formázott: Betűtípus: Félkövér
formázott: Betűtípus: Félkövér
formázott: Betűtípus: Félkövér
formázott: Betűtípus: Félkövér
formázott: Betűtípus: Dőlt
formázott: Betűtípus: 8 pt
formázott: Betűtípus: Félkövér
formázott: Betűtípus: 8 pt
formázott: Betűtípus: Dőlt
formázott: Betűtípus: 8 pt
formázott: Betűtípus: Félkövér
formázott: Betűtípus: 8 pt
formázott: Betűtípus: Dőlt
formázott: Betűtípus: Dőlt
formázott: Betűtípus: 8 pt
formázott: Betűtípus: Félkövér
formázott: Betűtípus: 8 pt
formázott: Betűtípus: Dőlt
formázott: Betűtípus: 8 pt
formázott: Betűtípus: Félkövér
formázott: Betűtípus: Félkövér
formázott: Betűtípus: 8 pt

(95 : 5 $CHCl_3$-MeOH or 1 : 1 EtOAc-hexane) indicated complete disappearance of the starting material (~ 1 hour). The solvent and the excess of CF_3COOH were then removed under reduced pressure. The residue was dissolved in CH_2Cl_2 (50 mL) and extracted with sat. aq. solution of $NaHCO_3$ (25 mL) and with water (25 mL). The separated organic phase was dried over $MgSO_4$, filtered and the solvent was removed under diminished pressure. The residue was purified by column chromatography.

5.1.8. General procedure VII for the synthesis of half-sandwich platinum-group metal complexes

To a solution of the corresponding complex dimer (**Ru-dimer**, **Os-dimer** ([(η^6-*p*-cym)$M^{II}Cl_2$]$_2$ (M = Ru, Os) or **Ir-dimer**, **Rh-dimer** [(η^5-Cp*)$M^{III}Cl_2$]$_2$ (M = Ir, Rh)) in CH_2Cl_2 (1 mL / 10 mg dimer) the appropriate *C*-glucosaminyl azine (1.9-2.3 eq.) and $TlPF_6$ (2 eq.) were added. To this stirred reaction mixture MeOH (1 mL / 10 mg dimer) was added at rt in order to accelerate the precipitation of the TlCl. The heterogeneous mixture was then continued to stir at rt and the completion of the reaction was monitored by TLC (95 : 5 $CHCl_3$-MeOH). When the TLC showed total disappearance of the starting dimer (~ 1 hour) the precipitated TlCl was filtered off. The resulting solution was evaporated under diminished pressure. The remaining crude complex was purified by column chromatography and / or crystallization.

5.1.9. Synthesis and characterisation of the new Compounds

2-(2′-Deoxy-2′-nitro-3′,4′,6′-tri-*O*-benzyl-β-D-glucopyranosyl)pyridine (**2a**)

Prepared from 2-nitroglucal **1** (0.50 g, 1.08 mmol) and 2-bromopyridine (0.21 mL, 0.34 g, 2.16 mmol, 2 eq.) according to general procedure I, method A. Reaction time: 1 h. Purified by column chromatography (1 : 4 EtOAc-hexane) to give 0.30 g (52%) colourless syrup. R_f = 0.18 (1 : 4 EtOAc-hexane). ^{1}H NMR (400 MHz, $CDCl_3$) δ (ppm): 8.57 (1H, ddd, *J* = 4.9, 1.8, 0.9 Hz, H-6), 7.71 (1H, td, *J* = 7.8, 1.8 Hz, H-4), 7.42 (1H, ddd, *J* = 7.8, 1.8, 0.9 Hz, H-3), 7.32-7.18 (16H, m, Ar, H-5), 4.95 (1H, pt, *J* = 9.8, 9.2 Hz, H-2′ or H-3′ or H-4′), 4.91 (1H, d, *J* = 9.7 Hz, H-1′), 4.83, 4.61 (2 × 1H, 2 d, *J* = 10.6 Hz in both, PhCH_2), 4.81, 4.63 (2 × 1H, 2 d, *J* = 10.9 Hz in both, PhCH_2), 4.59, 4.53 (2 × 1H, 2 d, *J* = 12.1 Hz in both, PhCH_2), 4.46 (1H, pt, *J* = 8.6, 8.5 Hz, H-2′ or H-3′ or H-4′), 3.82 (1H, pt, *J* = 9.5, 8.5 Hz, H-2′ or H-3′ or H-4′), 3.81-3.77 (3H, m, H-5′, H-6′a,b); ^{13}C NMR (90 MHz, $CDCl_3$) δ (ppm): 154.9 (C-2), 149.6 (C-6), 137.1 (C-4), 138.0, 137.7, 137.4, 128.6-127.9 (Ar), 124.1, 122.4 (C-3, C-5), 90.0, 83.2, 80.0, 77.9 (2) (C-1′ – C-5′), 75.7, 75.4, 73.7 (3 × PhCH_2), 68.7 (C-6′). ^{1}H and ^{13}C NMR data correspond to the reported ones [50].

3-(2′-Deoxy-2′-nitro-3′,4′,6′-tri-*O*-benzyl-β-D-glucopyranosyl)pyridazine (**2b**)

Prepared from 2-nitroglucal **1** (2.00 g, 4.33 mmol) and 3-bromopyridazine (0.83 g, 5.20 mmol, 1.2 eq.) according to general procedure I, method B. Purification of the crude product by column chromatography (1 : 1 EtOAc-hexane) gave a syrup. It was triturated in a solvent mixture of EtOAc (0.5 mL) and diisopropyl ether (15 mL). The precipitated product was filtered off, washed with diisopropyl ether to give 0.30 g (13%) white amorphous solid. R_f = 0.21 (1 : 1 EtOAc-hexane). ^{1}H NMR (400 MHz, $CDCl_3$) δ (ppm): 9.19 (1H, dd, *J* = 5.0, 1.7 Hz, H-6), 7.65 (1H, dd, *J* = 8.5, 1.7 Hz, H-4), 7.53 (1H, dd, *J* = 8.5, 5.0 Hz, H-5), 7.35-7.19 (15H, m, Ar), 5.19 (1H, d, *J* = 10.0 Hz, H-1′), 4.95 (1H, pt, *J* = 10.0, 9.9 Hz, H-2′ or H-3′ or H-4′), 4.85, 4.63 (2 × 1H, 2 d, *J* = 10.8 Hz in both, PhCH_2), 4.83, 4.65 (2 × 1H, 2 d, *J* = 10.4 Hz in both, PhCH_2), 4.58, 4.52 (2 × 1H, 2 d, *J* = 12.2 Hz in both, PhCH_2), 4.51 (1H, pt, *J* = 9.8, 8.3 Hz, H-2′ or H-3′ or H-4′), 3.86 (1H, pt, *J* = 9.4, 8.3 Hz, H-2′ or H-3′ or H-4′), 3.83-3.74 (3H, m, H-5′, H-6′a,b); ^{13}C NMR (100 MHz, $CDCl_3$) δ (ppm): 158.0 (C-3), 151.9 (C-6), 137.9, 137.6, 137.2, 128.7-127.9 (Ar), 127.3, 125.5 (C-4, C-5), 89.5, 82.8, 80.0, 78.5, 77.6 (C-1′ – C-5′), 75.9, 75.4, 73.7 (3 × PhCH_2), 68.5 (C-6′). ESI-HRMS positive mode (m/z): calcd for $C_{31}H_{32}N_3O_6^+$ $[M+H]^+$ 542.2286; $C_{31}H_{31}N_3O_6Na^+$ $[M+Na]^+$ 564.2105; $C_{62}H_{62}N_6O_{12}Na^+$ $[2M+Na]^+$ 1105.4318. Found: $[M+H]^+$ 542.2291; $[M+Na]^+$ 564.2106; $[2M+Na]^+$ 1105.4318.

formázott: Térköz Utána: 6 pt

formázott: Betűtípus: 8 pt

formázott: Betűtípus: Félkövér

formázott: Betűtípus: 8 pt

formázott: Betűtípus: Félkövér

2-(2′-Deoxy-2′-nitro-3′,4′,6′-tri-*O*-benzyl-β-D-glucopyranosyl)pyrimidine (**2c**)

Prepared from 2-nitroglucal **1** (1.00 g, 2.17 mmol) and 2-iodopyrimidine (0.54 g, 2.60 mmol, 1.2 eq.) according to general procedure I, method B. Purified by column chromatography (1 : 2 EtOAc-hexane) to give 0.83 g (71%) white amorphous solid. R_f = 0.29 (1 : 2 EtOAc-hexane). ^{1}H NMR (360 MHz, $CDCl_3$) δ (ppm): 8.77 (2H, d, *J* = 4.9 Hz, H-4, H-6), 7.35-7.15 (16H, m, Ar, H-5), 5.24 (1H, pt, *J* = 10.1, 10.0 Hz, H-2′ or H-3′ or H-4′), 5.07 (1H, d, *J* = 10.0 Hz, H-1′), 4.82, 4.63 (2 × 1H, 2 d, *J* = 10.6 Hz in both, PhCH_2), 4.82, 4.58 (2 × 1H, 2 d, *J* = 10.6 Hz in both, PhCH_2), 4.58,4.49 (2 × 1H, 2 d, *J* = 12.2 Hz in both, PhCH_2), 4.46 (1H, pt, *J* = 9.9, 9.5 Hz, H-2′ or H-3′ or H-4′), 3.86 (1H, pt, *J* = 9.9, 8.5 Hz, H-2′ or H-3′ or H-4′), 3.84-3.74 (3H, m, H-5′, H-6′a,b); ^{13}C NMR (100 MHz, $CDCl_3$) δ (ppm): 163.6 (C-2), 157.8 (C-4, C-6), 137.8, 137.6, 137.3, 128.7-127.9 (Ar), 121.3 (C-5), 88.4, 83.0, 80.6, 80.2, 77.7 (C-1′ – C-5′), 75.7, 75.3, 73.6 (3 × PhCH_2), 68.4 (C-6′). ESI-HRMS positive mode (m/z): calcd for $C_{31}H_{32}N_3O_6^+$ $[M+H]^+$ 542.2286; $C_{31}H_{31}N_3O_6Na^+$ $[M+Na]^+$ 562.2105. Found: $[M+H]^+$ 542.2288; $[M+Na]^+$ 562.2105.

2-(2′-Deoxy-2′-nitro-3′,4′,6′-tri-*O*-benzyl-β-D-glucopyranosyl)pyrazine (**2d**)

Prepared from 2-nitroglucal **1** (1.00 g, 2.17 mmol) and 2-iodopyrazine (0.54 g, 2.60 mmol, 1.2 eq.) according to general procedure I, methode B. Purified by column chromatography (1 : 3 EtOAc-hexane) to give 0.74 g (63%) white amorphous solid. R_f = 0.54 (1 : 2 EtOAc-hexane). ^{1}H NMR (400 MHz, $CDCl_3$) δ (ppm): 8.75 (1H, d, *J* = 1.4 Hz, H-3), 8.58 (1H, d, *J* = 2.5 Hz, H-6), 8.52 (1H, dd, *J* = 2.5, 1.4 Hz, H-5), 7.35-7.19 (15H, m, Ar) 5.00 (1H, d, *J* = 9.9 Hz, H-1′), 4.94 (1H, pt, *J* = 9.9, 9.7 Hz, H-2′ or H-3′ or H-4′), 4.84, 4.62 (2 × 1H, 2 d, *J* = 10.8 Hz in both, PhCH_2), 4.82, 4.63 (2 × 1H, 2 d, *J* = 10.6 Hz in both, PhCH_2), 4.59, 4.53 (2 × 1H, 2 d, *J* = 12.1 Hz in both, PhCH_2), 4.45 (1H, pt, *J* = 8.7, 8.7 Hz, H-2′ or H-3′ or H-4′), 3.83 (1H, pt, *J* = 9.4, 8.7 Hz, H-2′ or H-3′ or H-4′), 3.82-3.76 (3H, m, H-5′, H-6′a,b); ^{13}C NMR (100 MHz, $CDCl_3$) δ (ppm): 150.7 (C-2), 145.3, 144.2, 143.9 (C-3, C-5, C-6), 137.8, 137.6, 137.2, 128.7-127.9 (Ar), 89.2, 83.0, 80.1, 77.8, 77.6 (C-1′ – C-5′), 75.9, 75.4, 73.7 (3 × PhCH_2), 68.5 (C-6′). ESI-HRMS positive mode (m/z): calcd for $C_{31}H_{31}N_3O_6Na^+$ $[M+Na]^+$ 564.2105. Found: 564.2107.

2-(2′-Deoxy-2′-nitro-3′,4′,6′-tri-*O*-benzyl-β-D-glucopyranosyl)quinoline (**2e**)

Prepared from 2-nitroglucal **1** (2.00 g, 4.33 mmol) and 2-bromoquinoline (1.83 g, 8.80 mmol, 2 eq.) according to general procedure I, method A. Reaction time: 2 h. Purified by column chromatography (1 : 9 EtOAc-hexane) to give 1.53 g (60%) colourless syrup. R_f = 0.35 (1 : 4 EtOAc-hexane). ^{1}H NMR (400 MHz, $CDCl_3$) δ (ppm): 8.18 (1H, d, *J* = 8.5 Hz, H-3 or H-4), 8.04 (1H, dd, *J* = 8.5, 1.0 Hz, H-5 or H-8), 7.79 (1H, dd, *J* = 8.2, 1.4 Hz, H-5 or H-8), 7.69 (1H, ddd, *J* = 8.5, 7.0, 1.4 Hz, H-6 or H-7), 7.57 (1H, d, *J* = 8.5 Hz, H-3 or H-4), 7.53 (1H, ddd, *J* = 8.2, 7.0, 1.0 Hz, H-6 or H-7), 7.35-7.20 (15H, m, Ar), 5.13 (1H, d, *J* = 9.7 Hz, H-1′), 5.10 (1H, pt, *J* = 9.8, 8.0 Hz, H-2′ or H-3′ or H-4′), 4.86, 4.65 (2 × 1H, 2 d, *J* = 10.9 Hz in both, PhCH_2), 4.84, 4.64 (2 × 1H, 2 d, *J* = 10.6 Hz in both, PhCH_2), 4.61, 4.53 (2 × 1H, 2 d, *J* = 12.2 Hz in both, PhCH_2), 4.50 (1H, pt, *J* = 8.5, 8.4 Hz, H-2′ or H-3′ or H-4′), 4.88 (1H, pt, *J* = 9.5, 8.4 Hz, H-2′ or H-3′ or H-4′), 3.86-3.80 (3H, m, H-5′, H-6′a,b); ^{13}C NMR (100 MHz, $CDCl_3$) δ (ppm): 155.0, 147.3 (C-2, C-8a), 138.0, 137.7, 137.3, 137.4, 130.0, 129.9, 128.7-127.8, 127.6, 127.2, 119.4 (Ar, C-3 – C-8, C-4a), 89.3, 83.3, 80.1, 80.0, 77.8 (C-1′ – C-5′), 75.8, 75.4, 73.7 (3 × PhCH_2), 68.6 (C-6′). ESI-HRMS positive mode (m/z): calcd for $C_{36}H_{34}N_2O_6Na^+$ $[M+Na]^+$ 613.2309. Found: 613.2309.

2-(2′-Amino-2′-deoxy-3′,4′,6′-tri-*O*-benzyl-β-D-glucopyranosyl)pyridine (**3a**)

Compound **2a** (0.19 g, 0.35 mmol) and Zn powder (0.69 g, 10.55 mmol, 30 eq.) were suspended in a solvent mixture of THF (10 mL) and water (5 mL). This suspension was cooled down in an ice bath and *cc*HCl solution was added (0.7 mL, 8.14 mmol, 23 eq.). The reaction mixture was stirred at rt until the TLC (1 : 1 EtOAc-hexane) showed total consumption of the starting material (1 h). The reaction was quenched by the addition of sat.

formázott: Betűtípus: 8 pt
formázott: Betűtípus: Félkövér
formázott: Betűtípus: 8 pt
formázott: Betűtípus: Félkövér
formázott: Betűtípus: 8 pt
formázott: Betűtípus: Félkövér
formázott: Betűtípus: 8 pt
formázott: Betűtípus: Félkövér

aq. $NaHCO_3$ solution (50 mL). The insoluble inorganic salts and the rest of the Zn were filtered off and the remaining solution was extracted with CH_2Cl_2 (2 × 50 mL). The combined organic phase was extracted with water (50 mL) and then with brine (50 mL), dried over $MgSO_4$ and filtered. The solvent was removed under reduced pressure. The residue was purified by column chromatography (95 : 5 $CHCl_3$-MeOH) to give 114 mg (64%) pale yellow amorphous solid. R_f = 0.34 (95 : 5 $CHCl_3$-MeOH); $[\alpha]_D$ = +30 (c 0.5, $CHCl_3$). ^1H NMR (400 MHz, $CDCl_3$) δ (ppm): 8.56 (1H, ddd, *J* = 4.9, 1.8, 1.0 Hz, H-6), 7.70 (1H, td, *J* = 7.7, 1.8 Hz, H-4), 7.47 (1H, ddd, *J* = 7.7, 1.8, 1.0 Hz, H-3), 7.37-7.20 (16H, m, Ar, H-5), 5.01, 4.80 (2 × 1H, 2 d, *J* = 11.4 Hz in both, PhCH_2), 4.84, 4.63 (2 × 1H, 2 d, *J* = 10.7 Hz in both, PhCH_2), 4.62, 4.56 (2 × 1H, 2 d, *J* = 12.2 Hz in both, PhCH_2), 4.27 (1H, d, *J* = 9.6 Hz, H-1′), 3.80-3.75 (3H, m, H-4′, H-6′a,b), 3.70 (1H, m, H-5′), 3.62 (1H, pt, *J* = 9.2, 9.2 Hz, H-3′), 3.22 (1H, pt, *J* = 9.7, 9.6 Hz, H-2′), 1.65 (2H, s, NH_2); ^{13}C NMR (90 MHz, $CDCl_3$) δ (ppm): 158.7 (C-2), 148.9 (C-6), 138.7, 138.3, 138.2 (Ar), 137.0 (C-4), 128.6-127.7 (Ar), 123.2, 122.7 (C-3, C-5), 87.0, 83.0, 79.8, 78.9 (C-1′, C-3′ – C-5′), 75.5, 75.0, 73.6 (3 × PhCH_2), 69.4 (C-6′), 57.2 (C-2′). ESI-HRMS positive mode (m/z): calcd for $C_{32}H_{34}N_2O_4Na^+$ $[M+Na]^+$ 533.2410. Found: 533.2411.

2-(2′-Amino-2′-deoxy-3′,4′,6′-tri-*O*-benzyl-β-D-glucopyranosyl)pyrazine (**3d**)

Compound **2d** (0.10 g, 0.19 mmol) and Zn powder (0.12 g, 1.84 mmol, 10 eq.) were suspended in a solvent mixture of THF (5 mL) and water (2.5 mL). To this stirred mixture a 1 M aq. solution of HCl (1.5 mL, 1.50 mmol, 8 eq.) was added dropwise over 1 hour by using a syringe pump. The stirring of the reaction mixture was continued at rt until the TLC (95 : 5 $CHCl_3$-MeOH) indicated the completion of the reaction (2 h). The reaction was quenched by the addition of sat. aq. $NaHCO_3$ solution (25 mL). The insoluble inorganic salts and the rest of the Zn were filtered off and the remaining solution was extracted with CH_2Cl_2 (2 × 25 mL). The combined organic phase was extracted with water (25 mL), dried over $MgSO_4$ and filtered. The solvent was removed under reduced pressure. Column chromatographic purification of the residue (95 : 5 $CHCl_3$-MeOH) gave 6.8 mg (7%) pale yellow syrup. R_f = 0.23 (95 : 5 $CHCl_3$-MeOH); $[\alpha]_D$ = +19 (c 0.1, $CHCl_3$). ^1H NMR (400 MHz, $CDCl_3$) δ (ppm): 8.77 (1H, d, *J* = 1.0 Hz, H-3), 8.53-8.52 (2H, m, H-5, H-6), 7.35-7.21 (15H, m, Ar), 5.03, 4.78 (2 × 1H, 2 d, *J* = 11.4 Hz in both, PhCH_2), 4.85, 4.64 (2 × 1H, 2 d, *J* = 10.8 Hz in both, PhCH_2), 4.61, 4.56 (2 × 1H, 2 d, *J* = 12.3 Hz in both, PhCH_2), 4.31 (1H, d, *J* = 9.7 Hz, H-1′), 3.81-3.73 (2H, m, H-6′a,b), 3.77 (1H, pt, *J* = 9.8, 8.5 Hz, H-3′ or H-4′), 3.71 (1H, m, H-5′), 3.60 (1H, pt, *J* = 9.2, 9.0 Hz, H-3′ or H-4′), 3.25 (1H, pt, *J* = 9.7, 9.6 Hz, H-2′), 1.68 (2H, br s, NH_2); ^{13}C NMR (100 MHz, $CDCl_3$) δ (ppm): 154.2 (C-2), 145.0, 144.3, 143.5 (C-3, C-5, C-6), 138.6, 138.2, 138.1, 129.9-127.8 (Ar), 86.9, 81.4, 80.0, 78.8 (C-1′, C-3′ – C-5′), 75.6, 75.0, 73.7 (3 × PhCH_2), 69.2 (C-6′), 56.8 (C-2′). ESI-HRMS positive mode (m/z): calcd for $C_{31}H_{34}N_3O_4^+$ $[M+H]^+$ 512.2544; $C_{31}H_{33}N_3O_4Na^+$ $[M+Na]^+$ 534.2363. Found: $[M+H]^+$ 512.2541, $[M+Na]^+$ 534.2359.

2-(2′-Deoxy-2′-nitro-β-D-glucopyranosyl)pyridine (**4a**)

Prepared from compound **2a** (0.30 g, 0.55 mmol) according to general procedure II. Reaction time: 0.5 h. Purification by column chromatography (9 : 1 $CHCl_3$-MeOH) yielded 128 mg (85%) white amorphous solid. R_f = 0.53 (4 : 1 $CHCl_3$-MeOH). ^1H NMR (400 MHz, CD_3OD) δ (ppm): 8.53 (1H, d, *J* = 4.4 Hz, H-6), 7.85 (1H, t, *J* = 7.7 Hz, H-4), 7.54 (1H, d, *J* = 7.8 Hz, H-3), 7.40 (1H, m, H-5), 4.95 (1H, d, *J* = 9.7 Hz, H-1′), 4.74 (1H, pt, *J* = 10.1, 9.9 Hz, H-2′ or H-3′ or H-4′), 4.21 (1H, pt, *J* = 9.1, 8.7 Hz, H-2′ or H-3′ or H-4′), 3.91 (1H, m, H-6′a), 3.76 (1H, dd, *J* = 12.0, 4.2 Hz, H-6′b), 3.62-3.55 (2H, m, H-2′ or H-3′ or H-4′, H-5′); ^{13}C NMR (90 MHz, CD_3OD) δ (ppm): 156.4 (C-2), 150.2 (C-6), 138.9 (C-4), 125.6, 124.4 (C-3, C-5), 92.7, 82.7, 80.7, 76.4, 71.1 (C-1′ – C-5′), 62.4 (C-6′). ESI-HRMS positive mode (m/z): calcd for $C_{11}H_{14}N_2O_6Na^+$ $[M+Na]^+$ 293.0744. Found: 293.0744.

3-(2′-Deoxy-2′-nitro-β-D-glucopyranosyl)pyridazine (**4b**)

Prepared from compound **2b** (0.30 g, 0.55 mmol) according to general procedure II. Reaction time: 0.5 h. Purification by column chromatography (9 : 1 $CHCl_3$-MeOH) yielded

formázott: Betűtípus: 8 pt
formázott: Betűtípus: Félkövér
formázott: Betűtípus: 8 pt
formázott: Betűtípus: Félkövér
formázott: Betűtípus: 8 pt
formázott: Betűtípus: Félkövér

133 mg (89%) white amorphous solid. R_f = 0.39 (4 : 1 $CHCl_3$-MeOH). ^1H NMR (360 MHz, CD_3OD) δ (ppm): 9.17 (1H, d, *J* = 4.9 Hz, H-6), 8.00 (1H, dd, *J* = 8.6, 1.4 Hz, H-4), 7.79 (1H, dd, *J* = 8.6, 4.9 Hz, H-5), 5.22 (1H, d, *J* = 10.0 Hz, H-1′), 4.82 (1H, pt, *J* = 10.1, 10.0 Hz, H-2′ or H-3′ or H-4′), 4.25 (1H, pt, *J* = 10.0, 9.9 Hz, H-2′ or H-3′ or H-4′), 3.94 (1H, dd, *J* = 12.2, 2.1 Hz, H-6′a), 3.77 (1H, dd, *J* = 12.2, 5.3 Hz, H-6′b), 3.67 (1H, ddd, *J* = 9.8, 5.3, 2.1 Hz, H-5′), 3.57 (1H, pt, *J* = 9.8, 9.5 Hz, H-2′ or H-3′ or H-4′); ^{13}C NMR (90 MHz, CD_3OD) δ (ppm): 160.3 (C-3), 153.0 (C-6), 129.7, 128.2 (C-4, C-5), 91.9, 82.9, 79.2, 76.3, 71.0 (C-1′ – C-5′), 62.4 (C-6′). ESI-HRMS positive mode (m/z): calcd for $C_{10}H_{13}N_3O_6Na^+$ $[M+Na]^+$ 294.0697. Found: 294.0698.

2-(2′-Deoxy-2′-nitro-β-D-glucopyranosyl)pyrimidine (**4c**)

Prepared from compound **2c** (0.10 g, 0.18 mmol) according to general procedure II. Reaction time: 0.5 h. Purification by column chromatography (9 : 1 $CHCl_3$-MeOH) yielded 49 mg (98%) white amorphous solid. R_f = 0.52 (2 : 1 $CHCl_3$-MeOH). ^1H NMR (360 MHz, CD_3OD) δ (ppm): 8.99 (2H, d, *J* = 5.0 Hz, H-4, H-6), 7.70 (1H, t, *J* = 5.0 Hz, H-5), 5.24 (1H, d, *J* = 10.1 Hz, H-1′), 4.85 (1H, pt, *J* = 10.1, 10.0 Hz, H-2′ or H-3′ or H-4′), 4.20 (1H, pt, *J* = 10.0, 9.9 Hz, H-2′ or H-3′ or H-4′), 3.96 (1H, dd, *J* = 12.2, 2.1 Hz, H-6′a), 3.76 (1H, dd, *J* = 12.2, 5.5 Hz, H-6′b), 3.68 (1H, ddd, *J* = 9.5, 5.5, 2.1 Hz, H-5′), 3.52 (1H, pt, *J* = 9.9, 9.5 Hz, H-2′ or H-3′ or H-4′); ^{13}C NMR (90 MHz, CD_3OD) δ (ppm): 165.2 (C-2), 159.0 (C-4, C-6), 122.8 (C-5), 91.2, 82.9, 80.8, 76.3, 71.0 (C-1′ – C-5′), 62.4 (C-6′). ESI-HRMS positive mode (m/z): calcd for $C_{10}H_{13}N_3O_6Na^+$ $[M+Na]^+$ 294.0697. Found: 294.0698.

2-(2′-Deoxy-2′-nitro-β-D-glucopyranosyl)pyrazine(**4d**)

Prepared from compound **2d** (0.30 g, 0.55 mmol) according to general procedure II. Reaction time: 0.5 h. Purification by column chromatography (9 : 1 $CHCl_3$-MeOH) yielded 117 mg (78%) white amorphous solid. R_f = 0.48 (4 : 1 $CHCl_3$-MeOH). ^1H NMR (400 MHz, CD_3OD) δ (ppm): 8.83 (1H, d, *J* = 1.5 Hz, H-3), 8.60 (1H, d, *J* = 2.6 Hz, H-6), 8.57 (1H, dd, *J* = 2.6, 1.5 Hz, H-5), 5.10 (1H, d, *J* = 9.9 Hz, H-1′), 4.81 (1H, pt, *J* = 10.0, 10.0 Hz, H-2′ or H-3′ or H-4′), 4.21 (1H, pt, *J* = 10.0, 9.7 Hz, H-2′ or H-3′ or H-4′), 3.93 (1H, dd, *J* = 12.2, 2.1 Hz, H-6′a), 3.76 (1H, dd, *J* = 12.2, 5.4 Hz, H-6′b), 3.64 (1H, ddd, *J* = 10.0, 5.4, 2.1 Hz, H-5′), 3.54 (1H, pt, *J* = 9.4, 9.3 Hz, H-2′ or H-3′ or H-4′); ^{13}C NMR (90 MHz, CD_3OD) δ (ppm): 152.9 (C-2), 146.2, 145.5, 145.2 (C-3, C-5, C-6), 91.6, 82.9, 78.6, 76.5, 71.1 (C-1′ – C-5′), 62.4 (C-6′). ESI-HRMS positive mode (m/z): calcd for $C_{10}H_{13}N_3O_6Na^+$ $[M+Na]^+$ 294.0697. Found: 294.0698.

2-(2′-Deoxy-2′-nitro-β-D-glucopyranosyl)quinoline (**4e**)

Prepared from compound **2e** (83 mg, 0.14 mmol) according to general procedure II. Reaction time: 1 h. Purification by column chromatography (9 : 1 $CHCl_3$-MeOH) yielded 31 mg (76%) white amporhous solid. R_f = 0.19 (9 : 1 $CHCl_3$-MeOH). ^1H NMR (400 MHz, CD_3OD) δ (ppm): 8.36, 7.70 (2 × 1H, 2 d, *J* = 8.5 Hz in both, H-3, H-4), 8.00, 7.93 (2 ×1H, 2 d, *J* = 7.9 Hz in both, H-5, H-8), 7.77, 7.61 (2 × 1H, 2 t, *J* = 7.9 Hz in both, H-6, H-7), 5.14 (1H, d, *J* = 9.9 Hz, H-1′), 4.90 (1H, pt, *J* = 10.1, 10.0 Hz, H-2′ or H-3′ or H-4′), 4.27 (1H, pt, *J* = 9.7, 9.0 Hz, H-2′ or H-3′ or H-4′), 3.96 (1H, dd, *J* = 12.2, < 1Hz, H-6′a), 3.80 (1H, dd, *J* = 12.2, 4.7 Hz, H-6′b), 3.67 (1H, m, H-5′), 3.61 (1H, pt, *J* = 9.2, 9.1 Hz, H-2′ or H-3′ or H-4′); ^{13}C NMR (90 MHz, CD_3OD) δ (ppm): 157.2, 148.3 (C-2, C-8a), 138.9, 131.2, 129.7, 129.0, 128.4, 121.2 (C-3 – C-8), 129.5 (C-4a), 92.3, 82.9, 81.1, 76.6, 71.2 (C-1′ – C-5′), 62.5 (C-6′). ESI-HRMS positive mode (m/z): calcd for $C_{15}H_{16}N_2O_6Na^+$ $[M+Na]^+$ 343.0901. Found: 343.0900.

2-(2′-Amino-2′-deoxy-β-D-glucopyranosyl)pyridine (**5a**)

Method A: Prepared from compound **3a** (65 mg, 0.13 mmol) according to general procedure II. Reaction time: 0.5 h. Purification by column chromatography (7 : 3 $CHCl_3$-MeOH) yielded 15 mg (42%) white amporhous solid.

Method B: Compound **3a** (0.22 g, 0.43 mmol) and pentamethylbenzene (0.58 g, 3.88 mmol, 9 eq.) were dissolved in dry CH_2Cl_2 (22 mL) and the solution was cooled down to

formázott: Betűtípus: 8 pt
formázott: Betűtípus: Félkövér
formázott: Betűtípus: 8 pt
formázott: Betűtípus: Félkövér
formázott: Betűtípus: 8 pt
formázott: Betűtípus: Félkövér
formázott: Betűtípus: 8 pt
formázott: Betűtípus: Félkövér

–78 °C. To this solution a 1 M solution of BCl_3 in CH_2Cl_2 (1.72 mL, 1.72 mmol, 4 eq.) was added dropwise over 5 minutes. The reaction mixture was stirred at this temperature until the TLC (9 : 1 $CHCl_3$-MeOH) showed the completion of the reaction (0.5 h). After that, the reaction was quenched by the addition of MeOH (10 mL) and allowed to warm to rt. The solvents were then removed under reduced pressure. Purification of the residue by column chromatography (7 : 3 $CHCl_3$-MeOH) yielded 113 mg (95%) white amorphous solid. R_f = 0.23 (7 : 3 $CHCl_3$-MeOH); $[\alpha]_D$ = +84 (c 0.5, MeOH). ^{1}H NMR (400 MHz, CD_3OD) δ (ppm): 8.57 (1H, d, *J* = 4.5 Hz, H-6), 7.90 (1H, td, *J* = 7.8, 1.7 Hz, H-4), 7.72 (1H, d, *J* = 7.8 Hz, H-3), 7.41 (1H, dd, *J* = 7.5, 5.0 Hz, H-5), 4.57 (1H, d, *J* = 10.0 Hz, H-1′), 3.94 (1H, dd, *J* = 12.1, 1.8 Hz, H-6′a), 3.76 (1H, dd, *J* = 12.1, 4.9 Hz, H-6′b), 3.66 (1H, pt, *J* = 9.0, 8.9 Hz, H-3′), 3.54-3.45 (2H, m, H-4′, H-5′), 3.21 (1H, pt, *J* = 10.0, 9.9 Hz, H-2′); ^{13}C NMR (90 MHz, CD_3OD) δ (ppm): 158.7 (C-2), 149.6 (C-6), 139.1 (C-4), 125.1, 123.9 (C-3, C-5), 82.5, 78.7, 76.4, 71.6 (C-1′, C-3′ – C-5′), 62.7 (C-6′), 57.6 (C-2′). ESI-HRMS positive mode (m/z): calcd for $C_{11}H_{17}N_2O_4^+$ $[M+H]^+$ 241.1183; $C_{11}H_{16}N_2O_4Na^+$ $[M+Na]^+$ 263.1001. Found: $[M+H]^+$ 241.1183; $[M+Na]^+$ 263.1002.

2-(2′-Amino-2′-deoxy-β-D-glucopyranosyl)pyrimidine (**5c**)

A degassed, vigorously stirred suspension of 10% Pd(C) (56 mg) in dry EtOH (11 mL) was saturated with H_2 and compound **4c** (0.11 g, 0.41 mmol) was added. The reaction mixture was heated at reflux temperature until the TLC (3 : 2 $CHCl_3$-MeOH) indicated complete conversion of the starting material. After completion of the reaction (2 h) the catalyst was filtered off through a pad of celite and washed with MeOH. The resulting solution was then evaporated under reduced pressure. Purification of the remaining crude product by column chromatography (3 : 2 $CHCl_3$-MeOH) yielded 37 mg (38%) white amorphous solid. R_f = 0.10 (3 : 2 $CHCl_3$-MeOH); $[\alpha]_D$ = +22 (c 0.1, MeOH). ^{1}H NMR (400 MHz, CD_3OD) δ (ppm): 8.85 (2H, d, *J* = 4.9 Hz, H-4, H-6), 7.48 (1H, t, *J* = 4.9 Hz, H-5), 4.42 (1H, d, *J* = 9.7 Hz, H-1′), 3.87 (1H, dd, *J* = 12.1, 1.5 Hz, H-6′a), 3.73 (1H, dd, *J* = 12.1, 4.5 Hz, H-6′b), 3.50 (1H, pt, *J* = 9.5, 9.0 Hz, H-3′ or H-4′), 3.50-3.45 (1H, m, H-5′), 3.44 (1H, pt, *J* = 9.2, 9.0 Hz, H-3′ or H-4′), 3.08 (1H, pt, *J* = 9.5, 9.4 Hz, H-2′); ^{13}C NMR (90 MHz, CD_3OD) δ (ppm): 167.7 (C-2), 158.8 (C-4, C-6), 122.2 (C-5), 83.8, 82.6, 79.3, 71.4 (C-1′, C-3′ – C-5′), 62.8 (C-6′), 57.6 (C-2′). ESI-HRMS positive mode (m/z): calcd for $C_{10}H_{15}N_3O_4Na^+$ $[M+Na]^+$ 264.0955. Found: 264.0957.

2-(2′-Amino-2′-deoxy-β-D-glucopyranosyl)pyrazine (**5d**)

A degassed, vigorously stirred suspension of 10% Pd(C) (60 mg) in dry EtOH (12 mL) was saturated with H_2 and compound **4d** (0.12 g, 0.43 mmol) was added. The reaction mixture was heated at reflux temperature until the TLC (3 : 2 $CHCl_3$-MeOH) indicated complete conversion of the starting material. After completion of the reaction (6 h) the catalyst was filtered off through a pad of celite and washed with MeOH. The resulting solution was then evaporated under reduced pressure. Purification of the remaining crude product by column chromatography (7 : 3 $CHCl_3$-MeOH) yielded 68 mg (66%) white amorphous solid. R_f = 0.15 (3:2 $CHCl_3$-MeOH); $[\alpha]_D$ = +41 (c 0.5, MeOH). ^{1}H NMR (400 MHz, CD_3OD) δ (ppm): 8.79 (1H, d, *J* = 1.3 Hz, H-3), 8.62 (1H, dd, *J* = 2.4, 1.3 Hz, H-5), 8.57 (1H, d, *J* = 2.4 Hz, H-6), 4.38 (1H, d, *J* = 9.7 Hz, H-1′), 3.90 (1H, dd, *J* = 12.1, 1.7 Hz, H-6′a), 3.73 (1H, dd, *J* = 12.1, 5.0 Hz, H-6′b), 3.51-3.40 (3H, m, H-3′, H-4′, H-5′), 3.00 (1H, pt, *J* = 9.5, 9.4 Hz, H-2′); ^{13}C NMR (90 MHz, CD_3OD) δ (ppm): 155.4 (C-2), 146.0, 145.4, 145.1 (C-3, C-5, C-6), 82.6, 81.4, 79.2, 71.6 (C-1′, C-3′ – C-5′), 62.8 (C-6′), 58.0 (C-2′). ESI-HRMS positive mode (m/z): calcd for $C_{10}H_{16}N_3O_4Na^+$ $[M+H]^+$ 242.1135. Found: 242.1133.

2-(2′-Amino-2′-deoxy-β-D-glucopyranosyl)quinoline (**5e**)

Compound **4e** (0.10 g, 0.33 mmol) and tin powder (1.17 g, 9.82 mmol, 30 eq.) were suspended in a solvent mixture of THF (5 mL) and water (2.5 mL). This heterogenous mixture was cooled down in an ice bath and *cc*HCl solution (0.85 mL, 9.88 mmol 30 eq.) was added. The reaction mixture was then stirred at rt. When the TLC (4 : 1 $CHCl_3$-MeOH)

formázott: Betűtípus: 8 pt
formázott: Betűtípus: Félkövér
formázott: Betűtípus: 8 pt
formázott: Betűtípus: Félkövér
formázott: Betűtípus: 8 pt
formázott: Betűtípus: Félkövér

showed complete conversion of **4e** (1 d) a 2 M aq. solution of NaOH was added to the reaction mixture to become a slightly basic solution. This was then neutralised by the addition of sat. aq. NH_4Cl solution. The solvents were removed under diminished pressure. The residue was treated with MeOH (20 mL) and the inseparable inorganic salts and the excess of the unreacted Sn were filtered off. The resulting solution was evaporated in vacuo. Column chromatographic purification of the residue (9 : 1 $CHCl_3$-MeOH) yielded 28 mg (29%) pale yellow amorphous solid. R_f = 0.11 (4 : 1 $CHCl_3$-MeOH); $[\alpha]_D$ = –11 (c 0.1, MeOH). ^{1}H NMR (400 MHz, CD_3OD) δ (ppm): 8.34 (1H, d, *J* = 8.5 Hz, H-4), 8.06 (1H, dd, *J* = 8.5, 1.2 Hz, H-8), 7.92 (1H, dd, *J* = 8.2, 1.4 Hz, H-5), 7.76 (1H, ddd, *J* = 8.5, 6.8, 1.4 Hz, H-7), 7.71 (1H, d, *J* = 8.5 Hz, H-3), 7.59 (1H, ddd, *J* = 8.2, 6.8, 1.2 Hz, H-6), 4.50 (1H, d, *J* = 9.7 Hz, H-1′), 3.94 (1H, dd, *J* = 12.2, 1.3 Hz, H-6′a), 3.79 (1H, ddd, *J* = 12.2, 3.2, 1.3 Hz, H-5′), 3.56-3.50 (3H, m, H-3′, H-4′, H-6′b), 3.12 (1H, pt, *J* = 9.5, 9.4 Hz, H-2′); ^{13}C NMR (90 MHz, CD_3OD) δ (ppm): 160.1, 148.3 (C-2, C-8a), 138.7, 131.0, 129.6, 129.0, 128.0, 121.7 (C-3 – C-8), 129.4 (C-4a), 83.3, 82.6, 79.1, 71.7 (C-1′, C-3′ – C-5′), 62.9 (C-6′) 58.3(C-2′). ESI-HRMS positive mode (m/z): calcd for $C_{15}H_{18}N_2O_4Na^+$ $[M+Na]^+$ 313.1159; $C_{30}H_{36}N_4O_8Na^+$ $[2M+Na]^+$ 603.2425. Found: $[M+Na]^+$ 313.1158; $[2M+Na]^+$ 603.2425.

2-(2′-Deoxy-2′-nitro-3′,4′,6′-tri-*O*-benzoyl-β-D-glucopyranosyl)pyridine (**6a**)

Prepared from compound **2a** (95 mg, 0.18 mmol) and benzoyl chloride (0.13 mL, 1.12 mmol, 6 eq.) according to general procedure III. Reaction time: 5 d. Purified by column chromatography (1 : 4 EtOAc-hexane) to give 90 mg (88%) white amorphous solid. R_f = 0.38 (1 : 2 EtOAc-hexane). ^{1}H NMR (400 MHz, $CDCl_3$) δ (ppm): 8.60 (1H, ddd, *J* = 4.9, 1.5, 0.9 Hz, H-6), 8.14-7.29 (18H, m, Ar, H-3, H-4, H-5), 6.39 (1H, pt, *J* = 10.0, 9.7 Hz, H-2′ or H-3′ or H-4′), 5.76 (1H, pt, *J* = 9.8, 9.8 Hz, H-2′ or H-3′ or H-4′), 5.46 (1H, pt, *J* = 10.1, 10.1 Hz, H-2′ or H-3′ or H-4′), 5.28 (1H, d, *J* = 9.9 Hz, H-1′), 4.66 (1H, dd, *J* = 12.4, 3.1 Hz, H-6′a), 4.53 (1H, dd, *J* = 12.4, 5.3 Hz, H-6′b), 4.41 (1H, ddd, *J* = 10.1, 5.3, 3.1 Hz, H-5′); ^{13}C NMR (100 MHz, $CDCl_3$) δ (ppm): 166.2, 165.4, 165.2 (3 × C=O), 153.8 (C-2), 149.7 (C-6), 137.4 (C-4), 133.8 (2), 133.3, 130.1-128.4 (Ar), 124.6, 123.1 (C-3, C-5), 87.2, 79.5, 76.9, 73.3, 69.4 (C-1′ – C-5′), 63.3 (C-6′). ESI-HRMS positive mode (m/z): calcd for $C_{32}H_{27}N_2O_9^+$ $[M+H]^+$ 583.1711; $C_{32}H_{26}N_2O_9Na^+$ $[M+Na]^+$ 605.1531. Found: $[M+H]^+$ 583.1713; $[M+Na]^+$ 605.1532.

3-(2′-Deoxy-2′-nitro-3′,4′,6′-tri-*O*-benzoyl-β-D-glucopyranosyl)pyridazine (**6b**)

Prepared from compound **2b** (50 mg, 0.092 mmol) and benzoyl chloride (64 µL, 0.55 mmol, 6 eq.) according to general procedure III. Reaction time: 10 d. Purified by column chromatography (1 : 1 EtOAc-hexane) to give 52 mg (97%) white amorphous solid. R_f = 0.32 (1 : 1 EtOAc-hexane). ^{1}H NMR (400 MHz, $CDCl_3$) δ (ppm): 9.21 (1H, d, *J* = 5.0 Hz, H-6), 8.01-7.33 (17H, m, Ar, H-4, H-5), 6.45 (1H, pt, *J* = 9.8, 9.2 Hz, H-2′ or H-3′ or H-4′), 5.79 (1H, pt, *J* = 9.5, 9.5 Hz, H-2′ or H-3′ or H-4′), 5.60-5.49 (2H, m, H-1′, H-2′ or H-3′ or H-4′), 4.73-4.43 (3H, m, H-5′, H-6′a,b); ^{13}C NMR (100 MHz, $CDCl_3$) δ (ppm): 166.2, 165.3, 165.2 (3 × C=O), 157.0 (C-3), 152.1 (C-6), 133.9, 133.4, 130.1-129.8, 129.4, 128.6-128.5, 128.4, 128.2 (Ar), 127.5, 126.2 (C-4, C-5), 86.4, 78.0, 77.0, 73.0, 69.0 (C-1′ – C-5′), 62.9 (C-6′). ESI-HRMS positive mode (m/z): calcd for $C_{31}H_{25}N_3O_9Na^+$ $[M+Na]^+$ 606.1483. Found: 606.1479.

2-(2′-Deoxy-2′-nitro-3′,4′,6′-tri-*O*-benzoyl-β-D-glucopyranosyl)pyrimidine (**6c**)

Prepared from compound **2c** (0.50 g, 0.92 mmol) and benzoyl chloride (0.65 mL, 5.60 mmol, 6 eq.) according to general procedure III. Reaction time: 30 d. Purified by column chromatography (1 : 2 EtOAc-hexane) to give 0.24 g (45%) white amorphous solid. R_f = 0.34 (1 : 2 EtOAc-hexane). ^{1}H NMR (360 MHz, $CDCl_3$) δ (ppm): 8.81 (2H, d, *J* = 4.8 Hz, H-4, H-6), 7.98-7.33 (16H, m, Ar, H-5), 6.39 (1H, pt, *J* = 10.0, 9.7 Hz, H-2′ or H-3′ or H-4′), 5.80 (1H, pt, *J* = 9.7, 9.6 Hz, H-2′ or H-3′ or H-4′), 5.68 (1H, pt, *J* = 10.2, 10.2 Hz, H-2′ or H-3′ or H-4′), 5.42 (1H, d, *J* = 10.0 Hz, H-1′), 4.65 (1H, dd, *J* = 12.3, 3.0 Hz, H-6′a), 4.52 (1H, dd, *J* = 12.3, 5.0 Hz, H-6′b), 4.44 (1H, ddd, *J* = 10.0, 5.0, 3.0 Hz, H-5′); ^{13}C NMR (100 MHz, $CDCl_3$) δ (ppm): 166.2, 165.3 (2), 162.8 (3 × C=O, C-2), 157.9 (C-4, C-6), 133.8, 133.2, 130.1-128.4 (Ar),

formázott: Betűtípus: 8 pt
formázott: Betűtípus: Félkövér
formázott: Betűtípus: 8 pt
formázott: Betűtípus: Félkövér
formázott: Betűtípus: 8 pt
formázott: Betűtípus: Félkövér

121.5 (C-5), 85.8, 80.4, 77.2, 73.0, 69.2 (C-1′ – C-5′), 63.2 (C-6′). ESI-HRMS positive mode (m/z): calcd for $C_{31}H_{25}N_3O_9Na^+$ $[M+Na]^+$ 606.1483. Found: 606.1483.

2-(2′-Deoxy-2′-nitro-3′,4′,6′-tri-*O*-benzoyl-β-D-glucopyranosyl)pyrazine (**6d**)

Prepared from compound **2d** (50 mg, 0.092 mmol) and benzoyl chloride (64 μL, 0.55 mmol, 6 eq.) according to general procedure III. Reaction time: 5 d. Purified by column chromatography (1 : 2 EtOAc-hexane) to give 44 mg (82%) white amorphous solid. R_f = 0.14 (1 : 2 EtOAc-hexane). ^{1}H NMR (400 MHz, $CDCl_3$) δ (ppm): 8.83 (1H, d, *J* = 1.5 Hz, H-3), 8.62 (1H, d, *J* = 2.5 Hz, H-6), 8.55 (1H, dd, *J* = 2.5, 1.5 Hz, H-5), 8.01-7.35 (15H, m, Ar), 6.38 (1H, pt, *J* = 9.4, 9.3 Hz, H-2′ or H-3′ or H-4′), 5.74 (1H, pt, *J* = 9.7, 9.7 Hz, H-2′ or H-3′ or H-4′), 5.43 (1H, pt, *J* = 9.9, 9.5 Hz, H-2′ or H-3′ or H-4′), 5.39 (1H, d, *J* = 9.8 Hz, H-1′), 4.68 (1H, dd, *J* = 12.3, 2.9 Hz, H-6′a), 4.52 (1H, dd, *J* = 12.3, 5.4 Hz, H-6′b), 4.28 (1H, ddd, *J* = 10.0, 5.4, 2.9 Hz, H-5′); ^{13}C NMR (100 MHz, $CDCl_3$) δ (ppm): 166.2, 165.3, 165.2 (3 × C=O), 149.7 (C-2), 145.7, 144.7, 144.0 (C-3, C-5, C-6), 133.9, 133.4, 130.1-129.9, 129.5, 128.7-128.6, 128.5, 128.3 (Ar), 86.3, 77.4, 77.1, 73.1, 69.1 (C-1′ – C-5′), 63.0 (C-6′). ESI-HRMS positive mode (m/z): calcd for $C_{31}H_{26}N_3O_9^+$ $[M+H]^+$ 584.1664; $C_{31}H_{25}N_3O_9Na^+$ $[M+Na]^+$ 606.1483. Found: $[M+H]^+$ 584.1659; $[M+Na]^+$ 606.1477.

2-(2′-Amino-2′-deoxy-3′,4′,6′-tri-*O*-benzoyl-β-D-glucopyranosyl)pyridine (**7a**)

Compound **6a** (0.10 g, 0.17 mmol) and Zn powder (0.11 g, 1.71 mmol, 10 eq.) were suspended in a solvent mixture of THF (10 mL) and water (5 mL). To this stirred mixture a 2 M aq. solution of HCl was added (2.6 mL, 5.14 mmol, 30 eq.). The stirring of the reaction mixture was continued at rt until the TLC (95 : 5 $CHCl_3$-MeOH) showed total consumption of the starting material (5 h). The reaction was quenched by the addition of sat. aq. $NaHCO_3$ solution (50 mL). The insoluble inorganic salts and the rest of the Zn were filtered off and the remaining solution was extracted with CH_2Cl_2 (2 × 50 mL). The combined organic phase was extracted with water (50 mL) and then with brine (50 mL), dried over $MgSO_4$ and filtered. The solvent was removed under reduced pressure. The residue was purified by column chromatography (100 : 1 $CHCl_3$-MeOH) to give 36 mg (38%) white amorphous solid. R_f = 0.47 (50 : 1 $CHCl_3$-MeOH); $[\alpha]_D$ = –16 (c 0.5, $CHCl_3$). ^{1}H NMR (400 MHz, $CDCl_3$) δ (ppm): 8.60 (1H, ddd, *J* = 4.9, 1.9, 0.9 Hz, H-6), 8.01-7.25 (18H, m, Ar, H-3, H-4, H-5), 5.71 (1H, pt, *J* = 9.5, 9.5 Hz, H-4′), 5.66 (1H, pt, *J* = 9.5, 9.5 Hz, H-3′), 4.63 (1H, dd, *J* = 12.2, 3.1 Hz, H-6′a), 4.53 (1H, d, *J* = 9.5 Hz, H-1′), 4.52 (1H, dd, *J* = 12.2, 5.3 Hz, H-6′b), 4.25 (1H, ddd, *J* = 9.4, 5.3, 3.1 Hz, H-5′), 3.58 (1H, pt, *J* = 9.7, 9.6 Hz, H-2′), 1.71 (2H, s, NH_2); ^{13}C NMR (100 MHz, $CDCl_3$) δ (ppm): 166.6, 166.3, 165.7 (3 × C=O), 157.7 (C-2), 149.1 (C-6), 137.2 (C-4), 133.4, 133.3, 133.1, 129.9-128.4 (Ar), 123.6, 122.9 (C-3, C-5), 83.9, 77.7, 76.6, 70.3 (C-1′, C-3′ – C-5′), 64.0 (C-6′), 56.7 (C-2′). ESI-HRMS positive mode (m/z): calcd for $C_{32}H_{29}N_2O_7^+$ $[M+H]^+$ 553.1969; $C_{32}H_{28}N_2O_7Na^+$ $[M+Na]^+$ 575.1789. Found: $[M+H]^+$ 553.1970; $[M+Na]^+$ 575.1789.

3-(2′-Amino-2′-deoxy-3′,4′,6′-tri-*O*-benzoyl-β-D-glucopyranosyl)pyridazine (**7b**)

Prepared from compound **9b** (105 mg, 0.16 mmol) according to general procedure VI. Purified by column chromatography (95 : 5 $CHCl_3$-MeOH) to yield 78 mg (88%) white amorphous solid. R_f = 0.31 (95 : 5 $CHCl_3$-MeOH); $[\alpha]_D$ = +7 (c 0.5, $CHCl_3$). ^{1}H NMR (400 MHz, $CDCl_3$) δ (ppm): 9.17 (1H, d, *J* = 5.0 Hz, H-6), 8.02-7.32 (17H, m, Ar, H-4, H-5), 5.70 (2H, m, H-3′, H-4′), 4.82 (1H, d, *J* = 9.7 Hz, H-1′), 4.65 (1H, dd, *J* = 12.2, 2.9 Hz, H-6′a), 4.52 (1H, dd, *J* = 12.2, 5.2 Hz, H-6′b), 4.32-4.27 (1H, m, H-5′), 3.55 (1H, pt, *J* = 9.7, 9.6 Hz, H-2′), 1.78 (2H, s, NH_2); ^{13}C NMR (100 MHz, $CDCl_3$) δ (ppm): 166.6, 166.3, 165.6 (3 × C=O), 160.6 (C-3), 151.5 (C-6), 133.5, 133.4, 133.2, 129.9-129.8, 129.7, 129.3, 129.0, 128.5-128.4 (Ar), 127.5, 125.8 (C-4, C-5), 82.3, 77.4, 76.7, 69.9 (C-1′, C-3′ – C-5′), 63.6 (C-6′), 56.7 (C-2′). ESI-HRMS positive mode (m/z): calcd for $C_{31}H_{28}N_3O_7^+$ $[M+H]^+$ 554.1922; $C_{31}H_{27}N_3O_7Na^+$ $[M+Na]^+$ 576.1741. Found: $[M+H]^+$ 554.1922; $[M+Na]^+$ 576.1740.

formázott: Betűtípus: 8 pt
formázott: Betűtípus: Félkövér
formázott: Betűtípus: 10 pt
formázott: Betűtípus: 8 pt
formázott: Betűtípus: Félkövér
formázott: Betűtípus: 8 pt
formázott: Betűtípus: Félkövér

2-(2′-Amino-2′-deoxy-3′,4′,6′-tri-*O*-benzoyl-β-D-glucopyranosyl)pyrimidine (**7c**)

Prepared from compound **9c** (90 mg, 0.14 mmol) according to general procedure VI. Purified by column chromatography (95 : 5 $CHCl_3$-MeOH) to yield 73 mg (96%) white amorphous solid. R_f = 0.33 (95 : 5 $CHCl_3$-MeOH); $[\alpha]_D$ = –15 (c 0.5, $CHCl_3$). ^1H NMR (400 MHz, $CDCl_3$) δ (ppm): 8.84 (2H, d, *J* = 4.9 Hz, H-4, H-6), 7.99-7.30 (16H, m, Ar, H-5), 5.74 (1H, pt, *J* = 9.7, 9.6 Hz, H-3′ or H-4′), 5.65 (1H, pt, *J* = 9.8, 9.6 Hz, H-3′ or H-4′), 4.67 (1H, d, *J* = 9.9 Hz, H-1′), 4.60 (1H, dd, *J* = 12.2, 3.2 Hz, H-6′a), 4.51 (1H, dd, *J* = 12.2, 5.4 Hz, H-6′b), 4.29 (1H, ddd, *J* = 9.2, 5.4, 3.2 Hz, H-5′), 3.88 (1H, pt, *J* = 10.0, 9.8 Hz, H-2′), 1.46 (2H, s, NH_2); ^{13}C NMR (90 MHz, $CDCl_3$) δ (ppm): 166.8, 166.3, 165.9, 165.6 (3 × C=O, C-2), 157.7 (C-4, C-6), 133.4, 133.3, 133.0, 130.0-129.8, 129.4, 129.2, 128.5-128.3 (Ar), 120.9 (C-5), 85.2, 77.8, 77.0, 70.4 (C-1′, C-3′ – C-5′), 64.2 (C-6′), 55.3 (C-2′). ESI-HRMS positive mode (m/z): calcd for $C_{31}H_{28}N_3O_7^+$ $[M+H]^+$ 554.1922; $C_{31}H_{27}N_3O_7Na^+$ $[M+Na]^+$ 576.1741. Found: $[M+H]^+$ 554.1916; $[M+Na]^+$ 576.1734.

2-(2′-Amino-2′-deoxy-3′,4′,6′-tri-*O*-benzoyl-β-D-glucopyranosyl)pyrazine (**7d**)

Prepared from compound **9d** (0.12 g, 0.18 mmol) according to general procedure VI. Purified by column chromatography (95 : 5 $CHCl_3$-MeOH) to yield 98 mg (96%) white amorphous solid. R_f = 0.32 (95 : 5 $CHCl_3$-MeOH); $[\alpha]_D$ = –7 (c 0.5, $CHCl_3$). ^1H NMR (400 MHz, $CDCl_3$) δ (ppm): 8.82 (1H, d, *J* = 1.2 Hz, H-3), 8.58-8.56 (2H, m, H-5, H-6), 8.01-7.31 (15H, m, Ar), 5.71 (1H, pt, *J* = 9.7, 9.4 Hz, H-3′ or H-4′), 5.68 (1H, pt, *J* = 9.7, 9.4 Hz, H-3′ or H-4′), 4.65 (1H, dd, *J* = 12.3, 3.0 Hz, H-6′a), 4.62 (1H, d, *J* = 9.8 Hz, H-1′), 4.51 (1H, dd, *J* = 12.3, 5.3 Hz, H-6′b), 4.28 (1H, ddd, *J* = 8.9, 5.3, 3.0 Hz, H-5′), 3.64 (1H, pt, *J* = 9.7, 9.7 Hz, H-2′), 1.82 (2H, s, NH_2); ^{13}C NMR (100 MHz, $CDCl_3$) δ (ppm): 166.6, 166.2, 165.6 (3 × C=O), 153.1 (C-2), 145.1, 144.6, 143.6 (C-3, C-5, C-6), 133.5, 133.4, 133.1, 129.9-129.8, 129.7, 129.2, 129.0, 128.5-128.4 (Ar), 81.9, 77.4, 76.7, 70.0 (C-1′, C-3′ – C-5′), 63.7 (C-6′), 56.1 (C-2′). ESI-HRMS positive mode (m/z): calcd for $C_{31}H_{28}N_3O_7^+$ $[M+H]^+$ 554.1922; $C_{31}H_{27}N_3O_7Na^+$ $[M+Na]^+$ 576.1741. Found: $[M+H]^+$ 554.1916; $[M+Na]^+$ 576.1735.

2-(2′-Amino-2′-deoxy-3′,4′,6′-tri-*O*-benzoyl-β-D-glucopyranosyl)quinoline (**7e**)

Prepared from compound **9e** (0.12 g, 0.16 mmol) according to general procedure VI. Purified by column chromatography (1 : 1 EtOAc-hexane) to yield 83 mg (84%) white amorphous solid. R_f = 0.18 (1 : 1 EtOAc-hexane); $[\alpha]_D$ = +30 (c 0.5, $CHCl_3$). ^1H NMR (500 MHz, $CDCl_3$) δ (ppm): 8.22-7.31 (21H, m, Ar, H-3 – H-8), 5.77-5.71 (2H, m, H-3′, H-4′), 4.73 (1H, d, *J* = 9.5 Hz, H-1′), 4.66 (1H, dd, *J* = 12.2, 2.8 Hz, H-6′a), 4.54 (1H, dd, *J* = 12.2, 5.4 Hz, H-6′b), 4.31 (1H, ddd, *J* = 9.1, 5.4, 2.8 Hz, H-5′), 3.69 (1H, pt, *J* = 9.5, 9.1 Hz, H-2′), 1.83 (2H, br s, NH_2); ^{13}C NMR (90 MHz, $CDCl_3$) δ (ppm): 166.6, 166.3, 165.7 (3 × C=O), 157.9, 147.2 (C-2, C-8a), 137.4, 133.4, 133.3, 133.1, 130.0-129.6, 129.5, 129.2, 128.5-128.4, 128.0, 127.7, 127.0, 119.9 (Ar, C-3 – C-8, C-4a), 84.2, 77.6, 76.7, 70.3 (C-1′, C-3′ – C-5′), 63.9 (C-6′), 56.5 (C-2′). ESI-HRMS positive mode (m/z): calcd for $C_{36}H_{31}N_2O_7^+$ $[M+H]^+$ 603.2126. Found: 603.2123.

2-(2′-(*tert*-Butoxycarbonyl)amino-2′-deoxy-β-D-glucopyranosyl)pyrimidine (**8c**)

Prepared from compound **5c** (60 mg, 0.25 mmol) and Boc_2O (0.11 g, 0.50 mmol) according to general procedure IV. Purification by column chromatography (9 : 1 $CHCl_3$-MeOH) yielded 57 mg (67%) amorphous white solid. R_f = 0.37 (4 : 1 $CHCl_3$-MeOH). ^1H NMR (400 MHz, D_2O) δ (ppm): 8.81 (2H, d, *J* = 5.0 Hz, H-4, H-6), 7.55 (1H, t, *J* = 5.0 Hz, H-5), 4.51 (1H, d, *J* = 9.7 Hz, H-1′), 3.94 (1H, dd, *J* = 12.4, 1.9 Hz, H-6′a), 3.86 (1H, dd, *J* = 12.4, 4.6 Hz, H-6′b), 3.74-3.61 (4H, m, H-2′ – H-5′), 1.21 (6H, s, 2 × CH_3), 1.10 (3H, s, CH_3); ^{13}C NMR (100 MHz, D_2O + 2 drops of CD_3OD) δ (ppm): 165.0 (C-2), 157.7 (C-4, C-6), 156.8 (C=O), 121.6 (C-5), 81.2, 79.7, 74.5, 69.8 (C-1′, C-3′ – C-5′), 80.9 ($C(CH_3)_3$), 60.9 (C-6′), 56.8 (C-2′), 27.6 (3 × CH_3). ESI-HRMS positive mode (m/z): calcd for $C_{15}H_{23}N_3O_6Na^+$ $[M+Na]^+$ 364.1479; $C_{30}H_{46}N_6O_{12}Na^+$ $[2M+Na]^+$ 705.3066. Found: $[M+Na]^+$ 364.1474; $[2M+Na]^+$ 705.3057.

formázott: Betűtípus: 8 pt
formázott: Betűtípus: Félkövér
formázott: Betűtípus: 8 pt
formázott: Betűtípus: Félkövér
formázott: Betűtípus: 8 pt
formázott: Betűtípus: Félkövér
formázott: Betűtípus: 8 pt
formázott: Betűtípus: Félkövér

2-(2′-(*tert*-Butoxycarbonyl)amino-2′-deoxy-β-D-glucopyranosyl)pyrazine (**8d**)

Prepared from compound **5d** (0.10 g, 0.42 mmol) and Boc_2O (0.18 g, 0.83 mmol) according to general procedure IV. Purification by column chromatography (9 : 1 $CHCl_3$-MeOH) yielded 94 mg (67%) white amorphous solid. R_f = 0.37 (4 : 1 $CHCl_3$-MeOH). ^1H NMR (400 MHz, CD_3OD) δ (ppm): 8.72 (1H, d, *J* = 1.5 Hz, H-3), 8.56 (1H, dd, *J* = 2.7, 1.5 Hz, H-5), 8.53 (1H, d, *J* = 2.7 Hz, H-6), 4.41 (1H, d, *J* = 9.1 Hz, H-1′), 3.90 (1H, dd, *J* = 12.1, 2.2 Hz, H-6′a), 3.77 (1H, dd, *J* = 12.1, 5.1 Hz, H-6′b), 3.62-3.52 (3H, m, H-2′, H-3′, H-4′), 3.44 (1H, ddd, *J* = 9.0, 5.1, 2.2 Hz, H-5′), 1.22 (9H, s, 3 × C*H*$_3$); ^{13}C NMR (100 MHz, CD_3OD) δ (ppm): 157.5, 155.3 (C=O, C-2), 145.0, 144.9, 144.8 (C-3, C-5, C-6), 82.3, 81.3, 76.6, 71.8 (C-1′, C-3′ – C-5′), 79.9 (*C*(CH$_3$)$_3$), 62.7 (C-6′), 58.6 (C-2′), 28.6 (3 × CH$_3$). ESI-HRMS positive mode (m/z): calcd for $C_{15}H_{23}N_3O_6Na^+$ $[M+Na]^+$ 364.1479. Found: 364.1471.

2-(2′-(*tert*-Butoxycarbonyl)amino-2′-deoxy-β-D-glucopyranosyl)quinoline (**8e**)

Prepared from compound **5e** (25 mg, 0.086 mmol) and Boc_2O (37.6 mg, 0.172 mmol) according to general procedure IV. Purification by column chromatography (9 : 1 $CHCl_3$-MeOH) yielded 27 mg (80%) white amorphous solid. R_f = 0.35 (4:1 $CHCl_3$-MeOH). ^1H NMR (360 MHz, CD_3OD) δ (ppm): 8.29 (1H, d, *J* = 8.5 Hz, H-4), 8.05 (1H, dd, *J* = 8.5, 1.2 Hz, H-8), 7.90 (1H, dd, *J* = 8.1, 1.4 Hz, H-5), 7.75 (1H, ddd, *J* = 8.5, 6.9, 1.5 Hz, H-7), 7.69 (1H, d, *J* = 8.5 Hz, H-3), 7.58 (1H, ddd, *J* = 8.1, 6.9, 1.2 Hz, H-6), 4.49 (1H, d, *J* = 9.4 Hz, H-1′), 3.94 (1H, dd, *J* = 12.1, 2.3 Hz, H-6′a), 3.82 (1H, dd, *J* = 12.1, 5.2 Hz, H-6′b), 3.70-3.56 (3H, m, H-2′, H-3′, H-4′), 3.49 (1H, ddd, *J* = 9.5, 5.2, 2.3 Hz, H-5′), 1.00 (6H, s, 2 × C*H*$_3$), 0.79 (3H, s, C*H*$_3$); ^{13}C NMR (90 MHz, CD_3OD) δ (ppm): 160.2, 157.4, 148.0 (C=O, C-2, C-8a,), 138.2, 130.9, 129.2, 128.9, 127.8, 121.7 (C-3 – C-8), 129.4 (C-4a), 83.6, 82.3, 77.0, 72.0 (C-1′, C-3′ – C-5′), 79.8 (*C*(CH$_3$)$_3$), 62.9 (C-6′) 58.8 (C-2′), 28.4 (3 × CH$_3$). ESI-HRMS positive mode (m/z): calcd for $C_{20}H_{26}N_2O_6Na^+$ $[M+Na]^+$ 413.1683. Found: 413.1683.

3-(2′-(*tert*-Butoxycarbonyl)amino-2′-deoxy-3′,4′,6′-tri-*O*-benzoyl-β-D-glucopyranosyl)pyridazine (**9b**)

A degassed, vigorously stirred suspension of 10% Pd(C) (65 mg) in dry EtOH (13 mL) was saturated with H_2 and compound **4b** (0.13 g, 0.48 mmol) was added. The reaction mixture was heated at reflux temperature until the TLC (3 : 2 $CHCl_3$-MeOH) indicated complete conversion of the starting material. After completion of the reaction (3 h) the catalyst was filtered off through a pad of celite and washed with EtOH. The resulting solution was then evaporated under reduced pressure. Purification of the residue by column chromatography (3 : 2 $CHCl_3$-MeOH) yielded 100 mg of white amorphous solid containing the desired 3-(2′-amino-2′-deoxy-β-D-glucopyranosyl)pyridazine **5b** along with unidentified impurities. This mixture was dissolved in a solvent mixture of water (5 mL) and 1,4-dioxane (5 mL), and Boc_2O (0.21 g, 0.96 mmol) was added. The reaction mixture was stirred at rt until the TLC (9 : 1 $CHCl_3$-MeOH) showed complete transformation of **5b** (1 day). After that, the solvents were removed under reduced pressure. Column chromatographic purification of the residue (9 : 1 $CHCl_3$-MeOH) resulted in 70 mg of 3-(2′-(*tert*-butoxycarbonyl)amino-2′-deoxy-β-D-glucopyranosyl)pyridazine (**8b**) contaminated with inseparable impurities. To a solution of the resulting **8b** in dry pyridine (5 mL) benzoyl chloride (0.2 mL, 1.72 mmol) was added at rt. The reaction mixture was stirred at 60 °C for 1 hour. Since the TLC (1 : 1 EtOAc-hexane) showed incompleteness of the reaction, an additional portion of benzoyl chloride (0.2 mL, 1.72 mmol) was added to the reaction mixture and the heating was continued for 1 hour. The reaction mixture was allowed to cool to rt and further stirred overnight. The reaction mixture was then diluted with CH_2Cl_2 (50 mL) and extracted with sat. aq. solution of $NaHCO_3$ (25 mL), then with water (25 mL). The separated organic phase was dried over $MgSO_4$, filtered and the solvents were removed under diminished pressure. The residue was purified by column chromatography to give the title compound **9b** (83 mg, 27% for 3 steps) as white amorphous solid. R_f = 0.28 (1 : 1 EtOAc-hexane. ^1H NMR (400 MHz, $CDCl_3$) δ (ppm): 9.12 (1H, dd, *J* = 4.9, 1.7 Hz, H-6), 8.04-7.32 (17H, m, Ar, H-4, H-5), 5.82 (1H, pt, *J* = 9.3, 9.3 Hz, H-3′ or H-4′), 5.79 (1H, pt, *J* =

formázott: Betűtípus: 8 pt
formázott: Betűtípus: Félkövér
formázott: Betűtípus: 8 pt
formázott: Betűtípus: Félkövér
formázott: Betűtípus: 8 pt
formázott: Betűtípus: Félkövér

9.7, 9.5 Hz, H-3′ or H-4′), 5.12 (1H, d, *J* = 9.9 Hz, NH), 5.02 (1H, d, *J* = 10.3 Hz, H-1′), 4.67 (1H, dd, *J* = 12.3, 2.8 Hz, H-6′a), 4.50 (1H, dd, *J* = 12.3, 4.8 Hz, H-6′b), 4.30 (1H, ddd, *J* = 9.5, 4.8, 2.8 Hz, H-5′), 4.28 (1H, pt, *J* = 10.1, 10.0 Hz, H-2′), 1.05 (9H, s, 3 × CH_3); ^{13}C NMR (100 MHz, $CDCl_3$) δ (ppm): 166.7, 166.2, 165.4 (3 × C=O), 159.6, 155.0 (C=O, C-3), 151.4 (C-6), 133.6, 133.4, 133.2, 130.0-129.8, 129.7, 129.1, 128.9, 128.6-128.4 (Ar), 127.3, 125.7 (C-4, C-5), 81.3, 76.7, 74.3, 69.8 (C-1′, C-3′ – C-5′), 80.0 (*C*(CH_3)$_3$), 63.3 (C-6′), 55.9 (C-2′), 27.9 (3 × *C*H_3). ESI-HRMS positive mode (m/z): calcd for $C_{36}H_{35}N_3O_9Na^+$ [M+Na]$^+$ 676.2266; $C_{72}H_{70}N_6O_{18}Na^+$ [2M+Na]$^+$ 1329.4639. Found: [M+Na]$^+$ 676.2256; [2M+Na]$^+$ 1329.4641.

2-(2′-(*tert*-Butoxycarbonyl)amino-2′-deoxy-3′,4′,6′-tri-*O*-benzoyl-β-D-glucopyranosyl)pyrimidine (**9c**)

Prepared from compound **8c** (60 mg, 0.18 mmol) and benzoyl chloride (0.15 mL, 1.29 mmol, 7.2 eq.) according to general procedure V. Purification by column chromatography (1 : 1 EtOAc-hexane) gave 92 mg (80%) white amorphous solid. R_f = 0.22 (1 : 1 EtOAc-hexane). ^{1}H NMR (400 MHz, $CDCl_3$) δ (ppm): 8.82 (2H, d, *J* = 4.9 Hz, H-4, H-6), 7.98-7.27 (16H, m, Ar, H-5), 5.86 (1H, pt, *J* = 9.9, 9.6 Hz, H-3′ or H-4′), 5.80 (1H, pt, *J* = 9.6, 9.4 Hz, H-3′ or H-4′), 4.98 (1H, d, *J* = 9.5 Hz, NH), 4.90 (1H, d, *J* = 10.2 Hz, H-1′), 4.63 (1H, dd, *J* = 12.3, 3.5 Hz, H-6′a), 4.58 (1H, dd, *J* = 12.3, 5.4 Hz, H-6′b), 4.55 (1H, pt, *J* = 10.2, 9.7 Hz, H-2′), 4.30 (1H, ddd, *J* = 9.2, 5.4, 3.5 Hz, H-5′), 1.09 (9H, s, 3 × CH_3); ^{13}C NMR (100 MHz, $CDCl_3$) δ (ppm): 166.7, 166.3, 165.4, 165.2 (3 × C=O, C-2), 154.6 (C=O), 157.4 (C-4, C-6), 133.4, 133.3, 133.0, 130.0-129.8, 129.7, 129.2, 129.0, 128.4-128.2 (Ar), 120.7 (C-5), 82.8, 76.7, 74.6, 70.2 (C-1′, C-3′ – C-5′), 79.6 (*C*(CH_3)$_3$), 64.1 (C-6′), 55.2 (C-2′), 28.0 (3 × *C*H_3). ESI-HRMS positive mode (m/z): calcd for $C_{36}H_{35}N_3O_9Na^+$ [M+Na]$^+$ 676.2266. Found: 676.2256.

2-(2′-(*tert*-Butoxycarbonyl)amino-2′-deoxy-3′,4′,6′-tri-*O*-benzoyl-β-D-glucopyranosyl)pyrazine (**9d**)

Prepared from compound **8d** (90 mg, 0.26 mmol) and benzoyl chloride (0.22 mL, 1.89 mmol, 7.2 eq.) according to general procedure V. Purification by column chromatography (1 : 1 EtOAc-hexane) gave 122 mg (71%) white amorphous solid. R_f = 0.36 (1 : 1 EtOAc-hexane). ^{1}H NMR (400 MHz, $CDCl_3$) δ (ppm): 8.83 (1H, s, H-3), 8.55-8.53 (2H, m, H-5, H-6), 8.02-7.30 (15H, m, Ar), 5.88 (1H, d, *J* = 9.8, 9.6 Hz, H-3′ or H-4′), 5.83 (1H, d, *J* = 9.5, 9.3 Hz, H-3′ or H-4′), 5.15 (1H, d, *J* = 9.3 Hz, NH), 4.83 (1H, d, *J* = 10.2 Hz, H-1′), 4.68 (1H, dd, *J* = 12.3, 2.9 Hz, H-6′a), 4.53 (1H, dd, *J* = 12.3, 4.9 Hz, H-6′b), 4.35 (1H, pt, *J* = 9.8, 9.7 Hz, H-2′), 4.34-4.29 (H, m, H-5′), 1.09 (9H, s, 3 × CH_3); ^{13}C NMR (90 MHz, $CDCl_3$) δ (ppm): 166.8, 166.3, 165.4 (3 × C=O), 154.8, 152.4 (C=O, C-2), 144.6 (2), 143.4 (C-3, C-5, C-6), 133.5, 133.4, 133.2, 130.0-129.8, 129.7, 129.1, 129.0, 128.5-128.4 (Ar), 80.7, 76.8, 74.3, 70.0 (C-1′, C-3′ – C-5′), 79.9 (*C*(CH_3)$_3$), 63.5 (C-6′), 55.9 (C-2′), 28.0 (3 × *C*H_3). ESI-HRMS positive mode (m/z): calcd for $C_{36}H_{35}N_3O_9Na^+$ [M+Na]$^+$ 676.2266. Found: 676.2260.

2-(2′-(*tert*-Butoxycarbonyl)amino-2′-deoxy-3′,4′,6′-tri-*O*-benzoyl-β-D-glucopyranosyl)quinoline (**9e**)

Prepared from compound **8e** (50 mg, 0.13 mmol) and benzoyl chloride (0.11 mL, 0.95 mmol, 7.2 eq.) according to general procedure V. Purification by column chromatography (1 : 2 EtOAc-hexane) gave 73 mg (81%) white amorphous solid. R_f = 0.21 (1 : 2 EtOAc-hexane). ^{1}H NMR (500 MHz, $CDCl_3$) δ (ppm): 8.23-7.32 (21H, m, Ar, H-3 – H-8), 5.84 (1H, pt, *J* = 9.6, 9.5 Hz, H-3′ or H-4′), 5.77 (1H, dd, *J* = 10.0, 9.8 Hz, H-3′ or H-4′), 4.98 (1H, d, *J* = 9.8 Hz, NH), 4.89 (1H, d, *J* = 10.2 Hz, H-1′), 4.67 (1H, dd, *J* = 12.2, 2.9 Hz, H-6′a), 4.52 (1H, dd, *J* = 12.2, 4.8 Hz, H-6′b), 4.36 (1H, q, *J* = 10.2 Hz, H-2′), 4.28 (1H, ddd, *J* = 9.7, 4.8, 2.9 Hz, H-5′), 0.86 (9H, s, 3 × CH_3); ^{13}C NMR (90 MHz, $CDCl_3$) δ (ppm): 170.8, 166.4, 165.5 (3 × C=O), 157.4, 155.1, 146.5 (C=O, C-2, C-8a), 137.9, 133.5, 133.3, 133.2, 130.3-129.8, 129.4, 129.1, 128.5-128.3, 128.2, 127.9, 127.0, 119.5 (Ar, C-3 – C-8, C-4a), 82.5, 76.6, 74.7, 70.1 (C-1′, C-3′ – C-5′), 79.5 (*C*(CH_3)$_3$), 63.5 (C-6′), 56.1 (C-2′), 27.7 (3 × CH_3). ESI-HRMS positive mode (m/z): calcd for $C_{41}H_{38}N_2O_9Na^+$ [M+Na]$^+$ 725.2470. Found: 725.2473.

formázott: Betűtípus: 8 pt

formázott: Betűtípus: Félkövér

formázott: Betűtípus: 8 pt

formázott: Betűtípus: Félkövér

formázott: Betűtípus: 8 pt

formázott: Betűtípus: Félkövér

Complex **Ru-3a**

Prepared from compound **3a** (47 mg, 0.092 mmol, 1.9 eq.), **Ru-dimer** (30 mg, 0.049 mmol) and $TlPF_6$ (34 mg, 0.097 mmol) according to general procedure VII. Purification by column chromatography (95 : 5 $CHCl_3$-MeOH) gave 63 mg (74%) yellow solid. R_f = 0.50 (95 : 5 $CHCl_3$-MeOH). ^1H NMR (400 MHz, $CDCl_3$) δ (ppm): 9.02 (1H, d, *J* = 5.5 Hz, H-6), 7.86 (1H, dd, *J* = 8.1, 1.8 Hz, H-3), 7.82 (1H, td, *J* = 8.1, 1.5 Hz, H-4), 7.40-7.26 (16H, m, Ar, H-5), 5.84, 5.80, 5.59, 5.13 (4 × 1H, 4 d, *J* = 5.9 Hz in each, 4 × *p*-cym-CH_{Ar}), 5.34 (1H, pt, *J* = 10.8 Hz, NH_2), 4.89, 4.59 (2 × 1H, 2 d, *J* = 12.1 Hz in both, PhCH_2), 4.78, 4.56 (2 × 1H, 2 d, *J* = 12.3 Hz in both, PhCH_2), 4.75, 4.65 (2 × 1H, 2 d, *J* = 11.3 Hz in both, PhCH_2), 4.54 (1H, d, *J* = 10.2 Hz, H-1′), 4.23 (1H, pt, *J* = 8.9, 8.8 Hz, H-3′), 3.99 (1H, ddd, *J* = 9.4, 5.6, 2.6, H-5′), 3.84-3.77 (2H, m, H-6′a,b), 3.53 (1H, pt, *J* = 9.1, 9.0 Hz, H-4′), 3.20 (1H, dd, *J* = 10.8, 5.3 Hz, NH_2), 2.58 (1H, hept, *J* = 6.9 Hz, *i*-Pr-C*H*), 2.03-1.94 (1H, m, H-2′), 1.70 (3H, s, C_6H_4-CH_3), 1.16, 1.02 (2 × 3H, 2 d, *J* = 6.9 Hz in both, 2 × *i*-Pr-CH_3); ^{13}C NMR (100 MHz, $CDCl_3$) δ (ppm): 162.0 (C-2), 156.8 (C-6), 139.4 (C-4), 138.4, 138.1 (2), 129.1-127.8 (Ar), 124.5, 123.2 (C-3, C-5), 104.9, 98.7 (2 × *p*-cym-C_{qAr}), 86.6, 84.8, 83.8, 83.4, 82.9, 77.7, 76.8, 76.0 (4 × *p*-cym-CH_{Ar}, C-1′, C-3′ – C-5′), 75.1, 74.2, 73.5 (3 × PhCH_2), 68.7 (C-6′), 53.6 (C-2′), 31.0 (*i*-Pr-CH), 23.2, 21.5 (2 × *i*-Pr-CH_3), 17.7 (C_6H_4-CH_3). ESI-HRMS positive mode (m/z): calcd for $C_{42}H_{48}ClN_2O_4Ru^+$ $[M\text{-}PF_6]^+$ 781.2349. Found: 781.2346.

Complex **Os-3a**

Prepared from compound **3a** (12.3 mg, 0.024 mmol, 1.9 eq.), **Os-dimer** (10.0 mg, 0.013 mmol) and $TlPF_6$ (8.7 mg, 0.025 mmol) according to general procedure VII. After purification by column chromatography (95 : 5 $CHCl_3$-MeOH) the complex was dissolved in $CHCl_3$ (1 mL) and diisopropyl ether (8 mL) was added. The precipitated product was filtered off, then washed with $CHCl_3$-diisopropyl ether (1 : 8, 1 mL) to give 15.6 mg (64%) dark purple solid. R_f = 0.58 (95 : 5 $CHCl_3$-MeOH). ^1H NMR (400 MHz, $CDCl_3$) δ (ppm): 8.87 (1H, dd, *J* = 6.0, 1.5 Hz, H-6), 7.90 (1H, d, *J* = 7.8 Hz, H-3), 7.81 (1H, td, *J* = 7.8, 1.5 Hz, H-4), 7.41-7.26 (16H, m, Ar, H-5), 6.09, 6.08, 5.82, 5.27 (4 × 1H, 4 d, *J* = 5.7 Hz in each, 4 × *p*-cym-CH_{Ar}), 5.90-5.76 (1H, broad signal, NH_2), 4.91, 4.77 (2 × 1H, 2 d, *J* = 12.3 Hz in both, PhCH_2), 4.76, 4.67 (2 × 1H, 2 d, *J* = 11.5 Hz in both, PhCH_2), 4.59, 4.55 (2 × 1H, 2 d, *J* = 12.2 Hz in both, PhCH_2), 4.50 (1H, d, *J* = 10.2 Hz, H-1′), 4.22 (1H, pt, *J* = 9.0, 8.8 Hz, H-3′ or H-4′), 4.00-3.98 (1H, m, H-5′), 3.84-3.77 (2H, m, H-6′a,b), 3.67 (1H, dd, *J* = 11.4, 4.6 Hz, NH_2), 3.57 (1H, pt, *J* = 9.2, 9.1 Hz, H-3′ or H-4′), 2.47 (1H, hept, *J* = 7.0 Hz, *i*-Pr-C*H*), 2.32-2.23 (1H, m, H-2′), 1.75 (3H, s, C_6H_4-CH_3), 1.19, 0.98 (2 × 3H, 2 d, *J* = 6.9 Hz in both, 2 × *i*-Pr-CH_3); ^{13}C NMR (100 MHz, $CDCl_3$) δ (ppm): 161.3 (C-2), 157.7 (C-6), 139.5 (C-4), 138.4, 138.1 (2), 129.9-127.8 (Ar), 124.9, 122.5 (C-4, C-5), 95.0, 89.9 (2 × *p*-cym-C_{qAr}), 82.7, 78.3, 77.7, 76.8, 76.3, 75.6, 75.4, 73.6 (4 × *p*-cym-CH_{Ar}, C-1′, C-3′ – C-5′), 75.2, 74.2, 73.5 (3 × PhCH_2), 68.7 (C-6′), 53.6 (C-2′), 31.1 (*i*-Pr-CH), 23.6, 21.6 (2 × *i*-Pr-CH_3), 17.6 (C_6H_4-CH_3). ESI-HRMS positive mode (m/z): calcd for $C_{42}H_{47}N_2O_4Os^+$ $[M\text{-}HCl\text{-}PF_6]^+$ 835.3148. Found: 835.3143.

Complex **Ir-3a**

Prepared from compound **3a** (12.2 mg, 0.024 mmol, 1.9 eq.), **Ir-dimer** (10.0 mg, 0.013 mmol) and $TlPF_6$ (8.8 mg, 0.025 mmol) according to general procedure VII. Purification by column chromatography (95 : 5 $CHCl_3$-MeOH) gave 22.7 mg (93%) yellow solid. R_f = 0.51 (95 : 5 $CHCl_3$-MeOH). ^1H NMR (400 MHz, $CDCl_3$) δ (ppm): 8.58 (1H, d, *J* = 5.8 Hz, H-6), 7.92-7.87 (2H, m, H-3, H-4), 7.42-7.27 (16H, m, Ar, H-5), 4.83, 4.70 (2 × 1H, 2 d, *J* = 12.6 Hz in both, PhCH_2), 4.78, 4.69 (2 × 1H, 2 d, *J* = 11.4 Hz in both, PhCH_2), 4.60, 4.56 (2 × 1H, 2 d, *J* = 12.1 Hz in both, PhCH_2), 4.25 (1H, d, *J* = 10.0 Hz, H-1′), 4.12-4.05 (2H, m, H-5′, NH_2), 4.08 (1H, pt, *J* = 8.1, 8,0 Hz, H-3′ or H-4′), 3.95 (1H, dd, *J* = 11.5, 5.5 Hz, NH_2), 3.85 (1H, dd, *J* = 10.8, 4.1 Hz, H-6′a), 3.79 (1H, dd, *J* = 10.8, 3.0 Hz, H-6′b), 3.69 (1H, pt, *J* = 8.0, 7.9 Hz, H-3′ or H-4′), 2.55-2.47 (1H, m, H-2′), 1.41 (15H, s, Cp*-CH_3); ^{13}C NMR (100 MHz, $CDCl_3$) δ (ppm): 160.8 (C-2), 155.3 (C-6), 139.9 (C-4), 138.3, 138.1, 137.8, 129.9, 129.3-127.9 (Ar), 126.0, 123.0 (C-4, C-5), 88.1 (Cp*), 81.5, 77.5, 77.4, 77.1 (C-1′, C-3′ – C-5′), 74.3, 74.1, 73.5 (3 ×

formázott: Betűtípus: Félkövér

formázott: Betűtípus: Félkövér

formázott: Betűtípus: Félkövér

PhCH_2), 69.0 (C-6′), 54.1 (C-2′), 8.5 (Cp*-CH_3). ESI-HRMS positive mode (m/z): calcd for $C_{42}H_{49}ClN_2O_4Ir^+$ [M-PF_6]$^+$ 873.2999. Found: 873.2997.

Complex **Rh-3a**

Prepared from compound **3a** (15.7 mg, 0.031 mmol, 1.9 eq.), **Rh-dimer** (10.0 mg, 0.016 mmol) and $TlPF_6$ (11.3 mg, 0.032 mmol) according to general procedure VII. After purification by column chromatography (95 : 5 $CHCl_3$-MeOH) the complex was dissolved in $CHCl_3$ (1 mL) and diisopropyl ether (8 mL) was added. The precipitated product was filtered off, then washed with $CHCl_3$-diisopropyl ether (1 : 8, 1 mL) to give 23.6 mg (83%) orange solid. R_f = 0.30 (95 : 5 $CHCl_3$-MeOH).^{1}H NMR (400 MHz, $CDCl_3$) δ (ppm): 8.61 (1H, dd, *J* = 5.7, 1.7 Hz, H-6), 7.94-7.85 (2H, m, H-3, H-4), 7.46-7.28 (16H, m, Ar, H-5), 4.81, 4.68 (2 × 1H, 2 d, *J* = 12.5 Hz in both, PhCH_2), 4.77, 4.70 (2 × 1H, 2 d, *J* = 11.2 Hz in both, PhCH_2), 4.61, 4.58 (2 × 1H, 2 d, *J* = 12.8 Hz in both, PhCH_2), 4.26 (1H, d, *J* = 9.9 Hz, H-1′), 4.03 (1H, ddd, *J* = 7.6, 4.1, 3.2 Hz, H-5′), 3.96 (1H, pt, *J* = 7.7, 7.6 Hz, H-3′ or H-4′), 3.85 (1H, dd, *J* = 10.8, 4.1 Hz, H-6′a), 3.79 (1H, dd, *J* = 10.8, 3.2 Hz, H-6′b), 3.72 (1H, pt, *J* = 7.7, 7.7 Hz, H-3′ or H-4′), 3.47 (1H, dd, *J* = 11.1, 5.9 Hz, NH_2), 3.24 (1H, pt, *J* = 10.2 Hz, NH_2), 2.40-2.32 (1H, m, H-2′), 1.43 (15H, s, Cp*-CH_3); ^{13}C NMR (100 MHz, $CDCl_3$) δ (ppm): 160.8 (C-2), 154.2 (C-6), 139.8 (C-4), 138.2, 138.1, 137.7, 129.9, 129.2-127.9 (Ar), 125.6, 123.2 (C-3, C-5), 96.5, 96.4 (Cp*), 82.3, 77.7, 77.6, 76.9 (C-1′, C-3′ – C-5′), 74.3, 74.0, 73.6 (3 × PhCH_2), 69.0 (C-6′), 54.4 (C-2′), 8.9 (Cp*-CH_3). ESI-HRMS positive mode (m/z): calcd for $C_{42}H_{49}ClN_2O_4Rh^+$ [M-PF_6]$^+$ 783.2430. Found: 783.2430.

Complex **Ru-3d**

Prepared from compound **3d** (16.7 mg, 0.033 mmol, 2 eq.), **Ru-dimer** (10.0 mg, 0.016 mmol) and $TlPF_6$ (11.4 mg, 0.033 mmol) according to general procedure VII. After purification by column chromatography (100 : 1 $CHCl_3$-MeOH) the complex was dissolved in $CHCl_3$ (1.5 mL) and diisopropyl ether (12 mL) was added. The precipitated product was filtered off, then washed with diisopropyl ether (1 mL) to give 10.0 mg (33%) brown solid. R_f = 0.31 (95 : 5 $CHCl_3$-MeOH). ^{1}H NMR (400 MHz, $CDCl_3$) δ (ppm): 9.09 (1H, s, H-3), 8.94 (1H, dd, *J* = 3.2, 1.1 Hz, H-5), 8.65 (1H, d, *J* = 3.2 Hz, H-6), 7.43-7.26 (15H, m, Ar), 5.89, 5.85, 5.54, 5.15 (4 × 1H, 4 d, *J* = 6.0 Hz in each, 4 × *p*-cym-CH_{Ar}), 5.22-5.16 (1H, broad signal, NH_2), 4.92, 4.77 (2 × 1H, 2 d, *J* = 12.3 Hz in both, PhCH_2), 4.76, 4.66 (2 × 1H, 2 d, *J* = 11.3 Hz in both, PhCH_2), 4.67 (1H, d, *J* = 10.3 Hz, H-1′), 4.56 (2H, s, PhCH_2), 4.20 (1H, pt, *J* = 9.1, 8.9 Hz, H-3′ or H-4′), 3.99-3.94 (1H, m, H-5′), 3.81-3.77 (2H, m, H-6′a,b), 3.56 (1H, pt, *J* = 9.2, 9.1 Hz, H-3′ or H-4′), 3.16 (1H, dd, *J* = 11.1, 5.1 Hz, NH_2), 2.56 (1H, hept, *J* = 6.9 Hz, *i*-Pr-*CH*), 2.04-1.95 (1H, m, H-2′), 1.76 (3H, s, C_6H_4-CH_3), 1.16, 1.03 (2 × 3H, 2 d, *J* = 6.9 Hz in both, 2 × *i*-Pr-CH_3); ^{13}C NMR (100 MHz, $CDCl_3$) δ (ppm): 156.5 (C-2), 149.9, 145.3, 145.2 (C-3, C-5, C-6), 138.4, 138.0, 137.9, 129.1-127.9 (Ar), 105.7, 98.9 (2 × *p*-cym-C_{qAr}), 86.8, 85.2, 84.1, 84.0, 83.3, 77.5, 77.2, 75.1 (4 × *p*-cym-CH_{Ar}, C-1′, C-3′ – C-5′), 75.3, 74.4, 73.5 (3 × PhCH_2), 68.5 (C-6′), 53.2 (C-2′), 31.1 (*i*-Pr-*CH*), 23.0, 21.6 (2 × *i*-Pr-CH_3), 17.8 (C_6H_4-CH_3). ESI-HRMS positive mode (m/z): calcd for $C_{41}H_{47}ClN_3O_4Ru^+$ [M-PF_6]$^+$ 782.2307. Found: 782.2315.

Complex **Os-3d**

Prepared from compound **3d** (13.0 mg, 0.025 mmol, 2 eq.), **Os-dimer** (10.0 mg, 0.013 mmol) and $TlPF_6$ (8.7 mg, 0.025 mmol) according to general procedure VII. After purification by column chromatography (100 : 1 $CHCl_3$-MeOH) the complex was dissolved in $CHCl_3$ (1.5 mL) and diisopropyl ether (12 mL) was added. The precipitated product was filtered off, then washed with diisopropyl ether (1 mL) to give 12.0 mg (47%) greenish brown solid. R_f = 0.27 (95 : 5 $CHCl_3$-MeOH). ^{1}H NMR (400 MHz, $CDCl_3$) δ (ppm): 9.10 (1H, s, H-3), 8.76 (1H, dd, *J* = 3.3, 1.1 Hz, H-5), 8.56 (1H, d, *J* = 3.3 Hz, H-6), 7.42-7.27 (15H, m, Ar), 6.12, 6.11, 5.80, 5.29 (4 × 1H, 4 d, *J* = 5.8 Hz in each, 4 × *p*-cym-CH_{Ar}), 5.90-5.77 (1H, broad signal, NH_2), 4.92, 4.75 (2 × 1H, 2 d, *J* = 12.3 Hz in both, PhCH_2), 4.77, 4.68 (2 × 1H, 2 d, *J* = 11.4 Hz in both, PhCH_2), 4.70-4.65 (1H, broad signal, NH_2), 4.62 (1H, d, *J* = 10.4 Hz, H-1′), 4.56 (2H, s, PhCH_2), 4.23 (1H, pt, *J* = 9.1, 9.0 Hz, H-3′ or H-4′), 3.99-3.95 (1H, m, H-

formázott: Betűtípus: Félkövér

formázott: Betűtípus: Félkövér

formázott: Betűtípus: Félkövér

5′), 3.83-3.76 (2H, m, H-6′a,b), 3.59 (1H, pt, *J* = 9.3, 9.2 Hz, H-3′ or H-4′), 2.46 (1H, hept, *J* = 6.9 Hz, *i*-Pr-C*H*), 2.33-2.24 (1H, m, H-2′), 1.80 (3H, s, C_6H_4-CH_3), 1.18, 0.99 (2 × 3H, 2 d, *J* = 6.9 Hz in both, 2 × *i*-Pr-CH_3); ^{13}C NMR (100 MHz, $CDCl_3$) δ (ppm): 155.4 (C-2), 150.4, 146.0, 144.8 (C-3, C-5, C-6), 138.4, 138.0, 137.9, 129.1-127.9 (Ar), 96.2, 90.3 (2 × *p*-cym-C_{qAr}), 82.5, 78.5, 77.5, 77.1, 76.2, 76.0, 75.3, 74.7 (4 × *p*-cym-CH_{Ar}, C-1′, C-3′ – C-5′), 75.3, 74.4, 73.5 (3 × PhCH_2), 68.4 (C-6′), 53.0 (C-2′), 31.1 (*i*-Pr-CH), 23.4, 21.7 (2 × *i*-Pr-CH_3), 17.6 (C_6H_4-CH_3). ESI-HRMS positive mode (m/z): calcd for $C_{41}H_{47}ClN_3O_4Os^+$ $[M\text{-}PF_6]^+$ 872.2861. Found: 872.2867.

Complex **Ru-5a**

Prepared from compound **5a** (26 mg, 0.094 mmol, 2.3 eq.), **Ru-dimer** (25 mg, 0.041 mmol) and $TlPF_6$ (62 mg, 0.176 mmol, 4.3 eq.) according to general procedure VII. Column chromatographic purification (95 : 5 $CHCl_3$-MeOH) gave 23 mg (43%) yellow solid. R_f = 0.50 (7 : 3 $CHCl_3$-MeOH). ^{1}H NMR (400 MHz, CD_3OD) δ (ppm); 9.09 (1H, ddd, *J* = 5.8, 1.4, 0.8 Hz, H-6), 8.07-8.00 (2H, m, H-3, H-4), 7.53-4.49 (1H, ddd, *J* = 7.8, 5.8, 2.0 Hz, H-5), 5.96, 5.94, 5.81, 5.64 (4 × 1H, 4 d, *J* = 6.0 Hz in each, 4 × *p*-cym-CH_{Ar}), 5.70 (1H, dd, *J* = 11.8, 5.6 Hz, NH_2), 4.41 (1H, d, *J* = 10.1 Hz, H-1′), 4.01 (1H, dd, *J* = 12.2, 2.1 Hz, H-6′a), 3.87-3.79 (1H, broad signal, NH_2), 3.84 (1H, pt, *J* = 9.6, 8.9 Hz, H-3′), 3.82 (1H, dd, *J* = 12.2, 5.6 Hz, H-6′b), 3.67 (1H, ddd, *J* = 9.5, 5.6, 2.1 Hz, H-5′), 3.39 (1H, pt, *J* = 9.3, 9.2 Hz, H-4′), 2.83 (1H, hept, *J* = 6.9 Hz, *i*-Pr-C*H*), 2.22-2.18 (1H, m, H-2), 1.91 (3H, s, CH_3), 1.28, 1.23 (2 × 3H, 2 d, *J* = 6.9 Hz in both, 2 × *i*-Pr-CH_3); ^{13}C NMR (100 MHz, CD_3OD) δ (ppm): 161.8 (C-2), 158.1 (C-6), 140.9 (C-4), 125.8, 123.6 (C-3, C-5), 106.0, 100.8 (2 × *p*-cym-C_{qAr}), 87.8, 85.2, 84.1, 83.4, 81.8, 80.2, 77.5, 71.3 (4 × *p*-cym-CH_{Ar}, C-1′, C-3′ – C-5′), 62.6 (C-6′), 56.1 (C-2′), 32.3 (*i*-Pr-CH), 23.3, 21.9 (2 × *i*-Pr-CH_3), 18.0 (C_6H_4-CH_3). ESI-HRMS positive mode (m/z): calcd for $C_{21}H_{30}ClN_2O_4Ru^+$ $[M\text{-}PF_6]^+$ 511.0935. Found: 511.0934.

Complex **Ru-7a**

Prepared from compound **7a** (18.0 mg, 0.033 mmol, 2 eq.), **Ru-dimer** (10.0 mg, 0.016 mmol) and $TlPF_6$ (11.4 mg, 0.033 mmol) according to general procedure VII. The crude product was dissolved in $CHCl_3$ (3 mL) and diisopropyl ether (12 mL) was added. The precipitation was filtered off, then washed with $CHCl_3$-diisopropyl ether (1 : 2, 1 mL) to give 25.5 mg (81%) yellow solid. R_f = 0.49 (95 : 5 $CHCl_3$-MeOH). ^{1}H NMR (400 MHz, $CDCl_3$) δ (ppm): 9.02 (1H, d, *J* = 6.1 Hz, H-6), 8.12-7.31 (18H, m, Ar, H-3, H-4, H-5), 6.68-6.59 (1H, broad signal, NH_2), 6.15 (1H, d, *J* = 5.9 Hz, *p*-cym-CH_{Ar}), 6.10 (1H, pt, *J* = 9.4, 9.3 Hz, H-3′), 6.03, 6.00 (2 × 1H, 2 d, *J* = 6.0 Hz in both, 2 × *p*-cym-CH_{Ar}), 5.75 (1H, pt, *J* = 9.8, 9.6 Hz, H-4′), 5.47 (1H, d, *J* = 6.0 Hz, *p*-cym-CH_{Ar}), 5.01-4.97 (2H, m, H-1′, H-6′a), 4.86 (1H, ddd, *J* = 10.0, 3.4, 2.8 Hz, H-5′), 4.49 (1H, dd, *J* = 12.7, 3.4 Hz, H-6′b), 3.39 (1H, dd, *J* = 11.2, 7.3 Hz, NH_2), 2.89 (1H, hept, *J* = 6.9 Hz, *i*-Pr-C*H*), 2.65-2.57 (1H, m, H-2′), 1.81 (3H, s, C_6H_4-CH_3), 1.25, 1.23 (2 × 3H, 2 d, *J* = 6.9 Hz in both, 2 × *i*-Pr-CH_3); ^{13}C NMR (100 MHz, $CDCl_3$) δ (ppm): 168.7, 166.3, 165.6 (3 × C=O), 160.2 (C-2), 156.7 (C-6), 140.0 (C-4), 134.4, 133.8, 133.3, 130.4-130.0, 129.9, 128.7-128.6, 127.8 (Ar), 125.3, 122.9 (C-3, C-5), 104.3, 100.7 (2 × *p*-cym-C_{qAr}), 88.0, 84.5, 82.6, 82.3, 77.9, 77.2, 74.4, 67.6 (4 × *p*-cym-CH_{Ar}, C-1′, C-3′ – C-5′), 62.1 (C-6′), 54.3 (C-2′), 31.0 (*i*-Pr-CH), 22.8, 22.2 (2 × *i*-Pr-CH_3), 17.9 (C_6H_4-CH_3). ESI-HRMS positive mode (m/z): calcd for $C_{42}H_{42}ClN_2O_7Ru^+$ $[M\text{-}PF_6]^+$ 823.1727. Found: 823.1727.

Complex **Os-7a**

Prepared from compound **7a** (14.0 mg, 0.025 mmol, 2 eq.), **Os-dimer** (10.0 mg, 0.013 mmol) and $TlPF_6$ (8.7 mg, 0.025 mmol) according to general procedure VII. After purification by column chromatography (95 : 5 $CHCl_3$-MeOH) the complex was dissolved in $CHCl_3$ (2 mL) and diisopropyl ether (16 mL) was added. The precipitated product was filtered off, then washed with $CHCl_3$-diisopropyl ether (1 : 4, 1 mL) to give 11.5 mg (43%) dark purple solid. R_f = 0.45 (95 : 5 $CHCl_3$-MeOH). ^{1}H NMR (500 MHz, $CDCl_3$) δ (ppm): 8.86 (1H, dd, *J* = 5.9, 1.6 Hz, H-6), 8.15-7.34 (18H, m, Ar, H-3, H-4, H-5), 7.24-7.16 (1H, broad signal, NH_2), 6.52, 6.38, 6.20, 5.66 (4 × 1H, 4 d, *J* = 5.6 Hz in each, 4 × *p*-cym-CH_{Ar}),

formázott: Betűtípus: Félkövér

formázott: Betűtípus: Félkövér

formázott: Betűtípus: Félkövér

5.96 (1H, pt, *J* = 9.3, 9.1 Hz, H-3′ or H-4′), 5.78 (1H, pt, *J* = 9.7, 9.6 Hz, H-3′ or H-4′), 4.99 (1H, dd, *J* = 12.7, 2.1 Hz, H-6′a), 4.88 (1H, d, *J* = 10.1 Hz, H-1′), 4.84 (1H, ddd, *J* = 10.2, 3.3, 2.1 Hz, H-5′), 4.49 (1H, dd, *J* = 12.7, 3.3 Hz, H-6′b), 4.24 (1H, dd, *J* = 11.6, 7.2 Hz, NH_2), 2.87-2.78 (2H, m, H-2′, *i*-Pr-C*H*), 1.85 (3H, s, C_6H_4-CH_3), 1.27, 1.26 (2 × 3H, 2 d, *J* = 6.9 Hz in both, 2 × *i*-Pr-CH_3); ^{13}C NMR (100 MHz, $CDCl_3$) δ (ppm): 168.8, 166.3, 165.6 (3 × C=O), 159.6 (C-2), 156.8 (C-6), 140.2 (C-4), 134.5, 133.8, 133.3, 130.4-130.0, 129.9, 128.8-128.6, 127.7 (Ar), 125.5, 122.4 (C-3, C-5), 94.3, 92.2 (2 × *p*-cym-C_{qAr}), 80.6, 79.0, 77.1, 76.2, 74.3, 73.2, 73.1, 67.3 (4 × *p*-cym-CH_{Ar}, C-1′, C-3′ – C-5′), 62.0 (C-6′), 54.2 (C-2′), 31.2 (*i*-Pr-CH), 23.1, 22.6 (2 × *i*-Pr-CH_3), 17.8 (C_6H_4-CH_3). ESI-HRMS positive mode (m/z): calcd for $C_{42}H_{42}ClN_2O_7Os^+$ [M-PF_6]$^+$ 913.2292. Found: 913.2288.

Complex **Ir-7a**

Prepared from compound **7a** (13.9 mg, 0.025 mmol, 2 eq.), **Ir-dimer** (10.0 mg, 0.013 mmol) and $TlPF_6$ (8.8 mg, 0.025 mmol) according to general procedure VII. The crude product was dissolved in $CHCl_3$ (3 mL) and diisopropyl ether (12 mL) was added. The precipitation was filtered off, then washed with $CHCl_3$-diisopropyl ether (1 : 1, 1 mL) to give 20.1 mg (76%) yellow solid. R_f = 0.36 (95 : 5 $CHCl_3$-MeOH). ^{1}H NMR (400 MHz, $CDCl_3$) δ (ppm): 8.67 (1H, ddd, *J* = 5.8, 1.6, 0.7 Hz, H-6), 8.14-7.36 (18H, m, Ar, H-3, H-4, H-5), 6.08 (1H, dd, *J* = 11.9, 6.0 Hz, NH_2), 5.82 (1H, pt, *J* = 9.9, 9.7 Hz, H-4′), 5.69 (1H, pt, *J* = 9.6, 9.5 Hz, H-3′), 5.08 (1H, dd, *J* = 12.8, 2.2 Hz, H-6′a), 4.78 (1H, ddd, *J* = 10.0, 3.2, 2.2 Hz, H-5′), 4.53 (1H, dd, *J* = 12.8, 3.2 Hz, H-6′b), 4.49 (1H, d, *J* = 10.5 Hz, H-1′), 5.29 (1H, dd, *J* = 11.9, 8.1 Hz, NH_2), 3.09-3.00 (1H, m, H-2′), 1.76 (15H, s, Cp*-CH_3); ^{13}C NMR (100 MHz, acetone-d_6) δ (ppm): 167.9, 166.5, 166.0 (3 × C=O), 158.9 (C-2), 156.3 (C-6), 141.4 (C-4), 134.7, 134.6, 134.2, 130.8, 130.7-130.4, 130.0, 129.9, 129.5-129.4 (Ar), 127.2, 123.4 (C-3, C-5), 89.0 (Cp*), 81.8, 76.4, 76.3, 70.1 (C-1′, C-3′ – C-5′), 63.3 (C-6′), 54.8 (C-2′), 9.2 (Cp*-CH_3). ESI-HRMS positive mode (m/z): calcd for $C_{42}H_{43}ClN_2O_7Ir^+$ [M-PF_6]$^+$ 915.2377. Found: 915.2381.

Complex **Rh-7a**

Prepared from compound **7a** (17.9 mg, 0.032 mmol, 2 eq.), **Rh-dimer** (10.0 mg, 0.016 mmol) and $TlPF_6$ (11.3 mg, 0.032 mmol) according to general procedure VII. The crude product was dissolved in $CHCl_3$ (3 mL) and diisopropyl ether (12 mL) was added. The precipitation was filtered off, then washed with $CHCl_3$-diisopropyl ether (1 : 1, 0.5 mL) to give 27.1 mg (86%) orange solid. R_f = 0.32 (95 : 5 $CHCl_3$-MeOH). ^{1}H NMR (400 MHz, $CDCl_3$) δ (ppm): 8.68 (1H, d, *J* = 5.3 Hz, H-6), 8.13-7.43 (18H, m, Ar, H-3, H-4, H-5), 5.81 (1H, pt, *J* = 9.8, 9.7 Hz, H-3′ or H-4′), 5.66 (1H, pt, *J* = 9.8, 9.6 Hz, H-3′ or H-4′), 5.15 (1H, dd, *J* = 11.0, 5.0 Hz, NH_2), 5.06 (1H, dd, *J* = 12.9, 2.2 Hz, H-6′a), 4.72 (1H, ddd, *J* = 10.2, 3.1, 2.2 Hz, H-5′), 4.53 (1H, d, *J* = 10.0 Hz, H-1′), 4.51 (1H, dd, *J* = 12.9, 3.1 Hz, H-6′b), 3.51 (1H, pt, *J* = 10.2, 9.8 Hz, NH_2), 2.88-2.80 (1H, m, H-2′), 1.76 (15H, s, Cp*-CH_3); ^{13}C NMR (100 MHz, $CDCl_3$) δ (ppm): 169.3, 166.2, 165.6 (3 × C=O), 158.0 (C-2), 153.8 (C-6), 140.4 (C-4), 134.6, 133.8, 133.3, 130.5-130.0, 129.9, 128.8-128.7, 128.6, 127.6 (Ar), 126.0, 123.4 (C-3, C-5), 97.4, 97.3 (Cp*), 79.1, 78.3, 75.3, 67.2 (C-1′, C-3′ – C-5′), 62.0 (C-6′), 55.0 (C-2′), 9.3 (Cp*-CH_3). ESI-HRMS positive mode (m/z): calcd for $C_{42}H_{43}ClN_2O_7Rh^+$ [M-PF_6]$^+$ 825.1808. Found: 825.1807.

Complex **Ru-7b**

Prepared from compound **7b** (18.5 mg, 0.033 mmol, 2.05 eq.), **Ru-dimer** (10.0 mg, 0.016 mmol) and $TlPF_6$ (11.4 mg, 0.033 mmol) according to general procedure VII. The crude product was dissolved in $CHCl_3$ (3 mL) and diisopropyl ether (12 mL) was added. The precipitation was filtered off, then washed with $CHCl_3$-diisopropyl ether (1 : 2, 2 mL) to give 28.0 mg (88%) brownish orange solid. R_f = 0.51 (95 : 5 $CHCl_3$-MeOH). Diastereomeric ratio = 2 : 1. ^{1}H NMR (400 MHz, $CDCl_3$) δ (ppm): 9.18 (dd, *J* = 4.9, 2.0 Hz, major H-6), 9.08 (dd, *J* = 4.8, 2.0 Hz, minor H-6), 8.21 (dd, *J* = 8.5, 2.0 Hz, major H-4), 8.19 (dd, *J* = 8.4, 2.0 Hz, minor H-4), 8.08-7.25 (m, minor and major Ar), 7.79 (dd, *J* = 8.5, 4.9 Hz, minor H-5), 7.77 (dd, *J* = 8.5, 4.9 Hz, major H-5), 6.33 (pt, *J* = 10.6 Hz, major NH_2), 6.09 (pt, *J* = 9.2,

formázott: Betűtípus: Félkövér

formázott: Betűtípus: Félkövér

formázott: Betűtípus: Félkövér

9.0 Hz, major H-3'), 6.06 (pt, *J* = 9.5, 9.1 Hz, minor H-3'), 6.03-5.96 (broad signal, minor NH_2), 6.00, 5.94, 5.76, 5.42 (4 d, *J* = 6.0 Hz in each, 4 × major *p*-cym-CH_{Ar}), 5.82, 5.80, 5.77, 5.69 (4 d, *J* = 6.0 Hz in each, 4 × minor *p*-cym-CH_{Ar}), 5.65 (pt, *J* = 9.9, 9.6 Hz, major H-4'), 5.57 (pt, *J* = 9.2, 9.1 Hz, minor H-4'), 5.23 (d, *J* = 10.3 Hz, major H-1'), 5.18 (d, *J* = 10.5 Hz, minor H-1'), 4.97 (dd, *J* = 12.7, 2.2 Hz, major H-6'a), 4.72-4.68 (m, minor H-6'a or H-6'b), 4.68 (ddd, *J* = 10.1, 3.4, 2.2 Hz, major H-5'), 4.49-4.44 (m, minor H-6'a or H-6'b), 4.46 (dd, *J* = 12.7, 3.4 Hz, major H-6'b), 4.44-4.39 (m, minor H-5'), 4.13 (dd, *J* = 11.3, 4.9 Hz, major NH_2), 3.79 (pt, *J* = 11.9 Hz, minor NH_2), 3.22-3.15 (m, minor H-2'), 3.01 (hept, *J* = 6.9 Hz, minor *i*-Pr-C*H*), 2.93-2.85 (m, major H-2'), 2.80 (hept, *J* = 6.9 Hz, major *i*-Pr-C*H*), 2.28 (s, minor C_6H_4-CH_3), 1.85 (s, major C_6H_4-CH_3), 1.28, 1.27 (2 d, *J* = 6.9 Hz in both, 2 × minor *i*-Pr-CH_3), 1.22, 1.17 (2 d, *J* = 6.9 Hz in both, 2 × major *i*-Pr-CH_3); ^{13}C NMR (100 MHz, $CDCl_3$) δ (ppm): 167.7, 166.4, 165.4, 165.3 (3 × major C=O, major C-3), 166.9, 166.3, 165.3, 164.1 (3 × minor C=O, minor C-3), 152.3 (major C-6), 151.1 (minor C-6), 134.1, 133.9, 133.8, 133.7, 133.5 (2), 130.3-127.8 (minor and major Ar, C-4, C-5), 105.7, 100.5 (2 × minor *p*-cym-C_{qAr}), 104.9, 100.5 (2 × major *p*-cym-C_{qAr}), 88.5, 85.7, 85.5, 83.2 (4 × major *p*-cym-CH_{Ar}), 86.6, 86.5, 86.0, 83.3 (4 × minor *p*-cym-CH_{Ar}), 77.4, 75.0, 74.4, 67.7 (major C-1', C-3' – C-5'), 76.3, 75.7, 73.3, 69.2 (minor C-1', C-3' – C-5'), 62.7 (minor C-6'), 61.9 (major C-6'), 53.6 (minor C-2'), 53.6 (major C-2'), 30.9 (minor *i*-Pr-CH), 30.8 (major *i*-Pr-CH), 22.9, 21.8 (2 × major *i*-Pr-CH_3), 22.5, 22.3 (2 × minor *i*-Pr-CH_3), 18.2 (minor C_6H_4-CH_3), 17.9 (major C_6H_4-CH_3); ESI-HRMS positive mode (m/z): calcd for $C_{41}H_{41}ClN_3O_7Ru^+$ $[M\text{-}PF_6]^+$ 824.1679. Found: 824.1674.

Complex **Os-7b**

Prepared from compound **7b** (14.2 mg, 0.026 mmol, 2.05 eq.), **Os-dimer** (10.0 mg, 0.0126 mmol) and $TlPF_6$ (8.7 mg, 0.025 mmol) according to general procedure VII. The crude product was dissolved in $CHCl_3$ (3 mL) and diisopropyl ether (6 mL) was added. The precipitatation was filtered off, then washed with $CHCl_3$-diisopropyl ether (1 : 2, 3 mL) to give 19.6 mg (73%) dark green solid. R_f = 0.38 (95 : 5 $CHCl_3$-MeOH). Diastereomeric ratio = 5 : 4. ^{1}H NMR (400 MHz, $CDCl_3$) δ (ppm): 9.08 (dd, *J* = 4.9, 2.0 Hz, major H-6), 8.93 (dd, *J* = 4.8, 2.0 Hz, minor H-6), 8.30 (dd, *J* = 8.7, 2.0 Hz, minor H-4), 8.24 (dd, *J* = 8.6, 2.0 Hz, major H-4), 8.12-7.31 (m, minor and major Ar), 7.85 (dd, *J* = 8.7, 4.8 Hz, minor H-5), 7.69 (dd, *J* = 8.6, 4.9 Hz, major H-5), 6.89 (pt, *J* = 11.0 Hz, major NH_2), 6.72-6.65 (broad signal, minor NH_2), 6.27, 6.22, 6.19, 5.70 (4 d, *J* = 5.8 Hz in each, 4 × major *p*-cym-CH_{Ar}), 6.08, 6.04, 6.03, 5.92 (4 d, *J* = 5.7 Hz in each, 4 × minor *p*-cym-CH_{Ar}), 5.94 (pt, *J* = 9.0, 9.0 Hz, major H-3'), 5.88 (pt, *J* = 9.2, 8.9 Hz, minor H-3'), 5.73 (pt, *J* = 9.9, 9.8 Hz, major H-4'), 5.63 (pt, *J* = 9.4, 9.3 Hz, minor H-4'), 5.49 (d, *J* = 10.5 Hz, minor H-1'), 5.12 (d, *J* = 10.3 Hz, major H-1'), 4.98 (dd, *J* = 12.7, 2.2 Hz, major H-6'a), 4.73 (dd, *J* = 12.5, 2.5 Hz, minor H-6'a), 4.70 (ddd, *J* = 10.1, 3.4, 2.2 Hz, major H-5'), 4.64 (dd, *J* = 11.7, 4.9 Hz, major NH_2), 4.52-4.44 (m, minor and major H-6'b), 4.44-4.34 (m, minor H-5', NH_2), 3.38-3.27 (m, minor H-2'), 3.13-3.05 (m, major H-2'), 2.88 (hept, *J* = 6.9 Hz, minor *i*-Pr-C*H*), 2.77 (hept, *J* = 6.9 Hz, major *i*-Pr-C*H*), 2.26 (s, minor C_6H_4-CH_3), 1.93 (s, major C_6H_4-CH_3), 1.26-1.20 (m, 2 × minor and major *i*-Pr-CH_3); ^{13}C NMR (100 MHz, $CDCl_3$) δ (ppm): 167.9, 167.0, 166.4, 166.3, 165.4, 165.3, 164.4, 163.6 (3 × minor and major C=O, minor and major C-3), 152.7 (major C-6), 152.0 (minor C-6), 134.2, 133.9, 133.8, 133.7, 133.5, 133.4, 130.9-127.9 (minor and major Ar, C-4, C-5), 96.5, 94.2 (2 × minor *p*-cym-C_{qAr}), 94.9, 92.5 (2 × major *p*-cym-C_{qAr}), 80.3, 79.8 (2), 78.3 (2), 77.0, 76.5, 75.2 (2), 75.9, 75.8, 74.3, 73.6, 73.3, 69.0, 67.4 (4 × minor and major *p*-cym-CH_{Ar}, minor and major C-1', C-3' – C-5'), 62.6 (minor C-6'), 61.8 (major C-6'), 54.5 (minor C-2'), 53.5 (major C-2'), 31.0 (minor *i*-Pr-CH), 30.9 (major *i*-Pr-CH), 22.4, 21.9 (2 × major *i*-Pr-CH_3), 22.7, 22.6 (2 × minor *i*-Pr-CH_3), 18.2 (minor C_6H_4-CH_3), 17.9 (major C_6H_4-CH_3). ESI-HRMS positive mode (m/z): calcd for $C_{41}H_{41}ClN_3O_7Os^+$ $[M\text{-}PF_6]^+$ 914.2234. Found: 914.2239.

Complex **Ir-7b**

Prepared from compound **7b** (14.2 mg, 0.026 mmol, 2.05 eq.), **Ir-dimer** (10.0 mg, 0.013 mmol) and $TlPF_6$ (8.8 mg, 0.025 mmol) according to general procedure VII. The crude

formázott: Betűtípus: Félkövér

formázott: Betűtípus: Félkövér

product was dissolved in $CHCl_3$ (3 mL) and diisopropyl ether (6 mL) was added. The precipitation was filtered off, then washed with $CHCl_3$-diisopropyl ether (1 : 1, 4 mL) to give 18.5 mg (69%) yellow solid. R_f = 0.33 (95 : 5 $CHCl_3$-MeOH). Diastereomeric ratio = 9 : 1. ^{1}H NMR (400 MHz, $CDCl_3$) δ (ppm): 9.09 (dd, *J* = 4.9, 2.0 Hz, major H-6), 8.96 (dd, *J* = 4.8, 2.0 Hz, minor H-6), 8.34 (dd, *J* = 8.7, 2.0 Hz, major H-4), 8.29 (dd, *J* = 8.7, 2.0 Hz, minor H-4), 8.12-7.34 (m, minor and major Ar), 7.86 (dd, *J* = 8.7, 4.8 Hz, minor H-5), 7.78 (dd, *J* = 8.7, 4.9 Hz, major H-5), 5.96 (d, *J* = 10.2 Hz, minor H-1′), 5.87 (pt, *J* = 9.1, 9.0 Hz, major H-3′ or H-4′), 5.81 (pt, *J* = 9.8, 9.3 Hz, minor H-3′ or H-4′), 5.78 (pt, *J* = 9.9, 9.5 Hz, major H-3′ or H-4′), 5.66 (pt, *J* = 9.2, 9.1 Hz, minor H-3′ or H-4′), 5.59 (pt, *J* = 10.6 Hz, major NH_2), 5.36-5.29 (m, minor NH_2), 5.12-5.05 (m, minor NH_2), 4.99 (dd, *J* = 12.7, 2.2 Hz, major H-6′a), 4.89 (d, *J* = 10.3 Hz, major H-1′), 4.75 (ddd, *J* = 10.3, 3.6, 2.2 Hz, major H-5′), 4.77-4.66 (m, major NH_2, minor H-6′a), 4.54 (dd, *J* = 12.5, 5.2 Hz, minor H-6′b), 4.48 (dd, *J* = 12.7, 3.6 Hz, major H-6′b), 4.29 (ddd, *J* = 10.0, 5.2, 2.7 Hz, minor H-5′), 3.75-3.67 (m, minor H-2′), 3.44-3.35 (m, major H-2′), 1.69 (s, major Cp*-C*H*$_3$), 1.57 (s, minor Cp*-C*H*$_3$); ^{13}C NMR (100 MHz, $CDCl_3$) δ (ppm); only the major isomer can be clearly assigned: 168.4, 166.4, 165.5, 163.7 (3 × C=O, C-3), 153.5 (C-6), 134.3, 133.8, 133.4, 130.5-130.0, 129.8, 129.6-127.6, 127.9 (Ar, C-4, C-5), 89.3 (Cp*), 78.0, 76.4, 74.6, 67.3 (C-1′, C-3′ – C-5′), 61.9 (C-6′), 54.3 (C-2′), 8.8 (Cp*-*C*H$_3$). ESI-HRMS positive mode (m/z): calcd for $C_{41}H_{42}ClN_3O_7Ir^+$ $[M\text{-}PF_6]^+$ 916.2329. Found: 916.2322.

Complex **Rh-7b**

Prepared from compound **7b** (9.2 mg, 0.017 mmol, 2.05 eq.), **Rh-dimer** (5.0 mg, 0.008 mmol) and $TlPF_6$ (5.6 mg, 0.016 mmol) according to general procedure VII. The crude product was dissolved in $CHCl_3$ (1.5 mL) and diisopropyl ether (3 mL) was added. The precipitation was filtered off, then washed with $CHCl_3$-diisopropyl ether (1 : 1, 2 mL) to give 13.5 mg (86%) orange solid. R_f = 0.38 (95 : 5 $CHCl_3$-MeOH). Diastereomeric ratio = 5 : 1. ^{1}H NMR (400 MHz, $CDCl_3$) δ (ppm): 9.17 (dd, *J* = 4.9, 1.9 Hz, major H-6), 9.10 (dd, *J* = 4.8, 1.9 Hz, minor H-6), 8.28 (dd, *J* = 8.7, 1.9 Hz, major H-4), 8.17 (dd, *J* = 8.7, 1.9 Hz, minor H-4), 8.12-7.32 (m, minor and major Ar), 7.80 (dd, *J* = 8.7, 4.8 Hz, minor H-5), 7.77 (dd, *J* = 8.7, 4.9 Hz, major H-5), 6.01 (d, *J* = 10.0 Hz, minor H-1′), 5.89 (pt, *J* = 9.2, 9.1 Hz, major H-3′ or H-4′), 5.79 (pt, *J* = 9.7, 9.6 Hz, minor H-3′ or H-4′), 5.74 (pt, *J* = 9.8, 9.6 Hz, major H-3′ or H-4′), 5.61 (pt, *J* = 9.6, 9.4 Hz, minor H-3′ or H-4′), 5.07 (d, *J* = 10.3 Hz, major H-1′), 4.95 (dd, *J* = 12.7, 2.2 Hz, major H-6′a), 4.92-4.87 (broad signal, minor NH_2), 4.81 (pt, *J* = 10.6 Hz, major NH_2), 4.73 (ddd, *J* = 10.2, 3.7, 2.2 Hz, major H-5′), 4.63 (dd, *J* = 12.4, 2.6 Hz, minor H-6′a), 4.50 (dd, *J* = 12.4, 5.4 Hz, minor H-6′b), 4.48 (dd, *J* = 12.7, 3.7 Hz, major H-6′b), 4.37 (pt, *J* = 9.1 Hz, minor NH_2), 4.25 (dd, *J* = 10.6, 4.4 Hz, major NH_2), 4.21 (ddd, *J* = 10.1, 5.4, 2.6 Hz, minor H-5′), 3.57-3.47 (m, minor H-2′), 3.30-3.21 (m, major H-2′), 1.73 (s, major Cp*-C*H*$_3$); 1.65 (s, minor Cp*-C*H*$_3$); ^{13}C NMR (90 MHz, $CDCl_3$) δ (ppm): 170.0, 165.1, 164.5, 162.7 (3 × minor C=O, minor C-3), 168.3, 166.4, 165.5, 164.5 (3 × major C=O, major C-3), 152.8 (major C-6), 151.4 (minor C-6), 134.5, 134.2, 133.7 (2), 133.4, 133.3, 130.5-128.1 (minor and major C-4, C-5, Ar), 98.0, 97.9 (minor Cp*), 97.5, 97.4 (major Cp*), 79.1, 76.4, 74.3, 68.9 (minor C-1′, C-3′ – C-5′), 78.9, 75.5, 74.6, 67.5 (major C-1′, C-3′ – C-5′), 63.0 (minor C-6′), 62.0 (major C-6′), 54.8 (minor C-2′), 52.6 (major C-2′), 9.0 (major Cp*-CH$_3$), 8.7 (minor Cp*-CH$_3$). ESI-HRMS positive mode (m/z): calcd for $C_{41}H_{42}ClN_3O_7Rh^+$ $[M\text{-}PF_6]^+$ 826.1761. Found: 826.1757.

Complex **Ru-7c**

Prepared from compound **7c** (18.5 mg, 0.033 mmol, 2.05 eq.), **Ru-dimer** (10.0 mg, 0.016 mmol) and $TlPF_6$ (11.4 mg, 0.033 mmol) according to general procedure VII. The crude product was dissolved in $CHCl_3$ (3 mL) and diisopropyl ether (12 mL) was added. The precipitation was filtered off, then washed with $CHCl_3$-diisopropyl ether (1 : 2, 2 mL) to give 31.2 mg (99%) brownish orange solid. R_f = 0.44 (95 : 5 $CHCl_3$-MeOH). ^{1}H NMR (400 MHz, $CDCl_3$) δ (ppm): 9.33, 8.93 (2 ×1H, 2 dd, *J* = 5.8, 2.2 Hz and 4.7, 2.2 Hz, respectively, H-4, H-6), 8.02-7.21 (16H, m, Ar, H-5), 6.19 (1H, dd, *J* = 11.6, 8.3 Hz, NH_2), 6.11 (1H, pt, *J* = 9.2, 9.2 Hz, H-3′ or H-4′), 6.01, 5.91, 5.89, 5.40 (4 × 1H, 4 d, *J* = 6.0 Hz in each, 4 × *p*-cym-

formázott: Betűtípus: Félkövér

formázott: Betűtípus: Félkövér

CH_{Ar}), 5.71 (1H, pt, *J* = 9.7, 9.6 Hz, H-3′ or H-4′), 5.11 (1H, d, *J* = 10.3 Hz, H-1′), 4.82 (1H, dd, *J* = 12.7, 2.4 Hz, H-6′a), 4.73 (1H, m, H-5′), 4.60 (1H, dd, *J* = 12.7, 3.6 Hz, H-6′b), 3.67 (1H, dd, *J* = 11.6, 6.2 Hz, NH_2), 2.94-2.86 (1H, m, H-2′), 2.75 (1H, hept, *J* = 6.9 Hz, *i*-Pr-C*H*), 1.72 (3H, s, C_6H_4-CH_3), 1.23, 1.09 (2 × 3H, 2 d, *J* = 6.9 Hz in both, 2 × *i*-Pr-CH_3); ^{13}C NMR (90 MHz, $CDCl_3$) δ (ppm): 168.5, 166.4, 166.2, 165.2 (3 × C=O, C-2), 165.1 (C-6), 159.4 (C-4), 134.4, 133.8, 133.2, 130.3-128.5, 127.4 (Ar), 122.1 (C-5), 105.4, 100.8 (2 × *p*-cym-C_{qAr}), 86.2, 84.2, 83.5, 82.6 (4 × *p*-cym-CH_{Ar}), 78.0, 77.4, 74.3, 68.2 (C-1′, C-3′ – C-5′), 62.7 (C-6′), 54.2 (C-2′), 31.0 (*i*-Pr-CH), 23.0, 21.8 (2 × *i*-Pr-CH_3), 18.0 (C_6H_4-CH_3). ESI-HRMS positive mode (m/z): calcd for $C_{41}H_{41}ClN_3O_7Ru^+$ $[M\text{-}PF_6]^+$ 824.1679. Found: 824.1681.

Complex **Os-7c**

Prepared from compound **7c** (14.2 mg, 0.026 mmol, 2.05 eq.), **Os-dimer** (10.0 mg, 0.013 mmol) and $TlPF_6$ (8.7 mg, 0.025 mmol) according to general procedure VII. The crude product was dissolved in $CHCl_3$ (3 mL) and diisopropyl ether (6 mL) was added. The precipitation was filtered off, then washed with $CHCl_3$-diisopropyl ether (1 : 1, 2 mL) to give 26.3 mg (98%) dark green solid. R_f = 0.27 (95 : 5 $CHCl_3$-MeOH). ^{1}H NMR (400 MHz, $CDCl_3$) δ (ppm): 9.21, 8.86 (2 ×1H, 2 dd, *J* = 5.9, 2.2 Hz and 4.7, 2.2 Hz, respectively, H-4, H-6), 8.03-7.21 (16H, m, Ar, H-5), 6.86 (1H, dd, *J* = 12.0, 8.5 Hz, NH_2), 6.23, 6.18, 6.14, 5.57 (4 × 1H, 4 d, *J* = 5.7 Hz in each, 4 × *p*-cym-CH_{Ar}), 6.07 (1H, pt, *J* = 9.2, 9.2 Hz, H-3′ or H-4′), 5.74 (1H, pt, *J* = 9.8, 9.6 Hz, H-3′ or H-4′), 5.03 (1H, d, *J* = 10.3 Hz, H-1′), 4.82 (1H, dd, *J* = 12.7, 2.4 Hz, H-6′a), 4.71 (1H, ddd, *J* = 10.2, 3.5, 2.4 Hz, H-5′), 4.60 (1H, dd, *J* = 12.7, 3.5 Hz, H-6′b), 4.43 (1H, dd, *J* = 12.0, 6.0 Hz, NH_2), 3.19-3.10 (1H, m, H-2′), 2.68 (1H, hept, *J* = 6.9 Hz, *i*-Pr-C*H*), 1.75 (3H, s, C_6H_4-CH_3), 1.23, 1.06 (2 × 3H, 2 d, *J* = 6.9 Hz in both, 2 × *i*-Pr-CH_3); ^{13}C NMR (100 MHz, $CDCl_3$) δ (ppm): 168.4, 166.2, 165.6, 165.2 (3 × C=O, C-2), 165.5 (C-6), 159.2 (C-4), 134.5, 133.9, 133.2, 130.3-130.0, 129.8, 128.8-128.5, 127.3 (Ar), 122.4 (C-5), 96.0, 92.5 (2 × *p*-cym-C_{qAr}), 78.3, 77.9, 77.0, 75.8, 74.5, 74.2, 73.5, 68.0 (4 × *p*-cym-CH_{Ar}, C-1′, C-3′ – C-5′), 62.6 (C-6′), 53.9 (C-2′), 31.1 (*i*-Pr-CH), 23.4, 21.9 (2 × *i*-Pr-CH_3), 17.9 (C_6H_4-CH_3). ESI-HRMS positive mode (m/z): calcd for $C_{41}H_{41}ClN_3O_7Os^+$ $[M\text{-}PF_6]^+$ 914.2234. Found: 914.2234.

Complex **Ir-7c**

Prepared from compound **7c** (14.2 mg, 0.026 mmol, 2.05 eq.), **Ir-dimer** (10.0 mg, 0.013 mmol) and $TlPF_6$ (8.8 mg, 0.025 mmol) according to general procedure VII. The crude product was dissolved in $CHCl_3$ (3 mL) and diisopropyl ether (6 mL) was added. The precipitation was filtered off, then washed with $CHCl_3$-diisopropyl ether (1 : 1, 4 mL) to give 26.4 mg (99%) yellow solid. R_f = 0.30 (95 : 5 $CHCl_3$-MeOH). ^{1}H NMR (400 MHz, $CDCl_3$) δ (ppm): 8.98, 8.84 (2 ×1H, 2 dd, *J* = 4.8, 2.2 Hz and 5.9, 2.2 Hz, respectively, H-4, H-6), 8.01-7.29 (16H, m, Ar, H-5), 5.94 (1H, dd, *J* = 11.8, 5.2 Hz, NH_2), 5.83 (1H, pt, *J* = 9.6, 9.6 Hz, H-3′ or H-4′), 5.66 (1H, pt, *J* = 9.5, 9.6 Hz, H-3′ or H-4′), 4.81-4.56 (4H, m, H-1′, H-5′, H-6′a,b), 4.29 (1H, dd, *J* = 11.8, 8.2 Hz, NH_2), 3.37-3.29 (1H, m, H-2′), 1.74 (15H, s, Cp*-CH_3); ^{13}C NMR (90 MHz, $CDCl_3$) δ (ppm): 169.3, 166.3, 165.5, 164.1 (3 × C=O, C-2), 162.3, 160.5 (C-4, C-6), 134.8, 133.8, 133.2, 130.6-130.0, 129.8, 128.9-128.5, 127.5 (Ar), 123.2 (C-5), 89.4 (Cp*), 80.5, 77.9, 75.2, 67.7 (C-1′, C-3′ – C-5′), 62.8 (C-6′), 54.9 (C-2′), 9.1 (Cp*-CH_3). ESI-HRMS positive mode (m/z): calcd for $C_{41}H_{42}ClN_3O_7Ir^+$ $[M\text{-}PF_6]^+$ 916.2329. Found: 916.2324.

Complex **Rh-7c**

Prepared from compound **7c** (9.2 mg, 0.017 mmol, 2.05 eq.), **Rh-dimer** (5.0 mg, 0.008 mmol) and $TlPF_6$ (5.6 mg, 0.016 mmol) according to general procedure VII. The crude product was dissolved in $CHCl_3$ (1.5 mL) and diisopropyl ether (3 mL) was added. The precipitation was filtered off, then washed with $CHCl_3$-diisopropyl ether (1 : 1, 4 mL) to give 15.5 mg (99%) orange solid. R_f = 0.24 (95 : 5 $CHCl_3$-MeOH). ^{1}H NMR (400 MHz, $CDCl_3$) δ (ppm): 9.02, 8.92 (2 ×1H, 2 dd, *J* = 4.9, 2.3 Hz and 5.7, 2.3 Hz, respectively, H-4, H-6), 8.03-7.29 (16H, m, Ar, H-5), 5.84 (1H, pt, *J* = 9.6, 9.6 Hz, H-3′ or H-4′), 5.67 (1H, pt, *J* = 9.7, 9.6 Hz, H-3′ or H-4′), 5.15 (1H, dd, *J* = 12.1, 3.7 Hz, NH_2), 4.85-4.58 (3H, m, H-5′, H-

formázott: Betűtípus: Félkövér

formázott: Betűtípus: Félkövér

formázott: Betűtípus: Félkövér

6'a,b), 4.72 (1H, d, *J* = 10.2 Hz, H-1'), 3.46 (1H, pt, *J* = 10.0 Hz, NH_2), 3.21-3.13 (1H, m, H-2'), 1.81 (15H, s, Cp*-CH_3); ^{13}C NMR (90 MHz, $CDCl_3$) δ (ppm): 169.4, 166.3, 165.5, 164.7 (3 × C=O, C-2), 161.7, 160.4 (C-4, C-6), 134.8, 133.8, 133.2, 130.6-130.0, 129.9, 128.9-128.5, 127.5 (Ar), 122.8 (C-5), 97.9, 97.8 (Cp*), 80.0, 78.4, 75.4, 67.8 (C-1', C-3' – C-5'), 62.8 (C-6'), 55.3 (C-2'), 9.5 (Cp*-CH_3). ESI-HRMS positive mode (m/z): calcd for $C_{41}H_{42}ClN_3O_7Rh^+$ $[M\text{-}PF_6]^+$ 826.1761. Found: 826.1757.

Complex **Ru-7d**

Prepared from compound **7d** (18.5 mg, 0.033 mmol, 2.05 eq.), **Ru-dimer** (10.0 mg, 0.016 mmol) and $TlPF_6$ (11.4 mg, 0.033 mmol) according to general procedure VII. The crude product was dissolved in $CHCl_3$ (3 mL) and diisopropyl ether (6 mL) was added. The precipitation was filtered off, then washed with $CHCl_3$-diisopropyl ether (1 : 2, 6 mL) to give 28.8 mg (91%) brown solid. R_f = 0.35 (95 : 5 $CHCl_3$-MeOH). ^{1}H NMR (400 MHz, $CDCl_3$) δ (ppm): 9.09 (1H, s, H-3), 9.02 (1H, dd, *J* = 3.2, 1.1 Hz, H-5), 8.76 (1H, d, *J* = 3.2 Hz, H-6), 8.08-7.26 (15H, m, Ar), 6.26 (1H, dd, *J* = 11.5, 8.3 Hz, NH_2), 6.07 (1H, pt, *J* = 9.3, 9.2 Hz, H-3' or H-4'), 6.01-5.96 (3H, m, 3 × *p*-cym-CH_{Ar}), 5.72 (1H, pt, *J* = 9.7, 9.7 Hz, H-3' or H-4'), 5.44 (1H, d, *J* = 6.0 Hz, *p*-cym-CH_{Ar}), 5.03 (1H, d, *J* = 10.2 Hz, H-1'), 4.98 (1H, dd, *J* = 12.8, 2.2 Hz, H-6'a), 4.76 (1H, ddd, *J* = 10.2, 3.4, 2.2 Hz, H-5'), 4.48 (1H, dd, *J* = 12.8, 3.4 Hz, H-6'b), 3.54 (1H, dd, *J* = 11.5, 6.7 Hz, NH_2), 2.81 (1H, hept, *J* = 6.9 Hz, *i*-Pr-C*H*), 2.73-2.64 (1H, m, H-2'), 1.77 (3H, s, C_6H_4-CH_3), 1.23, 1.16 (2 × 3H, 2 d, *J* = 6.9 Hz in both, 2 × *i*-Pr-CH_3); ^{13}C NMR (90 MHz, $CDCl_3$) δ (ppm): 168.4, 166.3, 165.4 (3 × C=O), 154.7 (C-2), 150.1, 146.3, 144.6 (C-3, C-5, C-6), 134.4, 133.9, 133.4, 130.3-130.0, 129.7, 128.8-128.6, 127.6 (Ar), 105.4, 101.0 (2 × *p*-cym-C_{qAr}), 87.4, 84.9, 83.4, 83.3 (4 × *p*-cym-CH_{Ar}), 77.0, 76.9, 74.6, 67.7 (C-1', C-3' – C-5'), 61.9 (C-6'), 53.8 (C-2'), 31.0 (*i*-Pr-CH), 22.9, 21.9 (2 × *i*-Pr-CH_3), 17.9 (C_6H_4-CH_3). ESI-HRMS positive mode (m/z): calcd for $C_{41}H_{41}ClN_3O_7Ru^+$ $[M\text{-}PF_6]^+$ 824.1679. Found: 824.1673.

Complex **Os-7d**

Prepared from compound **7d** (14.2 mg, 0.026 mmol, 2.05 eq.), **Os-dimer** (10.0 mg, 0.013 mmol) and $TlPF_6$ (8.7 mg, 0.025 mmol) according to general procedure VII. The crude product was dissolved in $CHCl_3$ (3 mL) and diisopropyl ether (6 mL) was added. The precipitation was filtered off, then washed with $CHCl_3$-diisopropyl ether (1 : 2, 3 mL) to give 24.4 mg (91%) brown solid. R_f = 0.29 (95 : 5 $CHCl_3$-MeOH). ^{1}H NMR (400 MHz, $CDCl_3$) δ (ppm): 9.09 (1H, s, H-3), 8.87 (1H, dd, *J* = 3.2, 1.1 Hz, H-5), 8.69 (1H, d, *J* = 3.2 Hz, H-6), 8.09-7.28 (15H, m, Ar), 6.96 (1H, dd, *J* = 11.9, 8.4 Hz, NH_2), 6.27-6.24 (2H, m, 2 × *p*-cym-CH_{Ar}), 6.20 (1H, d, *J* = 5.7 Hz, *p*-cym-CH_{Ar}), 6.03 (1H, pt, *J* = 9.2, 9.2 Hz, H-3' or H-4'), 5.75 (1H, pt, *J* = 9.7, 9.6 Hz, H-3' or H-4'), 5.62 (1H, d, *J* = 5.7 Hz, *p*-cym-CH_{Ar}), 4.99 (1H, dd, *J* = 12.8, 2.2 Hz, H-6'a), 4.94 (1H, d, *J* = 10.2 Hz, H-1'), 4.75 (1H, ddd, *J* = 10.2, 3.4, 2.2 Hz, H-5'), 4.49 (1H, dd, *J* = 12.8, 3.4 Hz, H-6'b), 4.28 (1H, dd, *J* = 11.9, 6.4 Hz, NH_2), 2.97-2.88 (1H, m, H-2'), 2.74 (1H, hept, *J* = 6.9 Hz, *i*-Pr-C*H*), 1.80 (3H, s, C_6H_4-CH_3), 1.23, 1.14 (2 × 3H, 2 d, *J* = 6.9 Hz in both, 2 × *i*-Pr-CH_3); ^{13}C NMR (90 MHz, $CDCl_3$) δ (ppm): 168.5, 166.3, 165.3 (3 × C=O), 153.6 (C-2), 150.4, 147.1, 144.3 (C-3, C-5, C-6), 134.5, 133.9, 133.4, 130.3-130.0, 129.7, 128.8-128.6, 127.5 (Ar), 95.9, 92.7 (2 × *p*-cym-C_{qAr}), 79.5, 77.6, 76.7, 76.6, 74.6, 74.3, 74.1, 67.5 (4 × *p*-cym-CH_{Ar}, C-1', C-3' – C-5'), 61.8 (C-6'), 53.6 (C-2'), 31.1 (*i*-Pr-CH), 23.3, 22.1 (2 × *i*-Pr-CH_3), 17.7 (C_6H_4-CH_3). ESI-HRMS positive mode (m/z): calcd for $C_{41}H_{41}ClN_3O_7Os^+$ $[M\text{-}PF_6]^+$ 914.2234. Found: 914.2233.

Complex **Ir-7d**

Prepared from compound **7d** (14.2 mg, 0.026 mmol, 2.05 eq.), **Ir-dimer** (10.0 mg, 0.013 mmol) and $TlPF_6$ (8.8 mg, 0.025 mmol) according to general procedure VII. The crude product was dissolved in $CHCl_3$ (3 mL) and diisopropyl ether (6 mL) was added. The precipitation was filtered off, then washed with $CHCl_3$-diisopropyl ether (1 : 1, 4 mL) to give 26.5 mg (99%) yellow solid. R_f = 0.24 (95 : 5 $CHCl_3$-MeOH). ^{1}H NMR (400 MHz, $CDCl_3$) δ (ppm): 9.18 (1H, s, H-3), 8.76 (1H, d, *J* = 3.2 Hz, H-6), 8.54 (1H, dd, *J* = 3.2, 1.2 Hz, H-5),

formázott: Betűtípus: Félkövér

formázott: Betűtípus: Félkövér

formázott: Betűtípus: Félkövér

8.10-7.32 (15H, m, Ar), 5.94 (1H, dd, *J* = 11.8, 6.4 Hz, NH_2), 5.84 (1H, pt, *J* = 9.8, 9.7 Hz, H-3′ or H-4′), 5.68 (1H, pt, *J* = 9.6, 9.5 Hz, H-3′ or H-4′), 5.03 (1H, dd, *J* = 12.9, 2.2 Hz, H-6′a), 4.74 (1H, ddd, *J* = 10.1, 3.0, 2.2 Hz, H-5′), 4.56 (1H, d, *J* = 10.1 Hz, H-1′), 4.50 (1H, dd, *J* = 12.9, 3.0 Hz, H-6′b), 4.27 (1H, dd, *J* = 11.8, 7.9 Hz, NH_2), 3.17-3.09 (1H, m, H-2′), 1.73 (15H, s, Cp*-CH_3); ^{13}C NMR (90 MHz, $CDCl_3$) δ (ppm): 169.3, 166.2, 165.5 (3 × C=O), 152.1 (C-2), 147.8, 147.5, 145.5 (C-3, C-5, C-6), 134.8, 133.8, 133.3, 130.6-130.0, 129.8, 128.8-128.6, 128.5, 127.5 (Ar), 89.7 (Cp*), 78.9, 77.7, 75.4, 67.1 (C-1′, C-3′ – C-5′), 61.8 (C-6′), 54.5 (C-2′), 8.9 (Cp*-CH_3). ESI-HRMS positive mode (m/z): calcd for $C_{41}H_{42}ClN_3O_7Ir^+$ $[M\text{-}PF_6]^+$ 916.2329. Found: 916.2331.

Complex **Rh-7d**

Prepared compound **7d** (9.2 mg, 0.017 mmol, 2.05 eq.), **Rh-dimer** (5.0 mg, 0.008 mmol) and $TlPF_6$ (5.6 mg, 0.016 mmol) according to general procedure VII. The crude product was dissolved in $CHCl_3$ (1.5 mL) and diisopropyl ether (3 mL) was added. The precipitation was filtered off, then washed with $CHCl_3$-diisopropyl ether (1 : 1, 4 mL) to give 15.1 mg (96%) orange solid. R_f = 0.21 (95 : 5 $CHCl_3$-MeOH). ^{1}H NMR (400 MHz, $CDCl_3$) δ (ppm): 9.19 (1H, s, H-3), 8.83 (1H, d, *J* = 3.1 Hz, H-6), 8.61 (1H, dd, *J* = 3.1, 1.2 Hz, H-5), 8.11-7.32 (15H, m, Ar), 5.83 (1H, pt, *J* = 9.8, 9.7 Hz, H-3′ or H-4′), 5.69 (1H, pt, *J* = 9.7, 9.6 Hz, H-3′ or H-4′), 5.13 (1H, dd, *J* = 11.4, 6.1 Hz, NH_2), 5.05 (1H, dd, *J* = 12.9, 2.2 Hz, H-6′a), 4.75 (1H, ddd, *J* = 10.2, 2.9, 2.2 Hz, H-5′), 4.69 (1H, d, *J* = 10.1 Hz, H-1′), 4.51 (1H, dd, *J* = 12.9, 2.9 Hz, H-6′b), 3.54 (1H, pt, *J* = 9.9 Hz, NH_2), 3.02-2.93 (1H, m, H-2′), 1.78 (15H, s, Cp*-CH_3); ^{13}C NMR (100 MHz, $CDCl_3$) δ (ppm): 169.4, 166.2, 165.5 (3 × C=O), 152.6 (C-2), 147.1, 146.8, 145.6 (C-3, C-5, C-6), 134.8, 133.8, 133.3, 130.6-130.0, 129.8-128.7, 128.6, 127.5 (Ar), 98.1, 98.0 (Cp*), 78.3, 78.2, 75.5, 67.1 (C-1′, C-3′ – C-5′), 61.7 (C-6′), 54.9 (C-2′), 9.3 (Cp*-CH_3). ESI-HRMS positive mode (m/z): calcd for $C_{41}H_{42}ClN_3O_7Rh^+$ $[M\text{-}PF_6]^+$ 826.1761. Found: 826.1754.

Complex **Ru-7e**

Prepared from compound **7e** (21.2 mg, 0.035 mmol, 2.15 eq.), **Ru-dimer** (10.0 mg, 0.016 mmol) and $TlPF_6$ (11.4 mg, 0.033 mmol) according to general procedure VII. The crude product was dissolved in $CHCl_3$ (3 mL) and diisopropyl ether (12 mL) was added. The precipitation was filtered off, then washed with $CHCl_3$-diisopropyl ether (1 : 2, 2 mL) to give 27.2 mg (82%) orange solid. R_f = 0.66 (95 : 5 $CHCl_3$-MeOH). ^{1}H NMR (400 MHz, $CDCl_3$) δ (ppm): 9.38 (1H, d, *J* = 9.3 Hz, H-3 or H-4 or H-5 or H-8), 8.37 (1H, d, *J* = 8.7 Hz, H-3 or H-4 or H-5 or H-8), 8.16-7.34 (19H, m, Ar, H-3 and / or H-4 and / or H-5 and / or H-8, H-6, H-7), 6.58 (1H, dd, *J* = 11.4, 6.3 Hz, NH_2), 6.22-6.18 (3H, m, 3 × *p*-cym-CH_{Ar}), 6.04 (1H, pt, *J* = 9.5, 9.2 Hz, H-3′ or H-4′), 5.83 (1H, pt, *J* = 9.7, 9.7 Hz, H-3′ or H-4′), 5.51 (1H, d, *J* = 6.1 Hz, *p*-cym-CH_{Ar}), 5.14 (1H, d, *J* = 10.1 Hz, H-1′), 5.05 (1H, dd, *J* = 12.7, 2.1 Hz, H-6′a), 4.93 (1H, ddd, *J* = 9.8, 3.3, 2.1 Hz, H-5′), 4.53 (1H, dd, *J* = 12.7, 3.3 Hz, H-6′b), 3.61 (1H, dd, *J* = 11.4, 7.6 Hz, NH_2), 2.89 (1H, hept, *J* = 6.9 Hz, *i*-Pr-C*H*), 2.82-2.74 (1H, m, H-2), 1.59 (3H, s, C_6H_4-CH_3), 1.26, 1.19 (2 × 3H, 2 d, *J* = 6.9 Hz in both, 2 × *i*-Pr-CH_3); ^{13}C NMR (100 MHz, $CDCl_3$) δ (ppm): 168.9, 166.3, 165.7, 163.5, 149.3 (3 × C=O, C-2, C-8a), 141.3, 134.4, 133.8, 133.3, 131.4, 131.3, 130.4-130.0, 129.9, 129.3, 129.0-128.6, 127.8, 120.0 (Ar, C-3 – C-8, C-4a), 104.4, 100.6 (2 × *p*-cym-C_{qAr}), 87.3, 85.2, 83.3, 82.3, 79.9, 77.4, 74.6, 67.3 (4 × *p*-cym-CH_{Ar}, C-1′, C-3′ – C-5′), 62.1 (C-6′), 54.6 (C-2′), 31.0 (*i*-Pr-CH), 22.8, 21.7 (2 × *i*-Pr-CH_3), 17.7 (C_6H_4-CH_3). ESI-HRMS positive mode (m/z): calcd for $C_{46}H_{44}ClN_2O_7Ru^+$ $[M\text{-}PF_6]^+$ 873.1885. Found: $[M\text{-}PF_6]^+$ 873.1876.

Complex **Os-7e**

Prepared from compound **7e** (15.6 mg, 0.026 mmol, 2.05 eq.), **Os-dimer** (10.0 mg, 0.013 mmol) and $TlPF_6$ (8.7 mg, 0.025 mmol) according to general procedure VII. The crude product was dissolved in $CHCl_3$ (1 mL) and diisopropyl ether (8 mL) was added. The precipitation was filtered off, then washed with $CHCl_3$-diisopropyl ether (1 : 4, 2 mL) to give 26.9 mg (96%) dark green solid. R_f = 0.58 (95 : 5 $CHCl_3$-MeOH). ^{1}H NMR (400 MHz,

formázott: Betűtípus: Félkövér

formázott: Betűtípus: Félkövér

formázott: Betűtípus: Félkövér

$CDCl_3$) δ (ppm): 9.18 (1H, d, *J* = 9.1 Hz, H-3 or H-4 or H-5 or H-8), 8.29 (1H, d, *J* = 8.7 Hz, H-3 or H-4 or H-5 or H-8), 8.16-7.33 (19H, m, Ar, H-3 and / or H-4 and / or H-5 and / or H-8, H-6, H-7), 7.25 (1H, dd, *J* = 11.7, 6.9 Hz, NH_2), 6.54-6.51 (2H, m, 2 × *p*-cym-CH_{Ar}), 6.48 (1H, d, *J* = 5.7 Hz, *p*-cym-CH_{Ar}), 5.96 (1H, pt, *J* = 9.2, 9.1 Hz, H-3′ or H-4′), 5.83 (1H, pt, *J* = 9.8, 9.6 Hz, H-3′ or H-4′), 5.71 (1H, d, *J* = 5.7 Hz, *p*-cym-CH_{Ar}), 5.04 (1H, dd, *J* = 12.7, 2.3 Hz, H-6′a), 4.99 (1H, d, *J* = 10.2 Hz, H-1′), 4.90 (1H, ddd, *J* = 10.0, 3.4, 2.3 Hz, H-5′), 4.58 (1H, dd, *J* = 11.9, 7.3 Hz, NH_2), 4.52 (1H, dd, *J* = 12.7, 3.4 Hz, H-6′b), 3.03-2.95 (1H, m, H-2′), 2.82 (1H, hept, *J* = 6.9 Hz, *i*-Pr-C*H*), 1.63 (3H, s, C_6H_4-CH_3), 1.28, 1.18 (2 × 3H, 2 d, *J* = 6.9 Hz in both, 2 × *i*-Pr-CH_3); ^{13}C NMR (100 MHz, $CDCl_3$) δ (ppm): 168.9, 166.3, 165.7, 163.2, 149.4 (3 × C=O, C-2, C-8a), 141.6, 134.4, 133.8, 133.3, 132.5, 131.4, 130.5-130.0, 129.9, 129.4, 129.0-128.6, 127.8, 119.5 (C-3 – C-8, C-4a, Ar), 95.0, 92.4 (2 × *p*-cym-C_{qAr}), 81.0, 79.3, 77.4, 76.8, 75.2, 74.5, 73.5, 67.2 (4 × *p*-cym-CH_{Ar}, C-1′, C-3′ – C-5′), 62.1 (C-6′), 54.8 (C-2′), 31.1 (*i*-Pr-CH), 23.1, 21.9 (2 × *i*-Pr-CH_3), 17.6 (C_6H_4-CH_3). ESI-HRMS positive mode (m/z): calcd for $C_{46}H_{44}ClN_2O_7Os^+$ $[M\text{-}PF_6]^+$ 963.2439. Found: 963.2432.

Complex **Ir-7e**

Prepared from compound **7e** (15.5 mg, 0.026 mmol, 2.05 eq.), **Ir-dimer** (10.0 mg, 0.013 mmol) and $TlPF_6$ (8.8 mg, 0.025 mmol) by a slight modification of general procedure VII. During the reaction the desired product **Ir-7e** also precipitated from the reaction mixture. Therefore, after completion of the reaction removal of the solvents under reduced pressure was carried out first. After that, the residue was treated with CH_3CN (10 mL) and the insoluble TlCl was filtered off. The resulting solution was evaporated in vacuo. The residue was dissolved in a mixture of CH_3CN (0.1 mL) and $CHCl_3$ (2 mL) and diisopropyl ether (8 mL) was added. The precipitated product was filtered off, then washed with $CHCl_3$-diisopropyl ether (1 : 2, 2 mL) to give 24.6 mg (88%) dark yellow solid. R_f = 0.41 (95 : 5 $CHCl_3$-MeOH). ^{1}H NMR (400 MHz, CD_3CN) δ (ppm): 8.72 (1H, d, *J* = 9.0 Hz, H-3 or H-4 or H-5 or H-8), 8.60 (1H, d, *J* = 8.7 Hz, H-3 or H-4 or H-5 or H-8), 8.16-7.43 (19H, Ar, H-3 and / or H-4 and / or H-5 and / or H-8, H-6, H-7), 5.80 (1H, pt, *J* = 9.8, 9.4 Hz, H-3′ or H-4′), 5.73 (1H, pt, *J* = 9.6, 9.3 Hz, H-3′ or H-4′), 5.27 (1H, d, *J* = 12.9, NH_2), 4.80 (1H, dd, *J* = 12.4, 2.2 Hz, H-6′a), 4.82-4.73 (1H, broad signal, NH_2), 4.63 (1H, dd, *J* = 12.4, 3.9 Hz, H-6′b), 4.62-4.56 (1H, m, H-5′), 4.55 (1H, d, *J* = 10.5 Hz, H-1′), 3.50-3.52 (1H, m, H-2′), 1.70 (15H, s, Cp*-CH_3); ^{13}C NMR (90 MHz, CD_3CN) δ (ppm): 168.1, 166.8, 166.2, 162.6, 147.1 (3 × C=O, C-2, C-8a), 142.9, 134.9, 134.8, 134.4, 132.6, 131.9, 130.6-130.0, 129.9, 129.6-129.4, 120.4 (Ar, C-3 – C-8, C-4a), 89.7 (Cp*), 84.3, 76.4 (2), 70.0 (C-1′, C-3′ – C-5′), 63.3 (C-6′), 54.4 (C-2′), 9.9 (Cp*-CH_3). ESI-HRMS positive mode (m/z): calcd for $C_{46}H_{46}N_2O_7Ir^+$ $[M+H\text{-}Cl\text{-}PF_6]^+$ 931.2929. Found: 9631.2920.

Complex **Rh-7e**

Prepared from compound **7e** (20.0 mg, 0.033 mmol, 2.05 eq.), **Rh-dimer** (10.0 mg, 0.016 mmol) and $TlPF_6$ (11.3 mg, 0.032 mmol) by a slight modification of general procedure VII. During the reaction the desired product **Rh-7e** also precipitated from the reaction mixture. Therefore, after completion of the reaction the removal of the solvents under reduced pressure was carried out first. After that, the residue was treated with CH_3CN (10 mL) and the insoluble TlCl was filtered off. The resulting solution was evaporated in vacuo. The residue was dissolved in a mixture of CH_3CN (0.1 mL) and $CHCl_3$ (2 mL) and diisopropyl ether (8 mL) was added. The precipitated product was filtered off, then washed with $CHCl_3$-diisopropyl ether (1 : 4, 2 mL) to give 29.9 mg (90%) red solid. R_f = 0.58 (95 : 5 $CHCl_3$-MeOH). ^{1}H NMR (400 MHz, CD_3CN) δ (ppm): 8.86 (1H, d, *J* = 8.9 Hz, H-3 or H-4 or H-5 or H-8), 8.61 (1H, d, *J* = 8.7 Hz, H-3 or H-4 or H-5 or H-8), 8.12-7.43 (19H, m, Ar, H-3 and / or H-4 and / or H-5 and / or H-8, H-6, H-7), 5.83 (1H, dd, *J* = 10.2, 9.3 Hz, H-3′ or H-4′), 5.68 (1H, pt, *J* = 9.8, 9.4 Hz, H-3′ or H-4′), 4.80 (1H, dd, *J* = 12.6, 2.6 Hz, H-6′a), 4.71 (1H, d, *J* = 10.3 Hz, H-1′), 4.64 (1H, dd, *J* = 12.6, 4.0 Hz, H-6′b), 4.63-4.58 (1H, m, H-5′), 4.49 (1H, d, *J* = 12.6 Hz, NH_2), 3.95 (1H, pt, *J* = 10.4 Hz, NH_2), 3.24-3.16 (1H, m, H-2′), 1.68 (15H, s, Cp*-CH_3); ^{13}C NMR (90 MHz, CD_3CN) δ (ppm): 168.2, 166.9, 166.3, 162.7, 147.2

formázott: Betűtípus: Félkövér

formázott: Betűtípus: Félkövér

(3 × C=O, C-2, C-8a), 142.3, 134.9, 134.8, 134.4, 132.0, 131.6, 130.8, 130.7-130.5, 130.0, 129.9, 129.8-129.3, 120.8 (Ar, C-3 – C-8, C-4a), 98.1, 98.0 (Cp*), 82.1, 77.3, 76.3, 70.0 (C-1′, C-3′ – C-5′), 63.4 (C-6′), 54.4 (C-2′), 10.0 (Cp*-CH_3). ESI-HRMS positive mode (m/z): calcd for $C_{46}H_{44}ClN_2O_7Rh^+$ $[M\text{-}PF_6]^+$ 875.1965. Found: 875.1953.

5.2. X-Ray crystallography

X-ray-quality crystals of **Ru-3a** were grown by slow evaporation of a $CHCl_3$-MeOH solvent mixture. A crystal well-looking in polarized light microscope was fixed under a microscope onto a Mitegen loop using high-density oil. Diffraction intensity data were collected at room temperature using a Bruker-D8 Venture diffractometer (Bruker AXS GmbH, Karlsruhe, Germany) equipped with INCOATEC IμS 3.0 (Incoatec GmbH, Geesthacht, Germany) dual (Cu and Mo) sealed tube micro sources and a Photon II Charge-Integrating Pixel Array detector (Bruker AXS GmbH, Karlsruhe, Germany) using Mo Kα (λ = 0.71073 Å) radiation. High multiplicity data collection and integration were performed using APEX4 (version 2021-4.0, Bruker AXS Inc., 2021, Madison, USA) software. Data reduction and multi-scan absorption correction were performed using SAINT (version 8.40B, Bruker AXS Inc., 2019, Madison, USA). The structure was solved using direct methods and refined on F^2 using the SHELXL program [80] incorporated into the APEX4 suite. Refinement was performed anisotropically for all non-hydrogen atoms. Hydrogen atoms were placed into geometric positions except the amino protons which could be found on the difference electron density map and the respective N-H distances should be restrained. Multi-scan absorption correction had to be applied because of the presence of heavy atoms and shape of the crystal. Further experimental details are shown in Table S3. The CIF file was manually edited using Publcif software [81], while graphics were prepared using the Mercury program [82]. The results for the X-ray diffraction structure determinations were good enough and acceptable~~very good~~ according to the Checkcif functionality of PLATON software (Utrecht University, Utrecht, The Netherlands) [83].

and structural parameters such as bond length and angle data were in the expected range (Table S5) and except the short Ru-Cl distance. The solid state structure is stabilized by strong N-H..Cl and N-H..F as well as weak C-H..Cl hydrogen bonds (Figure S2 and Table S4)

5.3. Determination of the distribution coefficients (logD)

The logD values of the newly synthesized complexes were determined according to a procedure described in our previous publications [45].

5.4. Chemicals for biology experiments

In the cell biology and biochemistry assays all chemicals were from Sigma-Aldrich unless otherwise stated. The free ligands and complexes investigated in this study were dissolved in dimethyl-sulfoxide for biology experiments. As vehicle control 0.1% dimethyl-sulfoxide was used.

5.5. Cell lines

Cells were cultured under standard cell culture conditions, 37 °C, 5% CO_2, humidified atmosphere.

A2780 cells were cultured in RMPI 1640 medium supplemented with 10% fetal calf serum, 2 mM glutamine, 1% penicillin-streptomycin.

ID8 cells were cultured in high glucose DMEM (4.5 g/L glucose) medium supplemented with 4% fetal calf serum, 2 mM glutamine, 1% penicillin-streptomycin, 1% ITS supplement (I3146, Sigma-Aldrich).

Capan2 cells were maintained in MEM, 10% fetal bovine serum, 1% penicillin-streptomycin, 2 mM Glutamine.

formázott: Kiemelt

Human primary dermal fibroblasts were cultured in low glucose DMEM (1 g/L glucose) medium supplemented with 20% fetal calf serum, 2 mM glutamine, 1% penicillin-streptomycin.

U251 cells were maintained in MEM, 10% fetal bovine serum, 1% penicillin-streptomycin, 2 mM Glutamine.

MCF7 cells were maintained in MEM, 10% fetal bovine serum, 1% penicillin-streptomycin, 2 mM Glutamine.

5.6. Bacterial reference strains

We used the reference strains of *Staphylococcus aureus* (ATCC29213), and *Enterococcus faecalis* (ATCC29212) that were purchased from ATCC (Manassas, VA, USA).

5.7. Clinical isolates of S. aureus and E. faecium

We used a set of clinical isolates of *S. aureus and E. faecium* that were collected at the Medical Center of the University of Debrecen (Hungary) between 01. 01. 2018. – 31. 12. 2020. The isolates were reported in [31] and are presented in Table 9. The clinical isolates were identified using a Microflex MALDI-TOF mass spectrometer (Bruker, Billerica, MA, USA). Antibiotic susceptibility of the isolates was tested following the European Committee on Antimicrobial Susceptibility Testing (EUCAST) guidelines valid at the time of collection.

Table 9. The clinical isolates used in the study. VRE – vancomycin-resistant *Enterococcus*, MRSA – methicillin-resistant *Staphylococcus aureus*.

Species and strain identity		**Sample**	**Year**
Reference	*E. faecalis*		
VRE	25 051	Nephrostoma	2018
VRE	27 085	Wound	2018
VRE	25 498	Rectal swab for screening for multiresistant pathogens	2018
Reference	*S. aureus*		
MRSA	24 272	Throat	2018
MRSA	24 408	Bronchial	2018
MRSA	20 426	Blood	2020
MRSA	24 035	Wound	2018
MRSA	24 328	Throat	2018
MRSA	24 268	Throat	2018

5.8. Methylthiazolyldiphenyl-tetrazolium bromide (MTT) reduction assay

MTT reduction assay measures the activity of mitochondrial complex I and can be used to detect toxicity [60,61]. The assay was performed similar to [84]. Briefly, cells were plated to 96 well plates the day before the assay. Cells were treated with the compounds for 4 hours, then MTT was added in 0.5 mg/ml final concentration and cells were incubated at 37 °C in a cell incubator for 40-60 minutes as a function of the cell line assessed. Culture media was removed and the reduced MTT dye was dissolved in dimethyl-sulfoxide and plates were measured in a plate photometer (Thermo Scientific Multiscan GO spectrophotometer, Waltham, MA, USA) at 540 nm. On each plate wells were designed to contain vehicle-treated cells. In calculations the readings for these wells was considered as 1 and all readings were expressed relative to these values.

5.9. Sulforhodamine B (SRB) binding assay

formázott: Betűtípus: 10 pt

formázott: Betűtípus: 10 pt, Nem Dőlt, Nyelvhelyesség ellenőrzése

formázott: Betűtípus: 10 pt

formázott: Betűtípus: 10 pt

formázott: Betűtípus: 10 pt, Nem Dőlt, Nyelvhelyesség ellenőrzése

táblázatot formázott

formázott: Betűtípus: Nem Félkövér

táblázatot formázott

The SRB assay measures protein content of cells in correlation of cell number in an assay well, hence can be used to assess cell proliferation or long-term cytostasis [62]. Cells were seeded in 96 well plates the day before the assay. Cells were treated with the compounds for 48 hours. Then medium was removed and cells were fixed with 10 % trichloroacetic acid. Fixed cells were washed in distilled water 3 times followed by staining with SRB (0.4 m/V% dissolved in 1 % acetic acid) for 10 minutes. Stained cells were washed in 1% acetic acid 5 times; acetic acid was removed and cells were left to dry. Protein-bound SRB was released by adding 100 µl 10 mM Tris base. Plates were measured in a plate photometer (Thermo Scientific Multiscan GO spectrophotometer, Waltham, MA, USA) at 540 nm. On each plate wells were designed to contain vehicle-treated cells. In calculations the readings for these wells was considered as 1 and all readings were expressed relative to these values.

5.10. Broth microdilution

Microdilution experiments were performed according to the standards of EUCAST [85]. The bacterial isolates to be tested were grown on Mueller-Hinton agar plates. Inoculum density of bacteria was set at $5.0x10^5$ CFU/mL in microtiter plates in a final volume of 200 µL Mueller-Hinton broth. Tested concentration range was 0.08-40 µM (10 concentrations, two-fold serial dilutions), drug-free growth control and inoculum-free negative control were included. The inoculated plates were incubated for 24 hours at 37 °C then were assessed visually. Minimum inhibitory concentration (MIC) was defined as the lowest concentration with 50%≤ inhibitory effect compared to the growth control. All experiments were performed at least twice in duplicates.

5.11. Statistical evaluation

Statistical analysis was performed using 8.0.1 version of GraphPad Prism. Values were tested for normal distribution using the Shapiro-Wilk normality test. When necessary, values were log normalized or were normalized using the Box-Cox normalization method [86] as indicated in the figure captions. The following statistical test, post hoc test and the level of significance is indicated in the figure captions. Nonlinear regression was performed using the built-in "[Inhibitor] vs. response – Variable slope (four parameters), least square fit" utility of GraphPad that yielded IC_{50} and Hill slope values if the sigmoid curves reached a plateau of inhibition, there was no decrease between two subsequent data points, or, when inhibition was over 90%. In other cases, the percent of inhibition was taken for the maximum concentration (100 µM).

Conflicts of Interest: The authors declare that the research was conducted in the absence of any commercial or financial relationships that could be construed as a potential conflict of interest.

Author Contributions: I.K. synthesized the compounds and performed the stability and lipophilicity experiments, A.S. performed cell-based assays, statistical analysis and visualization, E.M. and N.B. determined MIC values, A. B. performed X-ray crystallography study, P.Buglyó contributed to the structural analysis of the complexes, coordinated the stability and lipophilicity experiments, L.S. wrote the paper and contributed to the manuscript editing, G.K. conceived, coordinated and supervised the research, contributed to visualization and wrote the paper, P.Bai conceived, coordinated and supervised the research, contributed to visualization and wrote the paper, É.B. conceived the research, coordinated the synthetic work, and wrote the paper.

Funding: Our work was supported by the National Research, Development and Innovation Office of Hungary (grants K142141 and FK125067), by the University of Debrecen, by the Thematic Excellence Programme (TKP2020-IKA-04, TKP2021-EGA-19, TKP2021-EGA-20) of the Ministry for Innovation and Technology in Hungary and by the Momentum fellowship and the POST-COVID2021-33 and NKM2022-30 grants of the Hungarian Academy of Sciences.

Acknowledgments: We are grateful for Mr. László Finta, Mr. Zsolt Hartman and Mr. György Attila Kiss for the technical assistance.

Supplementary Materials: The following supporting information can be downloaded at https://: Copies of ^{1}H and ^{13}C NMR spectra; Table S1. Changes of the chemical shifts of selected ^{1}H NMR resonances as a result of the complex formation; Table S2. Distribution coefficient of the synthesized complexes (logD); X-Ray diffraction study of **Ru-3a**: Figure S1. Ball and stick model of **Ru-3a** with partial numbering scheme, Table S3. Experimetal details, Figure S2. Packing diagram of **Ru-3a**, Table S4. Hydrogen-bond geometry (Å, º) for **Ru-3a**, Table S5. Geometric parameters (Å, º) for **Ru-3a**.

Data Availability Statement: The datasets generated and analyzed for this study can be found at Figshare.com https://figshare.com/s/9ec2a005e6b9e5874c07 (DOI: 10.6084/m9.figshare.21786020). The supplementary crystallographic data for the **Ru-3a** structure in this paper can be obtained free of charge from the Cambridge Crystallographic Data Centre via http://www.ccdc.cam.ac.uk/data_request/cif, using reference deposition number 2241543.

References

1. Zhang, C.; Xu, C.; Gao, X.; Yao, Q. Platinum-based drugs for cancer therapy and anti-tumor strategies. *Theranostics* **2022**, *12*, 2115-2132, doi:10.7150/thno.69424.
2. Kenny, R.G.; Marmion, C.J. Toward Multi-Targeted Platinum and Ruthenium Drugs-A New Paradigm in Cancer Drug Treatment Regimens? *Chemical reviews* **2019**, *119*, 1058-1137, doi:10.1021/acs.chemrev.8b00271.
3. Mukherjea, D.; Dhukhwa, A.; Sapra, A.; Bhandari, P.; Woolford, K.; Franke, J.; Ramkumar, V.; Rybak, L. Strategies to reduce the risk of platinum containing antineoplastic drug-induced ototoxicity. *Expert opinion on drug metabolism & toxicology* **2020**, *16*, 965-982, doi:10.1080/17425255.2020.1806235.
4. Lund, R.J.; Huhtinen, K.; Salmi, J.; Rantala, J.; Nguyen, E.V.; Moulder, R.; Goodlett, D.R.; Lahesmaa, R.; Carpen, O. DNA methylation and Transcriptome Changes Associated with Cisplatin Resistance in Ovarian Cancer. *Scientific Reports* **2017**, *7*, 1469, doi:10.1038/s41598-017-01624-4.
5. Yu, C.; Wang, Z.; Sun, Z.; Zhang, L.; Zhang, W.; Xu, Y.; Zhang, J.J. Platinum-Based Combination Therapy: Molecular Rationale, Current Clinical Uses, and Future Perspectives. *Journal of Medicinal Chemistry* **2020**, *63*, 13397-13412, doi:10.1021/acs.jmedchem.0c00950.
6. McMullen, M.; Madariaga, A.; Lheureux, S. New approaches for targeting platinum-resistant ovarian cancer. *Seminars in Cancer Biology* **2020**, doi:10.1016/j.semcancer.2020.08.013.
7. Fetoni, A.R.; Paciello, F.; Mezzogori, D.; Rolesi, R.; Eramo, S.L.; Paludetti, G.; Troiani, D. Molecular targets for anticancer redox chemotherapy and cisplatin-induced ototoxicity: the role of curcumin on pSTAT3 and Nrf-2 signalling. *British Journal of Cancer* **2015**, *113*, 1434-1444, doi:10.1038/bjc.2015.359.
8. Sipos, A.; Ujlaki, G.; Mikó, E.; Maka, E.; Szabó, J.; Uray, K.; Krasznai, Z.; Bai, P. The role of the microbiome in ovarian cancer: mechanistic insights into oncobiosis and to bacterial metabolite signaling. *Molecular medicine (Cambridge, Mass.)* **2021**, *27*, 33, doi:10.1186/s10020-021-00295-2.
9. Hartinger, C.G.; Phillips, A.D.; Nazarov, A.A. Polynuclear ruthenium, osmium and gold complexes. The quest for innovative anticancer chemotherapeutics. *Current topics in medicinal chemistry* **2011**, *11*, 2688-2702, doi:10.2174/156802611798040769.
10. Zeng, L.; Gupta, P.; Chen, Y.; Wang, E.; Ji, L.; Chao, H.; Chen, Z.-S. The development of anticancer ruthenium(II) complexes: from single molecule compounds to nanomaterials. *Chemical Society Reviews* **2017**, *46*, 5771-5804, doi:10.1039/C7CS00195A.
11. Štarha, P.; Trávníček, Z. Non-platinum complexes containing releasable biologically active ligands. *Coordination Chemistry Reviews* **2019**, *395*, 130-145, doi:10.1016/j.ccr.2019.06.001.
12. Meier-Menches, S.M.; Gerner, C.; Berger, W.; Hartinger, C.G.; Keppler, B.K. Structure–activity relationships for ruthenium and osmium anticancer agents – towards clinical development. *Chemical Society Reviews* **2018**, *47*, 909-928, doi:10.1039/C7CS00332C.
13. Coverdale, J.P.C.; Laroiya-McCarron, T.; Romero-Canelón, I. Designing Ruthenium Anticancer Drugs: What Have We Learnt from the Key Drug Candidates? *Inorganics* **2019**, *7*, 31, doi:10.3390/inorganics7030031.
14. Gichumbi, J.M.; Friedrich, H.B. Half-sandwich complexes of platinum group metals (Ir, Rh, Ru and Os) and some recent biological and catalytic applications. *Journal of Organometallic Chemistry* **2018**, *866*, 123-143, doi:10.1016/j.jorganchem.2018.04.021.
15. Melchart, M.; Sadler, P.J. Ruthenium Arene Anticancer Complexes. In *Bioorganometallics*, Jaouen, G., Ed.; Wiley-VCH Verlag GmbH & Co. KGaA: 2006; pp. 39-64.
16. Li, Y.; Liu, B.; Shi, H.; Wang, Y.; Sun, Q.; Zhang, Q. Metal complexes against breast cancer stem cells. *Dalton Transactions* **2021**, *50*, 14498-14512, doi:10.1039/d1dt02909f.
17. Konkankit, C.C.; Marker, S.C.; Knopf, K.M.; Wilson, J.J. Anticancer activity of complexes of the third row transition metals, rhenium, osmium, and iridium. *Dalton Transactions* **2018**, *47*, 9934-9974, doi:10.1039/c8dt01858h.
18. Hanif, M.; Babak, M.V.; Hartinger, C.G. Development of anticancer agents: wizardry with osmium. *Drug Discovery Today* **2014**, *19*, 1640-1648, doi:10.1016/j.drudis.2014.06.016.
19. Nabiyeva, T.; Marschner, C.; Blom, B. Synthesis, structure and anti-cancer activity of osmium complexes bearing Π-bound arene substituents and phosphane Co-Ligands: A review. *European Journal of Medicinal Chemistry* **2020**, *201*, doi:10.1016/j.ejmech.2020.112483.
20. Leung, C.H.; Zhong, H.J.; Chan, D.S.H.; Ma, D.L. Bioactive iridium and rhodium complexes as therapeutic agents. *Coordination Chemistry Reviews* **2013**, *257*, 1764-1776, doi:10.1016/j.ccr.2013.01.034.

21. Liu, Z.; Sadler, P.J. Organoiridium complexes: anticancer agents and catalysts. *Accounts of chemical research* **2014**, *47*, 1174-1185, doi:10.1021/ar400266c.
22. Máliková, K.; Masaryk, L.; Štarha, P. Anticancer Half-Sandwich Rhodium(III) Complexes. *Inorganics* **2021**, *9*, 26, doi:10.3390/inorganics9040026.
23. Mihajlovic, K.; Milosavljevic, I.; Jeremic, J.; Savic, M.; Sretenovic, J.; Srejovic, I.M.; Zivkovic, V.I.; Jovicic, N.; Paunovic, M.; Bolevich, S.; et al. Redox and apoptotic potential of novel ruthenium complexes in the rat blood and heart. *Canadian journal of physiology and pharmacology* **2020**, *99*, 207-217, doi: 10.1139/cjpp-2020-0349.
24. Liu, J.; Lai, H.; Xiong, Z.; Chen, B.; Chen, T. Functionalization and cancer-targeting design of ruthenium complexes for precise cancer therapy. *Chemical communications (Cambridge, England)* **2019**, *55*, 9904-9914, doi:10.1039/c9cc04098f.
25. Gano, L.; Pinheiro, T.; Matos, A.P.; Tortosa, F.; Jorge, T.F.; Gonçalves, M.S.; Martins, M.; Morais, T.S.; Valente, A.; Tomaz, A.I.; et al. Antitumour and Toxicity Evaluation of a Ru(II)-Cyclopentadienyl Complex in a Prostate Cancer Model by Imaging Tools. *Anti-Cancer Agents in Medicinal Chemistry* **2019**, *19*, 1262-1275, doi:10.2174/1871520619666190318152726.
26. Mello-Andrade, F.; Cardoso, C.G.; Silva, C.R.E.; Chen-Chen, L.; Melo-Reis, P.R.; Lima, A.P.; Oliveira, R.; Ferraz, I.B.M.; Grisolia, C.K.; Almeida, M.A.P.; et al. Acute toxic effects of ruthenium (II)/amino acid/diphosphine complexes on Swiss mice and zebrafish embryos. *Biomedicine & pharmacotherapy* **2018**, *107*, 1082-1092, doi:10.1016/j.biopha.2018.08.051.
27. Leijen, S.; Burgers, S.A.; Baas, P.; Pluim, D.; Tibben, M.; van Werkhoven, E.; Alessio, E.; Sava, G.; Beijnen, J.H.; Schellens, J.H. Phase I/II study with ruthenium compound NAMI-A and gemcitabine in patients with non-small cell lung cancer after first line therapy. *Investigational New Drugs* **2015**, *33*, 201-214, doi:10.1007/s10637-014-0179-1.
28. Burris, H.A.; Bakewell, S.; Bendell, J.C.; Infante, J.; Jones, S.F.; Spigel, D.R.; Weiss, G.J.; Ramanathan, R.K.; Ogden, A.; Von Hoff, D. Safety and activity of IT-139, a ruthenium-based compound, in patients with advanced solid tumours: a first-in-human, open-label, dose-escalation phase I study with expansion cohort. *ESMO Open* **2016**, *1*, e000154, doi:10.1136/esmoopen-2016-000154.
29. Kulkarni, G.S.; Lilge, L.; Nesbitt, M.; Dumoulin-White, R.J.; Mandel, A.; Jewett, M.A.S. A Phase 1b Clinical Study of Intravesical Photodynamic Therapy in Patients with Bacillus Calmette-Guérin-unresponsive Non-muscle-invasive Bladder Cancer. *European urology open science* **2022**, *41*, 105-111, doi:10.1016/j.euros.2022.04.015.
30. Yufanyi, D.M.; Abbo, H.S.; Titinchi, S.J.J.; Neville, T. Platinum(II) and Ruthenium(II) complexes in medicine: Antimycobacterial and Anti-HIV activities. *Coordination Chemistry Reviews* **2020**, *414*, 213285, doi:10.1016/j.ccr.2020.213285.
31. Balázs, B.; Tóth, Z.; Kacsir, I.; Sipos, A.; Buglyó, P.; Somsák, L.; Bokor, É.; Kardos, G.; Bai, P. Targeting multiresistant Gram-positive bacteria by ruthenium, osmium, iridium and rhodium half-sandwich type complexes with bidentate monosaccharide ligands. *Frontiers in Chemistry* **2022**, 868234, doi:10.3389/fchem.2022.868234.
32. Kacsir, I.; Sipos, A.; Kiss, T.; Major, E.; Bajusz, N.; Tóth, E.; Buglyo, P.; Somsak, L.; Kardos, G.; Bai, P.; et al. Half Sandwich-Type Osmium, Ruthenium, Iridium and Rhodium Complexes with Bidentate Glycosyl Heterocyclic Ligands Induce Cytostasis in Platinum-Resistant Ovarian Cancer Cells and Bacteriostasis in Gram-Positive Multiresistant Bacteria. *Frontiers in Chemistry* **2023**, doi:10.3389/fchem.2023.1086267.
33. Lapasam, A.; Adhikari, S.; Banothu, V.; Addepally, U.; Kollipara, M.R. Arene platinum group metal complexes containing imino-quinolyl ligands: synthesis and antibacterial studies. *Journal of Coordination Chemistry* **2020**, *73*, 737-753, doi:10.1080/00958972.2020.1753037.
34. Lapasam, A.; Mawnai, I.L.; Banothu, V.; Kaminsky, W.; Kollipara, M.R. Ruthenium, rhodium and iridium complexes containing pyrimidine based thienyl pyrazoles: Synthesis and antibacterial studies. *Journal of Organometallic Chemistry* **2020**, *911*, 121155, doi:10.1016/j.jorganchem.2020.121155.
35. Coverdale, J.P.C.; Guy, C.S.; Bridgewater, H.E.; Needham, R.J.; Fullam, E.; Sadler, P.J. Osmium-arene complexes with high potency towards Mycobacterium tuberculosis. *Metallomics* **2021**, *13*, mfab007, doi:10.1093/mtomcs/mfab007.
36. Kljun, J.; Leon, I.E.; Persic, S.; Cadavid-Vargas, J.F.; Etcheverry, S.B.; He, W.J.; Bai, Y.; Turel, I. Synthesis and biological characterization of organoruthenium complexes with 8-hydroxyquinolines. *Journal of inorganic biochemistry* **2018**, *186*, 187-196, doi:10.1016/j.jinorgbio.2018.05.009.
37. Karpin, G.W.; Merola, J.S.; Falkinham, J.O. Transition Metal-a-Amino Acid Complexes with Antibiotic Activity against *Mycobacterium* spp. *Antimicrobial Agents and Chemotherapy* **2013**, *57*, 3434-3436, doi:10.1128/aac.00452-13.
38. DuChane, C.M.; Brown, L.C.; Dozier, V.S.; Merola, J.S. Synthesis, Characterization, and Antimicrobial Activity of Rh^{III} and Ir^{III} b-Diketonato Piano-Stool Compounds. *Organometallics* **2018**, *37*, 530-538, doi:10.1021/acs.organomet.7b00742.
39. Bernier, C.M.; DuChane, C.M.; Martinez, J.S.; Falkinham, J.O.; Merola, J.S. Synthesis, Characterization, and Antimicrobial Activity of Rh^{III} and Ir^{III} N-Heterocyclic Carbene Piano-Stool Complexes. *Organometallics* **2021**, *40*, 1670-1681, doi:10.1021/acs.organomet.1c00166.
40. Holzer, I.; Desiatkina, O.; Anghel, N.; Johns, S.K.; Boubaker, G.; Hemphill, A.; Furrer, J.; Paunescu, E. Trithiolato-Bridged Dinuclear Arene Ruthenium(ll)- Glycoconjugates: Synthesis and Antiparasitic Activity. *ChemRxiv. Cambridge: Cambridge Open Engage* **2022**, doi:10.26434/chemrxiv-2022-kkcth.
41. Rajapakse, C.S.K.; Martinez, A.; Naoulou, B.; Jarzecki, A.A.; Suarez, L.; Deregnaucourt, C.; Sinou, V.; Schrevel, J.; Musi, E.; Ambrosini, G.; et al. Synthesis, Characterization, and in vitro Antimalarial and Antitumor Activity of New Ruthenium(II) Complexes of Chloroquine. *Inorganic Chemistry* **2009**, *48*, 1122-1131, doi:10.1021/ic802220w.
42. Martínez, A.; Carreon, T.; Iniguez, E.; Anzellotti, A.; Sánchez, A.; Tyan, M.; Sattler, A.; Herrera, L.; Maldonado, R.A.; Sánchez-Delgado, R.A. Searching for New Chemotherapies for Tropical Diseases: Ruthenium-Clotrimazole Complexes Display High in

Vitro Activity against Leishmania major and Trypanosoma cruzi and Low Toxicity toward Normal Mammalian Cells. *Journal of Medicinal Chemistry* **2012**, *55*, 3867-3877, doi:10.1021/jm300070h.
43. Chuong, C.; DuChane, C.M.; Webb, E.M.; Rai, P.; Marano, J.M.; Bernier, C.M.; Merola, J.S.; Weger-Lucarelli, J. Noble Metal Organometallic Complexes Display Antiviral Activity against SARS-CoV-2. *Viruses-Basel* **2021**, *13*, 980, doi:10.3390/v13060980.
44. Kljun, J.; Scott, A.J.; Rizner, T.L.; Keiser, J.; Turel, I. Synthesis and Biological Evaluation of Organoruthenium Complexes with Azole Antifungal Agents. First Crystal Structure of a Tioconazole Metal Complex. *Organometallics* **2014**, *33*, 1594-1601, doi:10.1021/om401096y.
45. Kacsir, I.; Sipos, A.; Ujlaki, G.; Buglyó, P.; Somsák, L.; Bai, P.; Bokor, É. Ruthenium Half-Sandwich Type Complexes with Bidentate Monosaccharide Ligands Show Antineoplastic Activity in Ovarian Cancer Cell Models through Reactive Oxygen Species Production. *International Journal of Molecular Sciences* **2021**, *22*, 10454, doi:10.3390/ijms221910454.
46. Kacsir, I.; Sipos, A.; Bényei, A.; Janka, E.; Buglyó, P.; Somsák, L.; Bai, P.; Bokor, É. Reactive oxygen species production is responsible for antineoplastic activity of osmium, ruthenium, iridium and rhodium half-sandwich type complexes with bidentate glycosyl hetero-cyclic ligands in various cancer cell models *International Journal of Molecular Sciences* **2022**, *23*, 813, doi:10.3390/ijms23020813.
47. Hamala, V.; Martišová, A.; Červenková Šťastná, L.; Karban, J.; Dančo, A.; Šimarek, A.; Lamač, M.; Horáček, M.; Kolářová, T.; Hrstka, R.; et al. Ruthenium tetrazene complexes bearing glucose moieties on their periphery: Synthesis, characterization, and in vitro cytotoxicity. *Applied Organometallic Chemistry* **2020**, *34*, e5896, doi:10.1002/aoc.5896.
48. Böge, M.; Fowelin, C.; Bednarski, P.; Heck, J. Diaminohexopyranosides as Ligands in Half-Sandwich Ruthenium(II), Rhodium(III), and Iridium(III) Complexes. *Organometallics* **2015**, *34*, 1507-1521, doi:10.1021/om5013117.
49. Dharuman, S.; Gupta, P.; Kancharla, P.K.; Vankar, Y.D. Synthesis of 2-Nitroglycals from Glycals Using the Tetrabutylammonium Nitrate-Trifluoroacetic Anhydride-Triethylamine Reagent System and Base-Catalyzed Ferrier Rearrangement of Acetylated 2-Nitroglycals. *Journal of Organic Chemistry* **2013**, *78*, 8442-8450, doi:10.1021/jo401165y.
50. Delaunay, T.; Poisson, T.; Jubault, P.; Pannecoucke, X. Stereoselective Access to b-*C*-Glycosamines by Nitro-Michael Addition of Organolithium Reagents. *European Journal of Organic Chemistry* **2014**, *2014*, 3341-3345, doi:10.1002/ejoc.201402001.
51. Schmidt, R.R.; Vankar, Y.D. 2-nitroglycals as powerful glycosyl donors: Application in the synthesis of biologically important molecules. *Accounts of chemical research* **2008**, *41*, 1059-1073, doi:10.1021/ar7002495.
52. Bokor, É.; Kun, S.; Goyard, D.; Tóth, M.; Praly, J.P.; Vidal, S.; Somsák, L. *C*-Glycopyranosyl Arenes and Hetarenes: Synthetic Methods and Bioactivity Focused on Antidiabetic Potential. *Chemical reviews* **2017**, *117*, 1687-1764, doi:10.1021/acs.chemrev.6b00475.
53. Yang, Y.; Yu, B. Recent Advances in the Chemical Synthesis of *C*-Glycosides. *Chemical reviews* **2017**, *117*, 12281-12356, doi:10.1021/acs.chemrev.7b00234.
54. Okano, K.; Okuyama, K.I.; Fukuyama, T.; Tokuyama, H. Mild debenzylation of aryl benzyl ether with BCl_3 in the presence of pentamethylbenzene as a non-Lewis-basic cation scavenger. *Synlett* **2008**, 1977-1980, doi:10.1055/s-2008-1077980.
55. Polat, T.; Linhardt, R.J. Zinc triflate-benzoyl bromide: a versatile reagent for the conversion of ether into benzoate protecting groups and ether glycosides into glycosyl bromides. *Carbohydrate Research* **2003**, *338*, 447-449, doi:10.1016/s0008-6215(02)00481-0.
56. Groom, C.R.; Bruno, I.J.; Lightfoot, M.P.; Ward, S.C. The Cambridge Structural Database. *Acta Crystallographica Section B-Structural Science Crystal Engineering and Materials* **2016**, *72*, 171-179, doi:10.1107/s2052520616003954.
57. Cremer, D.; Pople, J.A. General definition of ring puckering coordinates. *Journal of the American Chemical Society* **1975**, *97*, 1354-1358, doi:10.1021/ja00839a011.
58. Romero, M.J.; Sadler, P.J. Chirality in Organometallic Anticancer complexes. In *Bioorganometallic Chemistry*, Jaouen, G., Salmain, M., Eds.; Wiley-VCH Verlag GmbH & Co. KGaA 2015; pp. 85-116.
59. Parsons, S.; Flack, H.D.; Wagner, T. Use of intensity quotients and differences in absolute structure refinement. *Acta Crystallographica Section B-Structural Science Crystal Engineering and Materials* **2013**, *69*, 249-259, doi:10.1107/s2052519213010014.
60. Virág, L.; Salzman, A.L.; Szabó, C. Poly(ADP-ribose) synthetase activation mediates mitochondrial injury during oxidant-induced cell death. *Journal of immunology (Baltimore, Md. : 1950)* **1998**, *161*, 3753-3759, doi:10.4049/jimmunol.161.7.3753.
61. Henslee, E.A.; Torcal Serrano, R.M.; Labeed, F.H.; Jabr, R.I.; Fry, C.H.; Hughes, M.P.; Hoettges, K.F. Accurate quantification of apoptosis progression and toxicity using a dielectrophoretic approach. *Analyst* **2016**, *141*, 6408-6415, doi:10.1039/c6an01596d.
62. Skehan, P.; Storeng, R.; Scudiero, D.; Monks, A.; McMahon, J.; Vistica, D.; Warren, J.T.; Bokesch, H.; Kenney, S.; Boyd, M.R. New colorimetric cytotoxicity assay for anticancer-drug screening. *Journal of the National Cancer Institute* **1990**, *82*, 1107-1112, doi:10.1093/jnci/82.13.1107.
63. Hanif, M.; Meier, S.; Nazarov, A.; Risse, J.; Legin, A.; Casini, A.; Jakupec, M.; Keppler, B.; Hartinger, C. Influence of the π-coordinated arene on the anticancer activity of ruthenium(II) carbohydrate organometallic complexes. *Frontiers in Chemistry* **2013**, *1*, 27, doi:10.3389/fchem.2013.00027.
64. Berger, I.; Hanif, M.; Nazarov, A.A.; Hartinger, C.G.; John, R.O.; Kuznetsov, M.L.; Groessl, M.; Schmitt, F.; Zava, O.; Biba, F.; et al. In Vitro Anticancer Activity and Biologically Relevant Metabolization of Organometallic Ruthenium Complexes with Carbohydrate-Based Ligands. *Chemistry—A European Journal* **2008**, *14*, 9046-9057, doi:10.1002/chem.200801032.
65. Florindo, P.R.; Pereira, D.M.; Borralho, P.M.; Costa, P.J.; Piedade, M.F.M.; Rodrigues, C.M.P.; Fernandes, A.C. New [(η^5-C_5H_5)Ru(N-N)(PPh_3)][PF_6] compounds: colon anticancer activity and GLUT-mediated cellular uptake of carbohydrate-appended complexes. *Dalton Transactions* **2016**, *45*, 11926-11930, doi:10.1039/c6dt01571a.

66. Florindo, P.R.; Pereira, D.M.; Borralho, P.M.; Rodrigues, C.M.P.; Piedade, M.F.M.; Fernandes, A.C. Cyclopentadienyl-Ruthenium(II) and Iron(II) Organometallic Compounds with Carbohydrate Derivative Ligands as Good Colorectal Anticancer Agents. *Journal of Medicinal Chemistry* **2015**, *58*, 4339-4347, doi:10.1021/acs.jmedchem.5b00403.
67. Florindo, P.; Marques, I.J.; Nunes, C.D.; Fernandes, A.C. Synthesis, characterization and cytotoxicity of cyclopentadienyl ruthenium(II) complexes containing carbohydrate-derived ligands. *Journal of Organometallic Chemistry* **2014**, *760*, 240-247, doi:10.1016/j.jorganchem.2013.09.004.
68. Yuan, M.; Chua, S.L.; Liu, Y.; Drautz-Moses, D.I.; Yam, J.K.H.; Aung, T.T.; Beuerman, R.W.; Salido, M.M.S.; Schuster, S.C.; Tan, C.H.; et al. Repurposing the anticancer drug cisplatin with the aim of developing novel Pseudomonas aeruginosa infection control agents. *Beilstein journal of organic chemistry* **2018**, *14*, 3059-3069, doi:10.3762/bjoc.14.284.
69. McCarron, A.J.; Armstrong, C.; Glynn, G.; Millar, B.C.; Rooney, P.J.; Goldsmith, C.E.; Xu, J.; Moore, J.E. Antibacterial effects on acinetobacter species of commonly employed antineoplastic agents used in the treatment of haematological malignancies: an in vitro laboratory evaluation. *British Journal of Biomedical Science* **2012**, *69*, 14-17, doi:10.1080/09674845.2012.11669916.
70. Zhang, L.; Zheng, Y.; Callahan, B.; Belfort, M.; Liu, Y. Cisplatin inhibits protein splicing, suggesting inteins as therapeutic targets in mycobacteria. *Journal of Biological Chemistry* **2011**, *286*, 1277-1282, doi:10.1074/jbc.M110.171124.
71. Hummell, N.A.; Kirienko, N.V. Repurposing bioactive compounds for treating multidrug-resistant pathogens. *Journal of Medical Microbiology* **2020**, *69*, 881-894, doi:10.1099/jmm.0.001172.
72. Frei, A.; Ramu, S.; Lowe, G.J.; Dinh, H.; Semenec, L.; Elliott, A.G.; Zuegg, J.; Deckers, A.; Jung, N.; Bräse, S.; et al. Platinum Cyclooctadiene Complexes with Activity against Gram-positive Bacteria. *ChemMedChem* **2021**, *16*, 3165-3171, doi:10.1002/cmdc.202100157.
73. Mansour, A.M. Pd(ii) and Pt(ii) complexes of tridentate ligands with selective toxicity against Cryptococcus neoformans and Candida albicans. *RSC Advances* **2021**, *11*, 39748-39757, doi:10.1039/D1RA06559A.
74. Quirante, J.; Ruiz, D.; Gonzalez, A.; López, C.; Cascante, M.; Cortés, R.; Messeguer, R.; Calvis, C.; Baldomà, L.; Pascual, A.; et al. Platinum(II) and palladium(II) complexes with (N,N') and (C,N,N')- ligands derived from pyrazole as anticancer and antimalarial agents: synthesis, characterization and in vitro activities. *Journal of inorganic biochemistry* **2011**, *105*, 1720-1728, doi:10.1016/j.jinorgbio.2011.09.021.
75. Vieites, M.; Smircich, P.; Pagano, M.; Otero, L.; Fischer, F.L.; Terenzi, H.; Prieto, M.J.; Moreno, V.; Garat, B.; Gambino, D. DNA as molecular target of analogous palladium and platinum anti-Trypanosoma cruzi compounds: a comparative study. *Journal of inorganic biochemistry* **2011**, *105*, 1704-1711, doi:10.1016/j.jinorgbio.2011.07.018.
76. Hildebrandt, J.; Häfner, N.; Kritsch, D.; Görls, H.; Dürst, M.; Runnebaum, I.B.; Weigand, W. Highly Cytotoxic Osmium(II) Compounds and Their Ruthenium(II) Analogues Targeting Ovarian Carcinoma Cell Lines and Evading Cisplatin Resistance Mechanisms. *International Journal of Molecular Sciences* **2022**, *23*, 4976, doi:10.3390/ijms23094976.
77. Sun, Y.; Das, S.; Brown, S.R.; Blevins, E.R.; Qu, F.; Ward, N.A.; Gregory, S.A.; Boudreaux, C.M.; Kim, Y.; Papish, E.T. Ruthenium pincer complexes for light activated toxicity: Lipophilic groups enhance toxicity. *Journal of inorganic biochemistry* **2023**, *240*, 112110, doi:10.1016/j.jinorgbio.2022.112110.
78. Godó, A.J.; Bényei, A.C.; Duff, B.; Egan, D.A.; Buglyó, P. Synthesis and X-ray diffraction structures of novel half-sandwich Os(II)-and Ru(II)-hydroxamate complexes. *RSC Advances* **2012**, *2*, 1486-1495, doi:10.1039/C1RA00998B.
79. Das, J.; Schmidt, R.R. Convenient glycoside synthesis of amino sugars: Michael-Type addition to 2-nitro-D-galactal. *European Journal of Organic Chemistry* **1998**, *1998*, 1609-1613, doi:10.1002/(SICI)1099-0690(199808)1998:8<1609::AID-EJOC1609>3.0.CO;2-1.
80. Sheldrick, G.M. A short history of SHELX. *Acta Crystallographica a-Foundation and Advances* **2008**, *64*, 112-122, doi:10.1107/s0108767307043930.
81. Westrip, S.P. publCIF: software for editing, validating and formatting crystallographic information files. *Journal of Applied Crystallography* **2010**, *43*, 920-925, doi:10.1107/s0021889810022120.
82. Macrae, C.F.; Edgington, P.R.; McCabe, P.; Pidcock, E.; Shields, G.P.; Taylor, R.; Towler, M.; van De Streek, J. Mercury: visualization and analysis of crystal structures. *Journal of Applied Crystallography* **2006**, *39*, 453-457, doi:10.1107/s002188980600731x.
83. Spek, A.L. Single-crystal structure validation with the program PLATON. *Journal of Applied Crystallography* **2003**, *36*, 7-13, doi:10.1107/s0021889802022112.
84. Bakondi, E.; Gönczi, M.; Szabó, E.; Bai, P.; Pacher, P.; Gergely, P.; Kovács, L.; Hunyadi, J.; Szabó, C.; Csernoch, L.; et al. Role of intracellular calcium mobilization and cell-density-dependent signaling in oxidative-stress-induced cytotoxicity in HaCaT keratinocytes. *Journal of Investigative Dermatology* **2003**, *121*, 88-95, doi:10.1046/j.1523-1747.2003.12329.x.
85. EUCAST. MIC determination of non-fastidious and fastidious organisms. Available online: https://www.eucast.org/ast_of_bacteria/mic_determination/?no_cache=1 (accessed on 2021. 11. 04.).
86. Box, G.E.P.; Cox, D.R. An analysis of transformations. *Journal of the Royal Statistical Society, B* **1964**, *26*, 211-234, doi:10.1111/j.2517-6161.1964.tb00553.x.